

**SHEAR AND LOAD-INTRODUCTION DEFORMABILITY AND
STRENGTH OF COLUMN WEB PANELS IN STRONG AXIS
BEAM-TO-COLUMN JOINTS**

**EC3 FORMULAE : DISCUSSION AND
PROPOSALS FOR IMPROVEMENT**

J.P. JASPART

INTERNAL REPORT N° 202

APRIL 1990.

CONTAIN OF THE REPORT

1. INTRODUCTION
2. JOINT DEFORMABILITY COMPONENTS
3. NUMERICAL INVESTIGATIONS
4. STUDY OF THE LOAD-INTRODUCTION EFFECT
 - 4.1. Conclusions of the numerical simulations
 - 4.2. Theoretical developments and model for prediction
5. STUDY OF THE SHEAR EFFECT
 - 5.1. Conclusions of the numerical simulations
 - 5.2. Theoretical developments and model for prediction - unstiffened column web panels
 - 5.3. Theoretical developments and model for prediction - stiffened column web panels
6. ASSESSMENT OF THE ULTIMATE STRENGTH FOR UNSTIFFENED WEB PANELS
 - 6.1. Shear of the web panel
 - 6.2. Excessive yielding of the web
 - 6.3. Web instability
 - 6.3.1. Interior HE columns
 - 6.3.2. Exterior HE columns
 - 6.3.3. Extension to IPE columns
7. COMPARISON OF THE MODELS AND FORMULAE WITH THE RESULTS OF NUMERICAL SIMULATIONS
 - 7.1. Shear curves
 - 7.2. Load-introduction curves
 - 7.3. Ultimate loads
8. PASSAGE FROM MULTI-LINEAR MODELS TO MORE CONTINUOUS DEFORMABILITY CURVES
9. VALIDATION OF THE MODELS FOR JOINTS WITH STEEL BOLTED CONNECTIONS
 - 9.1. Shear curves
 - 9.2. Load-introduction curves
 - 9.2.1. Check of the ultimate load
 - 9.2.2. Check of the deformability model
 - 9.2.3. Amendments of the formulae for bolted connections
10. IMPROVEMENT OF THE EC3 FORMULAE FOR THE ASSESSMENT OF THE DESIGN RESISTANCE OF COLUMN WEB PANELS.
 - 10.1. Resistance of the shear panel
 - 10.2. Resistance to the introduction of transverse loads
 - 10.3. Resistance of the whole panel
 - 10.4. Summary of the proposals.

1. INTRODUCTION

For some years, experimental and/or theoretical research works have been devoted to the actual behaviour of beam-to-column joints in steel buildings and more especially to semi-rigid joints. This is the result of a search for simple and cheap connections with a view to a reduction of the labour cost, which grew much faster than the material cost. Thus for the sake of economy, bolted joints without any stiffener became a common practice. Unfortunately such joints have a non linear behaviour : when subject to an applied bending moment M , the axes of the connected members do not rotate a same angle, so that there is a relative rotation θ , which is not proportional to the applied bending moment M .

Both strength and stability of steel frames are affected by the semi-rigid behaviour of the joints [1]. Though several computer programmes [2], which allow for material and geometrical non linearities - including semi-rigid-joints are available, there is an urgent need of knowledge for the $M-\theta$ characteristics of the joints.

The first part of the present report is aimed at summarizing the studies performed [3] since two years at the University of Liège for the prediction of the shear and of the load-introduction behaviour of column web panels in strong axis beam-to-column welded joints. The models developed are then validated for beam-to-column joints with bolted connections.

The accuracy of the EC3 formulae (annex J of chapter 6) for the assessment of the design resistance of a column web panel subject to shear forces and to transverse compression and tension forces is discussed in the second part of the report and proposals for their improvement are suggested.

2. JOINT DEFORMABILITY COMPONENTS

The two following sources of deformability of a strong axis beam-to-column joint have to be clearly defined :

- a) the deformation of the connection associated to the deformation of the connection elements (end plate, angles, bolts,...), to that of the column flange and of the column web in the tension and compression zones (respectively a lengthening and a shortening) and to the slips ;
- b) the shear deformation of the column web associated mostly to the common presence of forces, equal and opposite, in tension and compression, carried over by the beam(s) and acting on the column web at the level of the joint.

The case of the end plate connection of figure 1 may be chosen to illustrate this. The rotation ϕ of the connection is mathematically defined by the difference of the two rotations θ_b and θ_c and includes the deformation of the end plate, of the bolts and of the column flange, the lengthening of the zone BC and the shortening of the zone AD of the web.

The rotation γ of the column web under shear is defined by the difference of the rotations θ_c and θ_f where θ_f represents the flexural rotation of the column.

It is important to know that the shear in the column web is the result of the combined action of the equal but opposite forces F_b in the beam flanges, which are statically equivalent to the beam moment, and of the shear forces in the column at the level of the beam flanges.

The difference between the loading of the connection and that of the column web in a same joint leads to take account separately of both deformability sources.

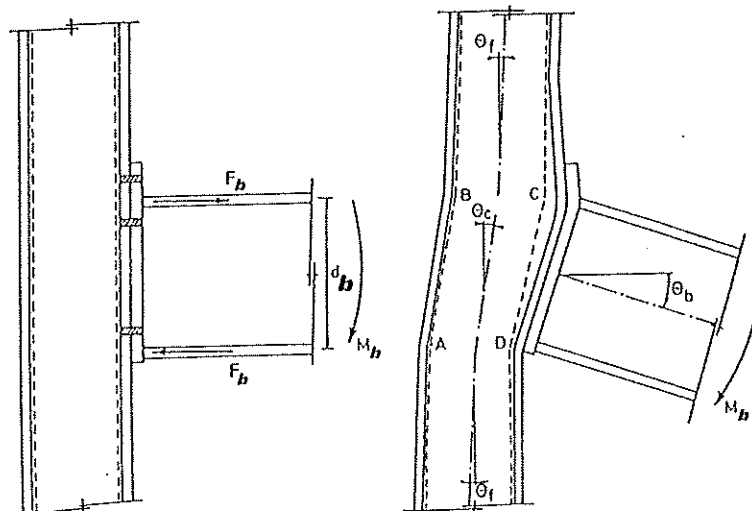


Figure 1 - Deformation of a strong axis joint with an end plate connection

The load-introduction deformability of a column web panel is defined as the component of the connection deformability relative to the local deformation of the column web in the tension and compression zones of the joint (respectively a lengthening and a shortening).

The deformability of a column web panel in the particular case of a joint between one beam and one column is schematized on figure 2.

The deformation of the ABCD column web panel (figure 2.a) has to be divided into two parts :

- the transverse effect of the forces F_b in the beam flanges (statically equivalent to the beam moment M_b) results in a relative rotation ϕ between the beam and the column axes ; this rotation concentrates mainly along edge CD (figure 2.b) and provides a first deformability curve $M_b - \phi$;
- the shear effect due to the shear force V_n results in a relative rotation γ between the beam and the column axes (figure 2.c); this rotation occurs mainly along edges BC and AD and makes it possible to establish a second deformability curve $V_n - \gamma$.

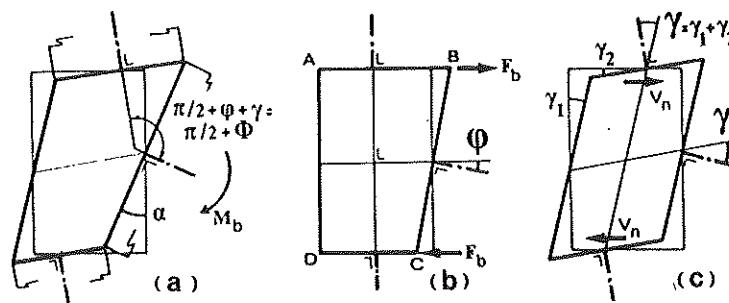


Figure 2 - Global deformation of column web panel (a) decomposed into the load-introduction effect (b) and the shear effect (c).

3. NUMERICAL INVESTIGATIONS

An important parametric study has been realized recently at the Polytechnic Federal School of Lausanne and at the University of Liège. All the results and all the conclusions of this study may be found in [3].

This study is based on numerical simulations with the non linear FE-program FINELG [4] of the loading up to failure of welded beam-to-column joints. Material and geometrical non-linear effects are taken into account, although the latter is far less important than the former. The specimens

of the chosen joints are analysed in three dimensions by using "shell" finite elements to model the webs and flanges of the profiles and "beam" finite elements to model the stiffeners. The adopted finite element meshes are shown on figure 3, respectively for a "T" joint (one column, one beam) and a "cross" joint (one column, two beams).

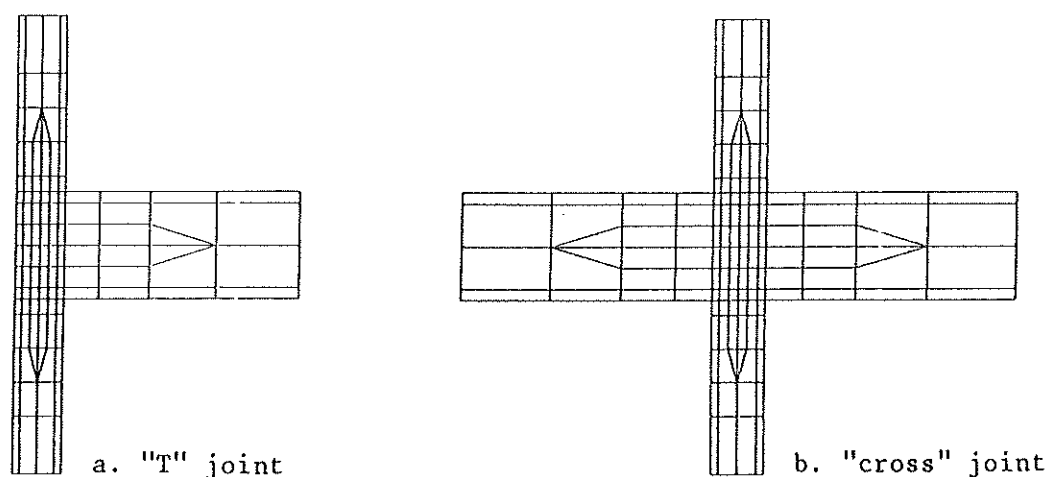


Figure 3 - Joint finite elements meshes

The numerical simulations allow to study the propagation of the plasticity in the profiles and to observe the exact failure modes.

Steel is supposed to follow a piecewise linear law shown on Fig. 4. The 2D elastoplastic state of stress is dealt with by using the incremental flow theory and the von MISES yield criterion. Parabolic patterns of rolling residual normal stresses in flanges and webs are taken according to the ECCS recommendations [5]. Welding imperfections are not considered. Complete data may be found in [3].

The good agreement between the numerical simulations and results of experimental tests on joints is shown in [6].

The moment-rotation curves characterizing the shear deformability and the load-introduction deformability of the column web panel have been reported for every simulation.

The following parameters have been taken into account in the parametric study of the joints :

- a) the type of the beam(s) ;
- b) the type of the column ;
- c) the loading of the joint ;
- d) the initial out-of-flatness of the column web ;

e) the presence or not of transverse stiffeners on the column web.

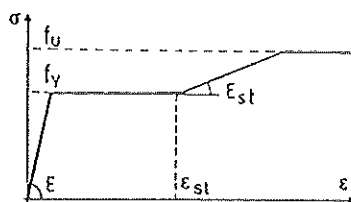


Figure 4 - Stress-strain curve (mild steel)

4. STUDY OF THE LOAD-INTRODUCTION EFFECT

4.1. Conclusions of the numerical simulations

Only the main conclusions of the numerical simulations relative to the load-introduction behaviour of the unstiffened column web panels are presented here.

a) The $M_b - \phi$ curve for a given joint depends on the actual loading of the joint.

Let us suppose that the two unstiffened welded joints of figure 5 are subjected to different types of loading (figure 6) and let us report, for each joint, the characteristic $M_b - \phi$ curve in a common diagram (figures 7 and 8). A similarly exists only in the elastic range of the web panel behaviour.

The difference between the $M_b - \phi$ curves in the non linear range of the panel behaviour can not be neglected.

In reality an unstiffened column web panel experiences to three types of stresses in its most stressed zone (figure 9) :

- the shear stresses τ ;
- the normal stresses σ_n resulting from the compression force and the bending moment in the column ;
- the normal stresses σ_1 resulting from the introduction of beam loads in the column web.

The load-introduction behaviour of a web panel will obviously be affected, except in the elastic range, by the relative importance of each of these stresses according to the type of joint loading.

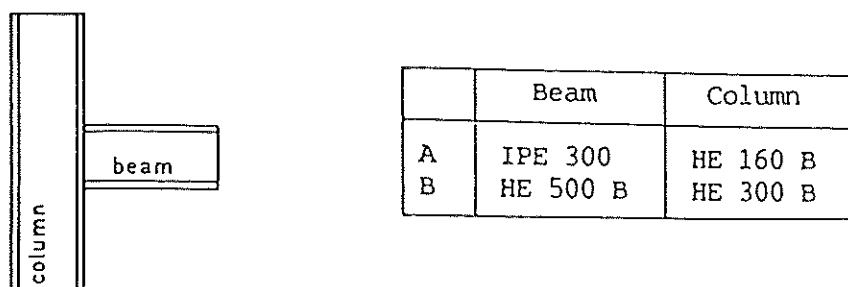
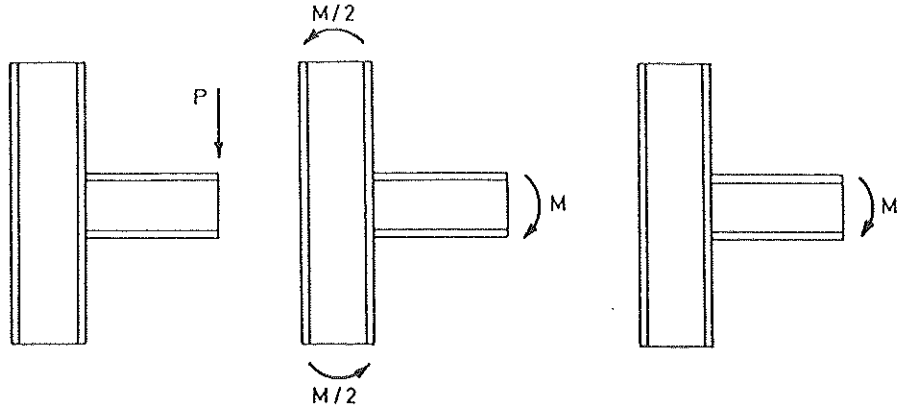


Figure 5 - Definition of two welded joints ("T" arrangement)



Simple bending (FS) Pure bending (FP) Pure bending in the beam (MP)
 Figure 6 - Different types of loading for "T" joints.

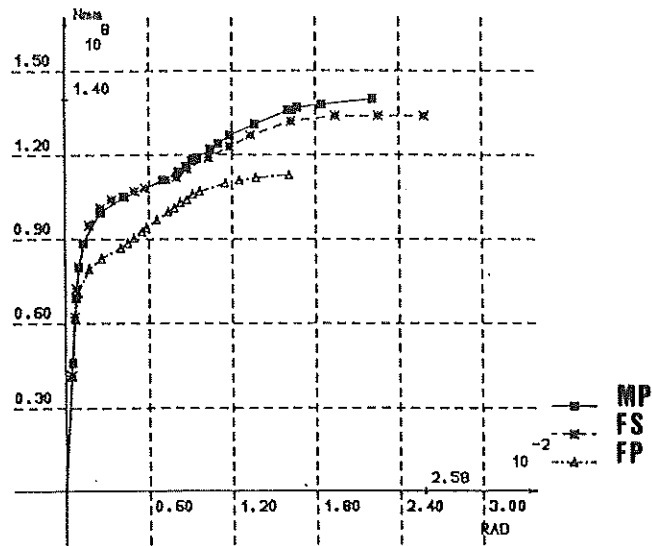


Figure 7 - Characteristic $M_b - \phi$ curves (joint A - 3 load cases).

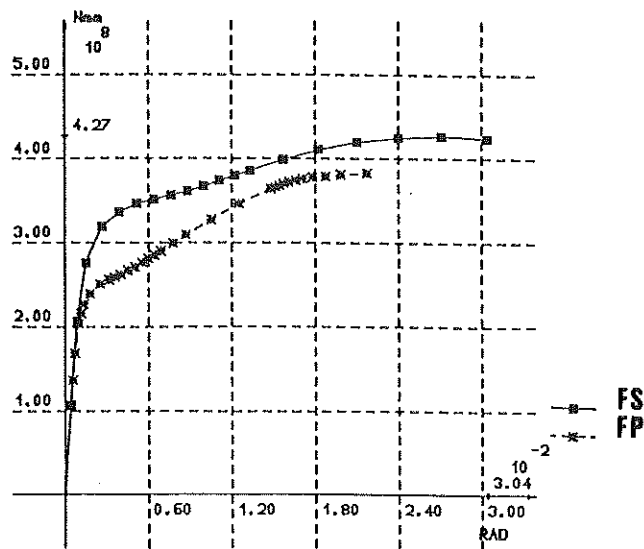


Figure 8 - Characteristic $M_b - \phi$ curves (joint B - 2 load cases)

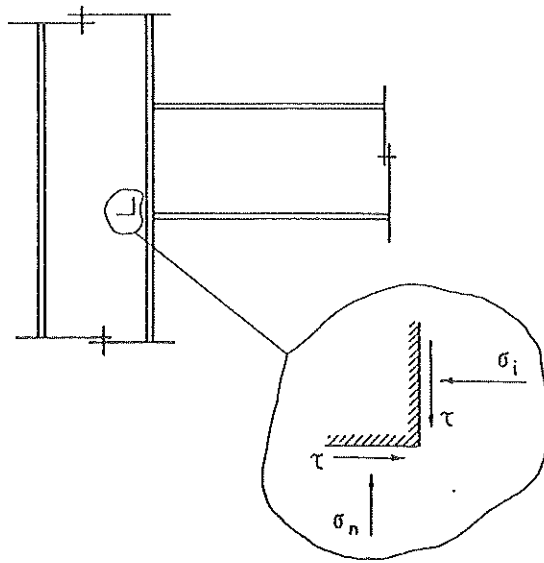


Figure 9 - Different types of stresses in a web panel

- b) It is not allowed to define the plastic capacity of a web subject to transverse loads as this may be done for sheared column web panels : the propagation of the plasticity in the column web transversally loaded does not end indeed in the apparition of a horizontal yield plateau when the strain-hardening is omitted in the numerical simulation (as in figure 10 for sheared webs), but rather in the development, till the attainment of the ultimate load, of a zone characterized by a progressive increase of the resistance and the deformability of the web (figure 11.a).

It will be consequently referred in this report to the so-called pseudo-plastic moment, $M_{b\text{pppl}}$; this beam moment corresponds to a limit state of the column web transversally loaded which is defined in figure 11.a.

This characteristic load level may obviously be similarly defined for the $M_b - \phi$ curves relative to "T" joints (see figure 11.b).

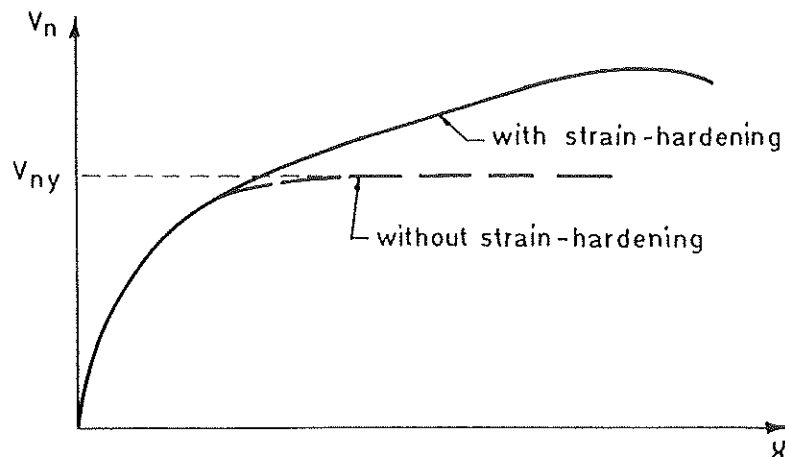
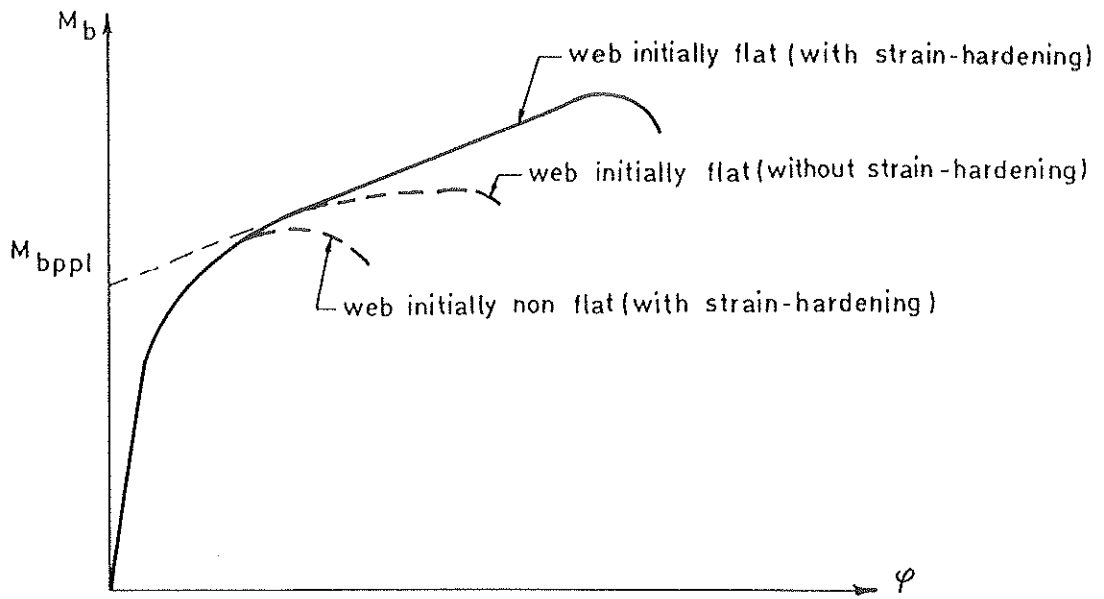
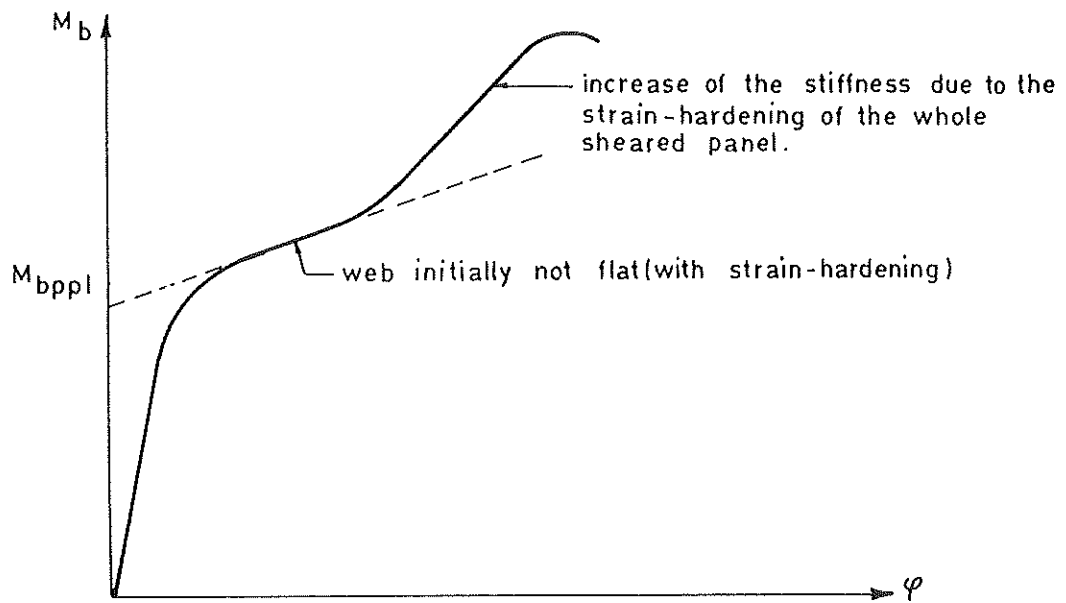


Figure 10-Definition of the plastic capacity for a sheared column web panel



a) "cross" nodes



b) "T" nodes

Figure 11 - Definition of the pseudo-plastic capacity of a web subject to transverse loads.

- c) The propagation of the plasticity in a web subject to transverse loads is not affected by the presence of σ_n stresses in the web insofar as their maximum value does not exceed a relatively high limit which should have to be explicitly determined.

This conclusion seems to confirm the result of an experimental study carried out in the Netherlands [7] and which tends to show that the influence, on the "plastic capacity" of the web, of σ_n stresses not exceeding 50 % of the column web yield stress is not significant.

ZOETEMEIJER [7] proposes, for larger values of σ_n ($\sigma_n > 0.5f_y$), to reduce the "plastic capacity" by means of a factor e given by :

$$e = 1.25 - 0.5 \frac{|\sigma_n|}{f_y} \quad (1)$$

KATO considers for his own [8] that the attainment of stresses σ_n greater than $0.5 f_y$ is not of practical interest because of the relative low values of the loads transmitted to the column in order to provide against instability.

- d) The amplitude of the column web out-of-flatness influences only the shape of the $M_b - \phi$ curves of joints whose collapse is linked up to the buckling of the web; this initial out-of-flatness affects the value of the web ultimate buckling load in a significant way but modified very slightly the deformability of the web as far as the collapse load is not reached (figure 11.a).

- e) The comparison (figure 12) of $M_b - \phi$ curves relative to a "T" joint (figure 3.a) and to the corresponding (same column and same type of beam) cruciform joint (figure 3.b) shows clearly the similarity of both web behaviours in the elastic range (it is not possible to compare the curves in the non elastic range on account of the different stresses interacting in the column webs).

This leads to the conclusion that the introduction of transverse loads in a column web constitutes, as far as the stability of the web is not concerned with, a local phenomena limited to the vicinity of the column flanges.

The influence of the joint loading (both joints are subject to simple bending - see figures 6 and 38) on the shape of the $M-\phi$ curves - as discussed in (a) - is seen to be very significant in this case.

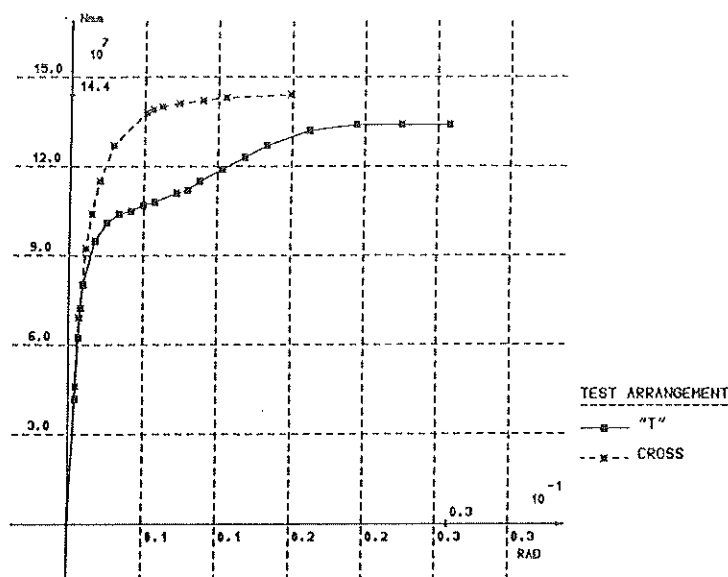


Figure 12 - Comparison between "T" and "cross" joint behaviour ($M_b - \phi$ curves)

4.2. Theoretical developments and model for prediction.

The theoretical developments carried out in Liège are presented in details in [3]; they have led to a piecewise multi-linear modelling of the $M_b - \phi$ deformability curves. Figure 13 shows its main characteristics.

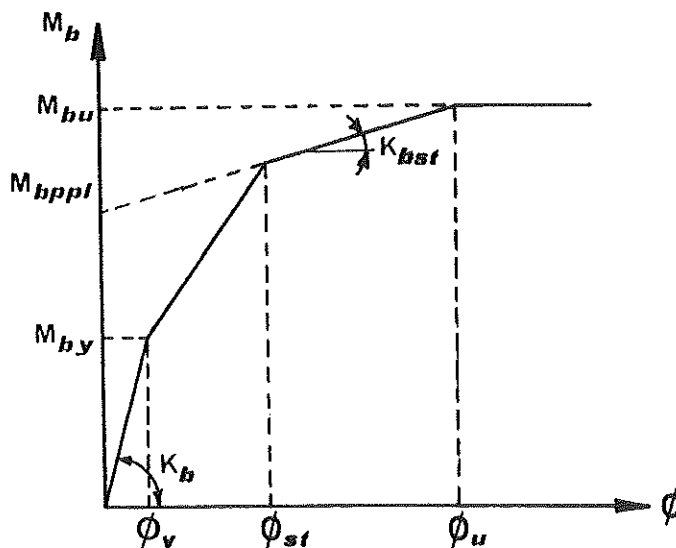


Figure 13 - Characteristics of the multi-linear model for prediction of $M_b - \phi$ curves

The initial stiffness K_b results from the study of an elastic beam (column flange) lying on an elastic foundation (column web) as shown in figure 14. Because of the stiffening of the column flange by the beam web (welded joints), the elastic beam in the model is assumed to be infinitely stiff in the zone located between the beam flanges (figure 15).

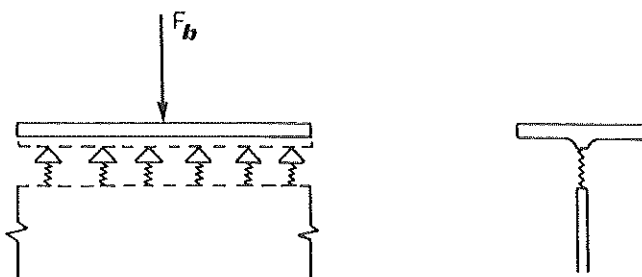


Figure 14 - Definition of beam and foundation

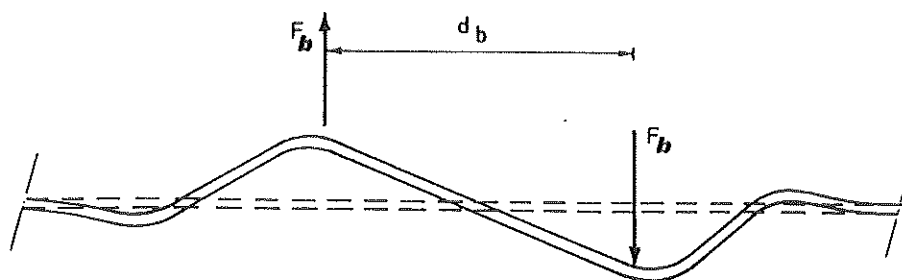


Figure 15 - Deformed shape of the beam

The stiffness K_b is given [3] by :

$$K_b = k \frac{d_b^2}{2} \left[\frac{1}{\lambda} + \frac{2}{\lambda^2 d_b} \left(1 + \frac{1}{\lambda d_b} \right) + \frac{d_b}{6} \right] \quad (2)$$

where : d_b = distance between the center of the beam flanges ;
 $k = E s_c / h_w$ (column geometrical characteristics are defined on figure 16) ;

$$\lambda = \sqrt[4]{k/4EI_f} \quad (I_f \text{ represents the inertia of the "elastic beam" defined on figure 16}).$$

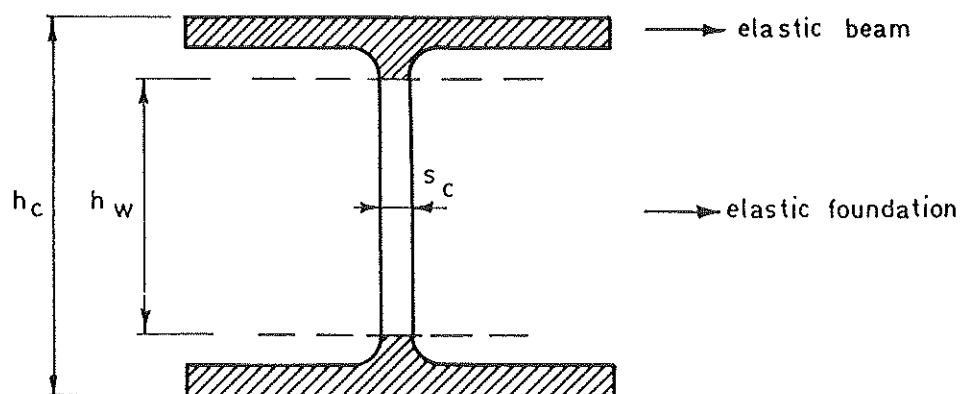


Figure 16 - Geometrical characteristics of the "beam" and of the "foundation".

The maximum elastic moment of the web, M_{by} , is a load level corresponding to the first yielding of the web under the combination of τ and σ_{iy} stresses (figure 9). τ stresses resulting from the action of the shear force V_n in the web panel will be defined in section 5.2.

The maximum σ_{iy} stresses in the web are given [3] by :

$$\sigma_{iy} = \frac{M_b}{d_b s_c} \frac{1}{\left[\frac{1}{\lambda} + \frac{2}{d_b \lambda^2} \left(1 + \frac{1}{d_b \lambda} \right) + \frac{d_b}{6} \right]} \quad (3)$$

where M_b = bending moment at the end of the beam (in the connection cross-section).

The introduction of σ_{iy} and τ_y stresses in the von MISES criterion

$$\sigma_c = \sqrt{\sigma_{iy}^c{}^2 + 3\tau_y^c{}^2} = f_y \quad (4)$$

will allow to determine σ_{iy}^c and τ_y^c (the particular values of σ_{iy} and τ_y which induce the first yielding of the web) and to deduce from them the value of the maximum elastic moment, M_{by} .

The relative rotation ϕ_{st} corresponds to the apparition of strain-hardening in the web, it is given by :

$$\phi_{st} = \frac{\epsilon_{st} h_w}{d_b} \quad (5)$$

ϵ_{st} is defined on figure 4.

The pseudo-plastic moment of the web (see section 4.1.) is approximated by the following formula (figure 17) :

$$M_{b ppl} = s_c \cdot l_p \cdot d_b \cdot \sigma_{iy}^c \quad (6)$$

where s_c = column web thickness ;

d_b = distance between the center of the beam flanges ;

$l_p = t_b + 2\sqrt{2} a + 5(t_c + r_c)$

with t_b = beam flange thickness ;

a = weld throat thickness ;

t_c = column flange thickness ;

r_c = radius of fillet of the column ;

σ_{iy}^c is deduced from (4).

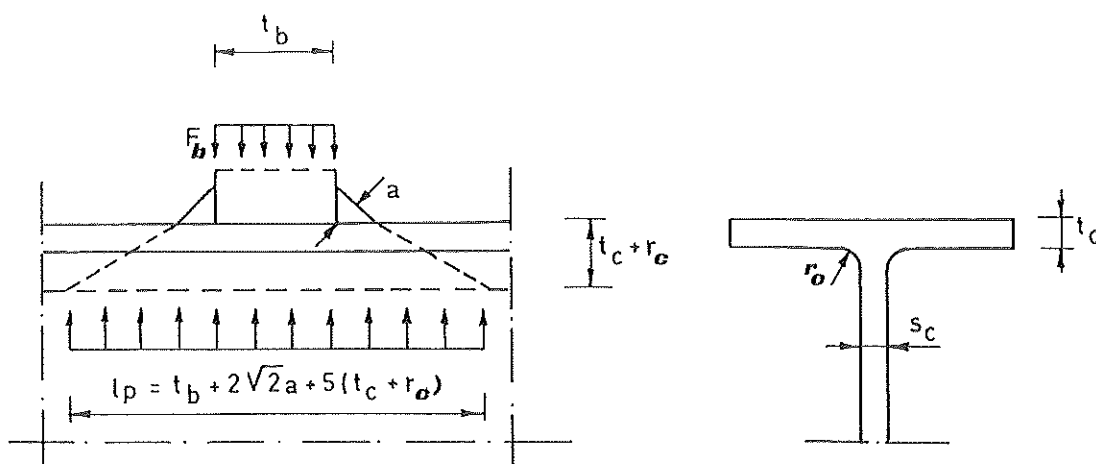


Figure 17 - Definition of l_p and s_c

The strain-hardening stiffness, K_{st} , is evaluated in a very simple way by means of the following expression :

$$K_{bst} = K_b \frac{E_{st}}{E}$$

The steel mechanical properties E and E_{st} are defined on figure 4.

Formulae for the assessment of the ultimate bending moment, M_{bu} , carried over from the beam to the column will be presented in chapter 6 of this report. This ultimate moment is linked either to the excessive shear or to the load-introduction resistance of the web.

5. STUDY OF THE SHEAR EFFECT

5.1. Conclusions of the numerical simulations

Only the main conclusions of the numerical simulations relative to the behaviour of the sheared column web panels are presented here.

- a) The shear stresses in the column web panels may be considered as uniformly distributed ; this is due to the action of the column flanges.
- b) The actual value of the shear force V_n may be obtained from the equilibrium equations of the web panel [3].

It is given by the following formula (figure 18) :

$$V_n = \frac{M_{b1} + M_{b2}}{d_b} - \frac{Q_{c1} + Q_{c2}}{2} \quad (7)$$

Some other researchers refer to another formula :

$$V_n = \frac{M_{b1} + M_{b2}}{d_b} \quad (8)$$

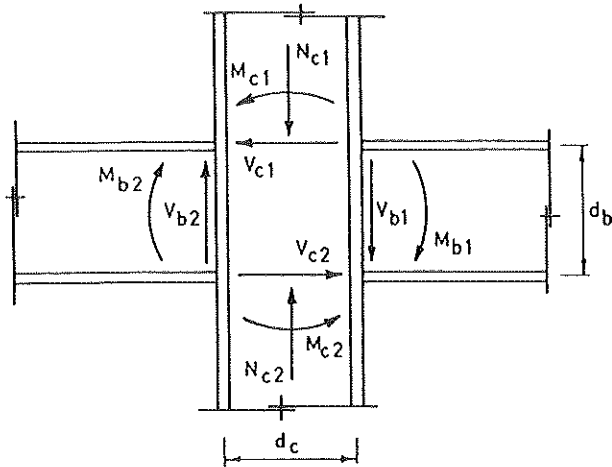
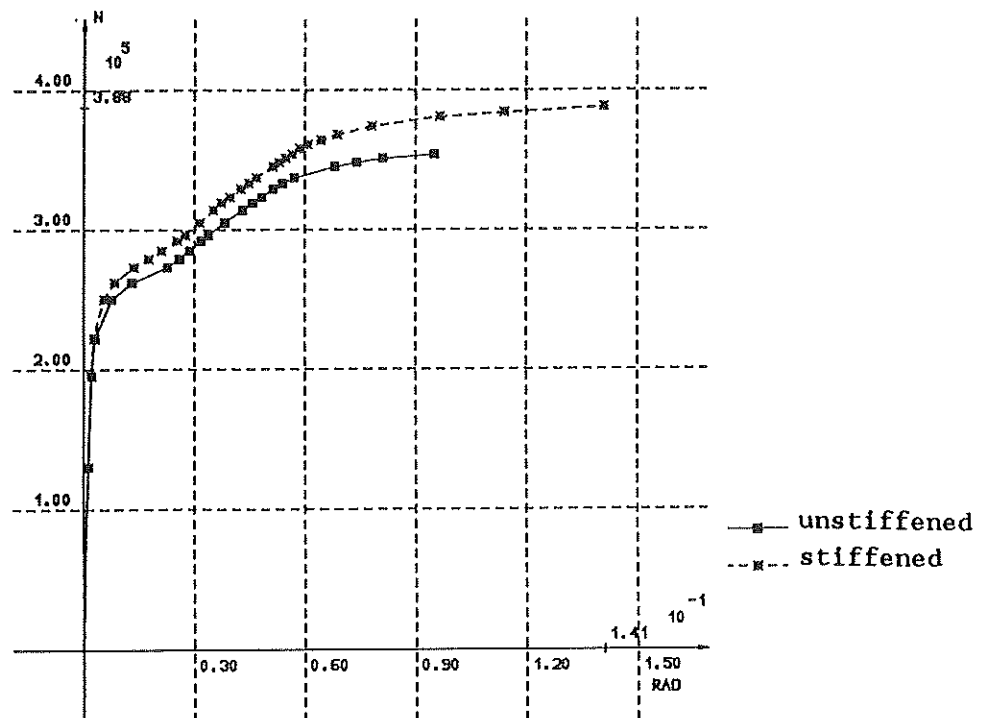


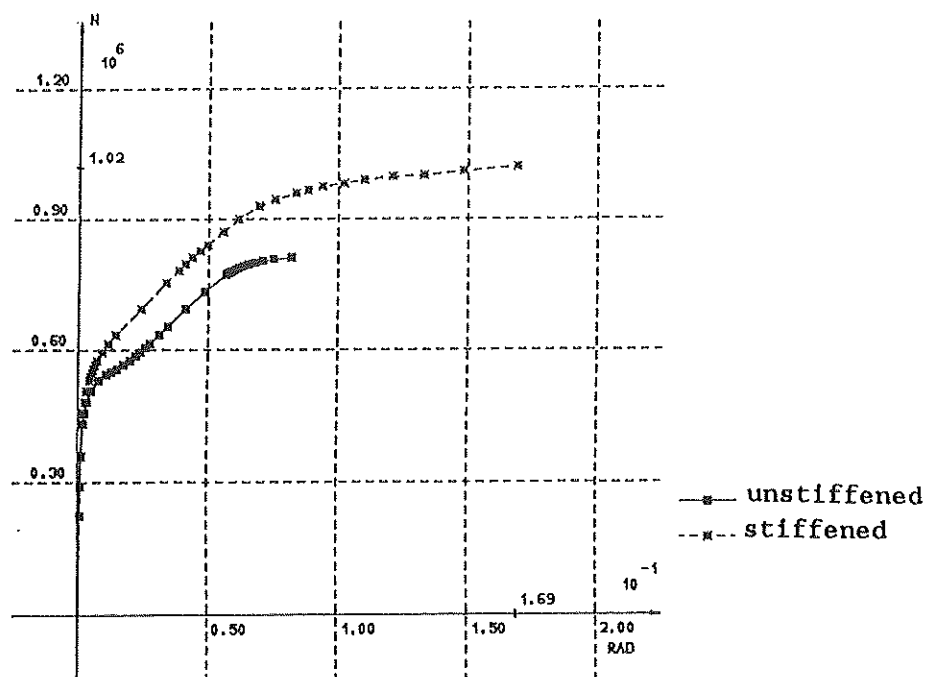
Figure 18 - Loading of an interior joint

The validity of the proposed formula (7) has been clearly demonstrated.

- c) The presence or not of transverse stiffeners welded on the column web at the level of the beam flanges influences the resistance as well as the collapse mode of the sheared webs in a quite significant manner; it has to be accounted for (see figure 19). The influence on both initial and strain-hardening stiffnesses may be neglected.



(a) Joint A (FP - see figure 21)

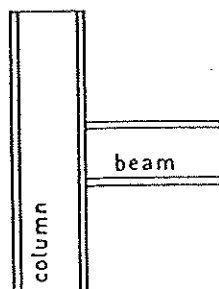


(b) Joint B (FP - see figure 21)

Figure 19 - Influence of the web transverse stiffening on the $V_n - \gamma$ curves

d) The $V_n - \gamma$ curve for a given joint depends on the actual loading of the joint.

Let us assume that the two unstiffened welded nodes of figure 20 are subject to different types of loading (figure 21) and let us report, for each node, the characteristic $V_n - \gamma$ curve in a common diagram (figures 22 and 23).



	Beam	Column
A	IPE 300	HE 160 B
B	HE 500 B	HE 300 B

Figure 20 - Definition of two welded joints ("T" arrangement)

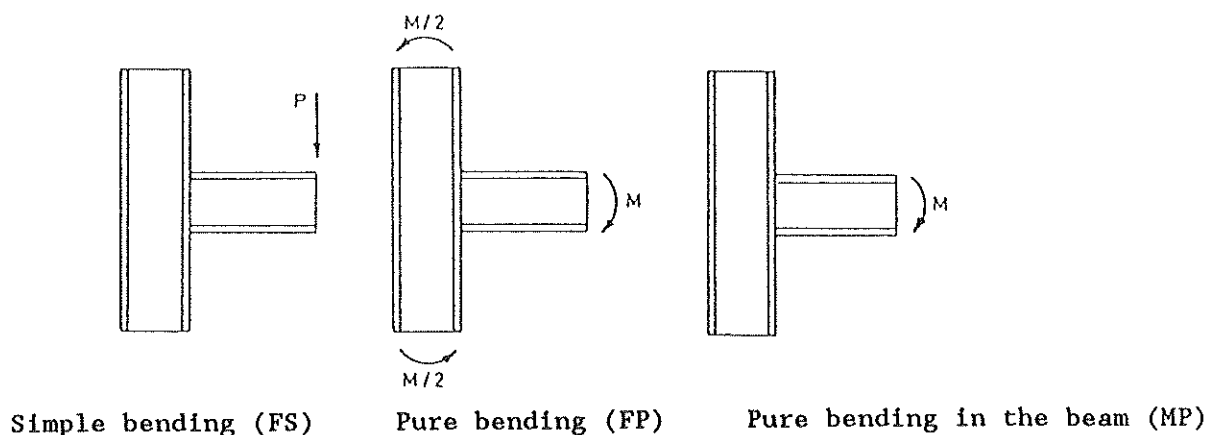


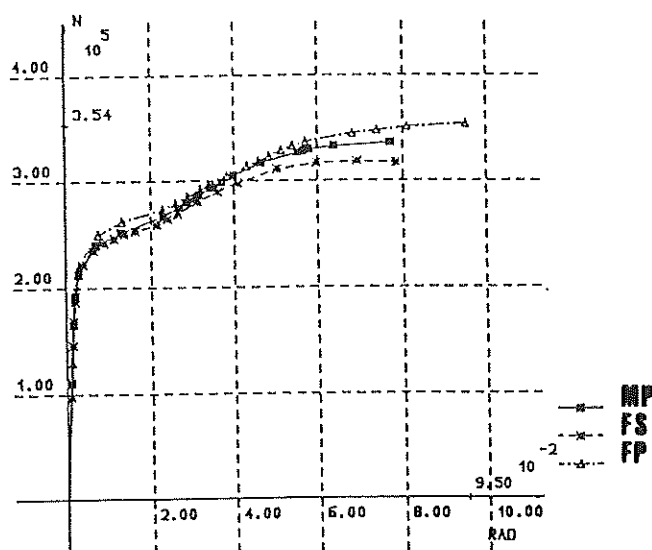
Figure 21 - Different types of loading

The shear force V_n takes account, by means of formula (7), of the loading of the joints ; in consequence one could believe that the $V_n - \gamma$ curves are identical for a given node. Actually only a similarity exists in the elastic range of the web panel behaviour and this demonstrates the validity of the proposed shear force definition (formula 7).

The differences between the $V_n - \gamma$ curves in the non-elastic range of the web panel behaviour are not negligible.

The existing methods for the prediction of the shear deformability of web panels - which have been detailed and compared to results of numerical simulations in [3] - do not account for the influence of the actual joint loading

Figures 22 and 23 show that this is questionable and has led to the elaboration of a new approach.

Figure 22 - Characteristic $V_n - \gamma$ curves ("T" joint A).

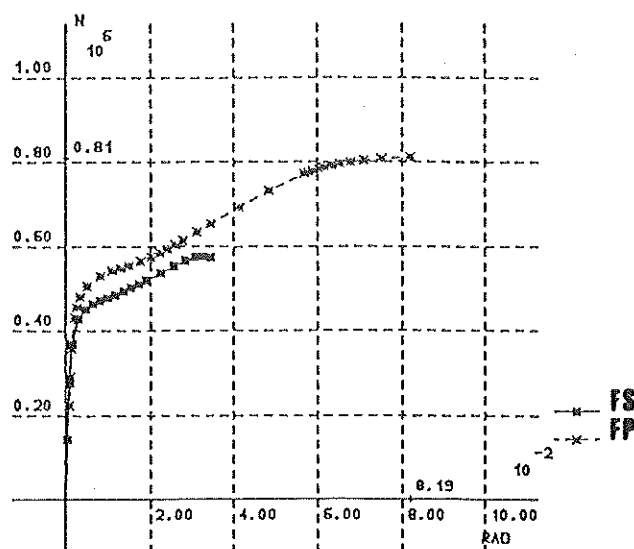


Figure 23 - Characteristic $V_n - \gamma$ curves ("T" joint B).

5.2. Theoretical developments and model for prediction - unstiffened column web panels

The theoretical developments in this section are related to the study of the unstiffened column web panels. It will be referred to section 5.3. for stiffened columns.

Let us consider a small column web element subject to shear stresses τ (figure 24.a) and whose material characteristic is elastic-perfectly plastic with strain-hardening (fig. 25.a). The shear deformability γ of this element (figure 24.b) versus the shear stress τ may be deduced.

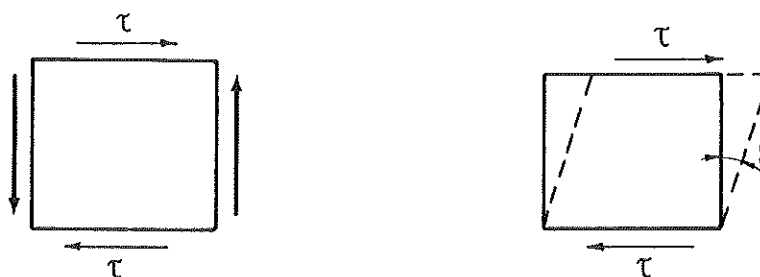


Figure 24 - Shear in a small web element.

The shear stresses being uniformly distributed in the web panel, a first approximation (pure shear) of the searched $V_n - \gamma$ curve may be easily obtained by multiplying the shear stress τ by the column web area (figure 25.b).

The theory of plasticity may be used in connection with the von MISES yield criterion to modify the characteristic values V_{ny} (γ_y), V_{nu} , γ_{st} and γ_u (figure 25.b) with a view to account for the actual node loading. How to proceed is explained in the following.

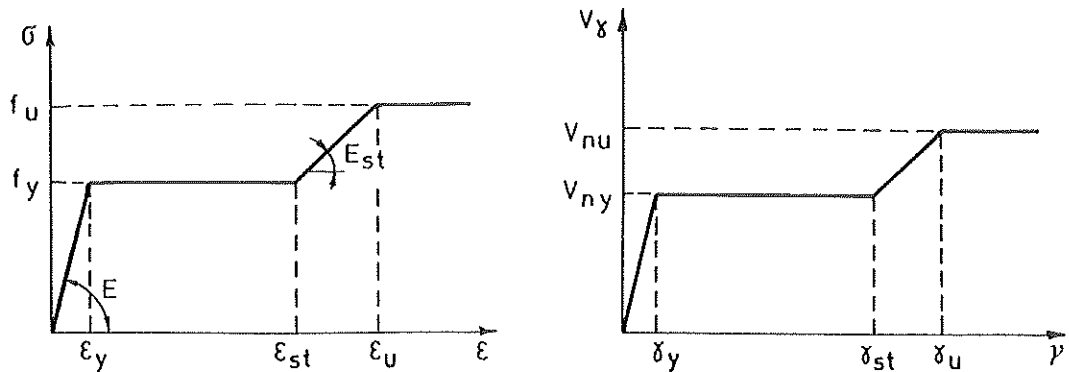


Figure 25 - Characteristic $\sigma - \epsilon$ and $V_n - \gamma$ curves (first approximation)

In its most stressed zone (figure 9) an unstiffened web panel is subject to three types of stresses :

- the shear stresses τ ;
- the normal stresses σ_n resulting from the compression force and the bending moment in the column ;
- the normal stresses σ_i resulting from the introduction of beam loads into the column web.

The load introduction constitutes only a local phenomena (see section 4.1.) which has no direct influence on the global behaviour of the web panel. The web panel deformability predicting model based on the modified value of V_{ny} (γ_y), V_{nu} , γ_{st} and γ_u (interaction between τ and σ_n stresses) is applied for instance in figure 26 to the unstiffened "T" node B submitted to pure bending (figures 20 and 21).

It may be seen that :

- the agreement between the values of the initial stiffness and of the strain-hardening stiffness given by the mathematical model and the numerical simulation is very good ;
- the mathematically predicted plastic load is slightly lower than the corresponding load obtained by means of the numerical simulation; the small difference which represents the bending resistance of the column flange may be neglected in the case of joints with unstiffened columns.

See JASPART Ph.D. Thesis for exact definition of σ_n

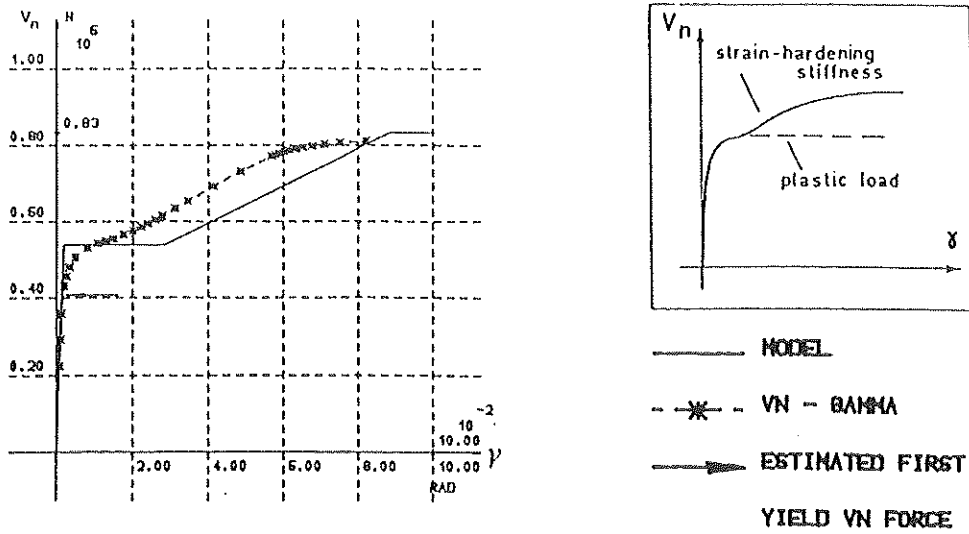


Figure 26- Comparison between the numerical simulation of the unstiffened node B subject to pure bending and the model modified to account for the node loading (second approximation).

However, the mathematical model differs from the result of the numerical simulation for what regards the length of the yield plateau and the collapse load.

It must be referred to the interaction in the web panel between the shear and load-introduction effects to explain these differences :

- the strain-hardening first appears locally in the most stressed zone of the column web (figure 9) where the three above-mentioned types of stresses interact and will depend on the importance of the σ_1 stresses relatively to the two other types of stresses; the length of the yield plateau has been consequently empirically reduced ;
- the collapse load of the web panel is linked up either to the excessive shear or to the load-introduction resistance of the web (web crippling for instance), what depends on the relative importance of σ_1 stresses too; formulae for the assessment of the resistance and the stability of column webs subject to transverse loads have then been developed and will be presented in chapter 6.

It is also easy to show the necessity of taking into account the interaction between shear and load-introduction by introducing the σ_1 and τ stresses into the von MISES yield criterion in order to determine the shear load corresponding to the beginning of yielding in the column web.

The agreement between the calculated elastic shear force and the result of the numerical simulation for the joint B (FP) is seen to be very good (figure 26). This elastic shear load is obviously associated to a bending moment in the beam equal to M_{by} (see section 4.2.).

The general shape of the $V_n - \gamma$ curve is therefore adapted accordingly as a multi-linear model shown in figure 27.

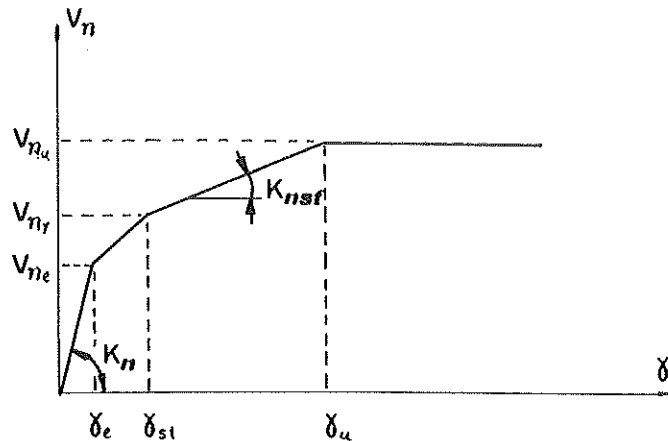


Figure 27 - Definitive general shape of the shear model for unstiffened column web panels.

The initial stiffness is given by :

$$K_n = G A_{sh} \tag{9}$$

with $G = E/2(1 + \nu)$

A_{sh} = sheared web area of the column defined in figure 28.

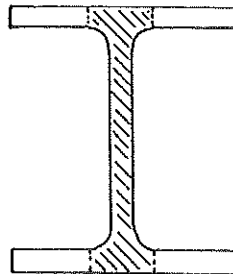


Figure 28 - Definition of the actual sheared web area

V_{ne} is the web shear resistance related to the apparition of yielding in the most stressed region of the web under the combination of σ_i and τ stresses (see figure 9 and section 4.2). This elastic shear force is associated by formula (7) to the elastic bending moment M_{by} defined in section 4.2.

V_{ny} , which has been defined in the previous section as the plastic resistance of the column sheared web, is evaluated in the following way :

$$V_{ny} = A_{sh} \cdot \tau_y^c \quad (10)$$

As explained in section 5.1., the introduction of the expression for σ_n and τ stresses in the von MISES criterion :

$$\sigma_c = \sqrt{\sigma_{ny}^2 + 3\tau_y^2} = f_y \quad (11)$$

allows to determine the value $\hat{\gamma}_y$ of the shear stress which induces yielding in the whole panel (shear stresses are uniformly distributed) and has to be introduced in (10).

The shear rotation γ_{st} which corresponds to the first onset of strain-hardening in the web has the following expression [3] :

$$\gamma_{st} = 0.5 [\gamma_y + \sqrt{3} (\epsilon_{st} - \epsilon_y)] \quad (12)$$

with : $\gamma_y = V_{ny}/G \cdot A_{sh}$
 $\epsilon_y =$ elastic steel strain = f_y/E (figure 4) ;
 $\epsilon_{st} =$ strain-hardening steel strain (figure 4).

The strain-hardening stiffness is expressed as [3]:

$$K_{nst} = G_{st} A_{sh} \quad (13)$$

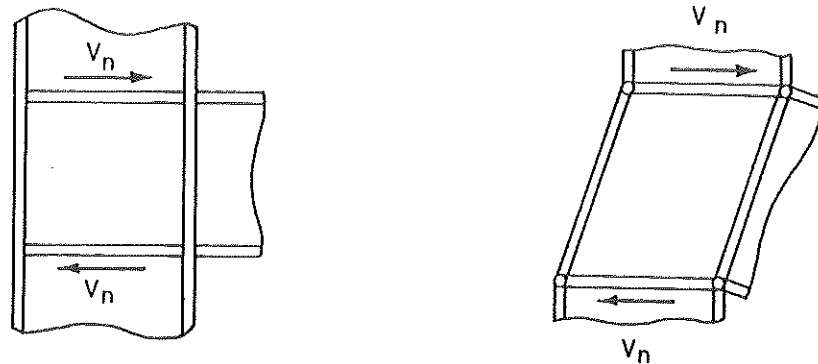
with $G_{st} = E_{st}/3$ (figure 4).

Formulae for the assessment of the ultimate strength of the web panel will be proposed in chapter 6.

5.3. Theoretical developments and model for prediction - stiffened column web panels.

Because of the presence of transverse stiffeners welded on the column web at the level of the beam flanges, no allowance for an interaction between σ_i and τ stresses may be considered from a theoretical point of view.

It may however be noted that the use of the multi-linear model presented in the previous section leads to an accurate prediction of the $V_n - \gamma$ curves for stiffened web panels providing the shear resistance of the frame constituted by the stiffeners and the column flanges is added (figure 29).



a) elastic resistance

b) frame plastic mechanism

Figure 29 - Illustration of the frame effect.

The shape of the piecewise multi-linear model for prediction is shown on figure 30.

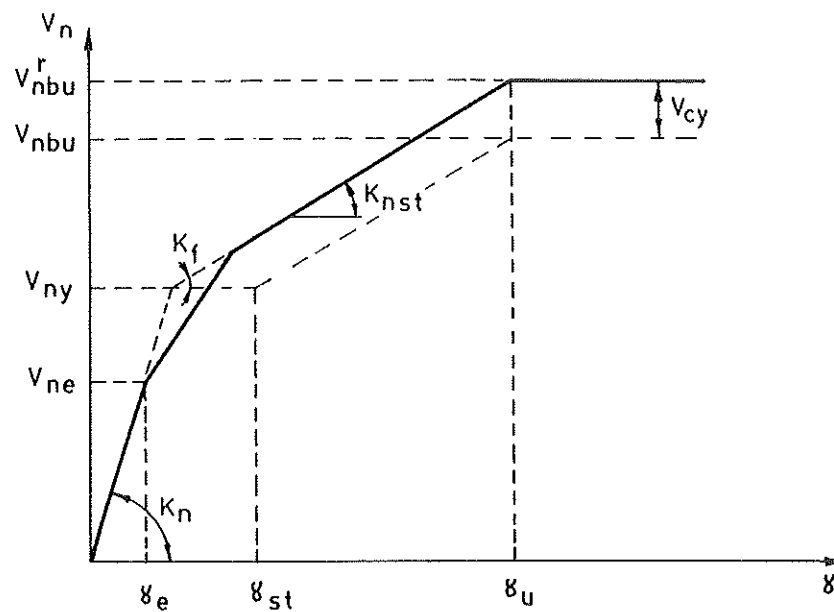


Figure 30 - Multi-linear model for prediction of the shear behaviour of stiffened column web panels.

The expressions for the assessment of K_n , K_{nst} , V_{ne} , V_{ny} and γ_{st} are quite similar to that described in the previous section.

In its range of elastic behaviour (which starts as soon as the plastic capacity of the web is reached), the frame is able to support a shear force V_f , the rate of increase K_f (figure 30) of which is given by :

$$K_f = \frac{24EI_f}{d_b^2} \quad (14)$$

where I_f represents the inertia of the column flanges and d_b the distance between the centers of the beam flanges.

The plastic capacity of the frame, V_{cy} , is reached when plastic hinges have formed in the column flanges at the level of the stiffeners (figure 29.b). The value of V_{cy} is the following :

$$V_{cy} = \frac{4M_{pf}}{d_b} \quad (15)$$

where M_{pf} represents the plastic moment of the column flanges.

The horizontal stiffeners are welded to the web and to the flanges of the column. They may be considered as infinitely rigid during the whole joint loading if they are correctly designed; this explains why their flexural deformation has not been accounted in the expression of K_F - which corresponds to the elastic flexural deformation of the column flanges rigidly connected to the stiffeners - and why the plastic mechanism of figure 29.b is associated to the formation of plastic hinges in the column flanges.

The ultimate shear resistance of the stiffened web panel is obtained by adding the plastic capacity of the frame, V_{cy} , to the ultimate shear resistance V_{nbu} of a similar web panel without stiffeners. The way to evaluate V_{nbu} will be presented in chapter 6.

6. ASSESSMENT OF THE ULTIMATE STRENGTH FOR UNSTIFFENED WEB PANELS

The ultimate strength of a column web may be associated to one of the three following types of collapse :

- the shear collapse of the column web panel (V_{nbu} to which corresponds by formula (7) a moment M_{nbu} in the beam) ;
- the excessive yielding of the web under transverse loads (M_{buy}) ;
- the instability of the web under compression transverse loads (M_{bub}).

The ultimate moment in the beam corresponding to the collapse of the column web panel is equal to :

$$- M_{nbu} \quad \text{if} \quad \begin{matrix} M_{nbu} < M_{buy} \\ \text{and} \quad M_{nbu} < M_{bub} \end{matrix} \quad (16.a)$$

$$- M_{buy} \quad \text{if} \quad \begin{matrix} M_{buy} < M_{nbu} \\ \text{and} \quad M_{buy} < M_{bub} \end{matrix} \quad (16.b)$$

$$- M_{bub} \text{ if } M_{bub} < M_{buy} \text{ and } M_{bub} < M_{nbu} \quad (16.c)$$

6.1. Shear of the web panel.

The ultimate carrying capacity of a sheared web panel is given by :

$$V_{nbu} = \tau_u^c \cdot A_{sh} \quad (17)$$

where A_{sh} represents the column web area (figure 28).

The shear force V_n has been defined in section 5.1.(formula 7).

τ_u^c is the ultimate shear stress evaluated, as in formula (11), by means of the von MISES criterion allowing for the interaction between σ_n and τ stresses, but based this time on the attainment of the ultimate stress f_u in the column web (figure 4).

6.2. Excessive yielding of the web.

The ultimate resistance associated to the excessive yielding of a web subject to transverse loading is given by :

$$M_{buy} = \sigma_{iu}^c \cdot s_c \cdot l_p \cdot d_b \quad (18)$$

The expression is quite similar to that proposed for the assessment of the pseudo-plastic moment of the web (formula 6), except that σ_{iu}^c , the maximum permissible compression stress in the web, results, as in formula (4), from the consideration of the local interaction between σ_i and τ stresses by means of the von MISES criterion based, as for the shear resistance, on the attainment of the ultimate stress f_u in the web.

6.3. Web instability

The instability of the web under compression affects either the whole depth of the column (web buckling - figure 31.a) or the region located just under the beam flange (web crippling - figure 31.b).

The associated instability load is given by :

$$M_{bub} = M_{bb} \uparrow M_{bppl} \quad (19.a)$$

with :

$$M_{bb} = \sqrt{M_{by} M_{bcr}} \quad (19.b)$$

M_{bppl} is the pseudo-plastic moment of the web (formula 6).

M_{by} is the elastic resistance of the transversally loaded web which corresponds to the onset of yielding in the web; it results from the

study of a "beam on elastic foundation" model as presented in section 4.2. (only the interaction between σ_i and τ stresses must however be considered).

M_{bcr} is the elastic linear instability load of the web which is expressed as :

$$M_{bcr} = (h_c - 2.t_c) \cdot s_c \cdot d_b \cdot k \cdot \frac{\pi^2 \cdot E}{12 \cdot (1-\nu^2)} \cdot \left(\frac{s_c}{h_c - 2.t_c} \right)^2 \quad (20)$$

h_c is the total depth of the column. t_c and s_c are defined in figure 17. The values to give to the k coefficient as well as the physical explanation of formula (19) will be found in the following sub-sections.

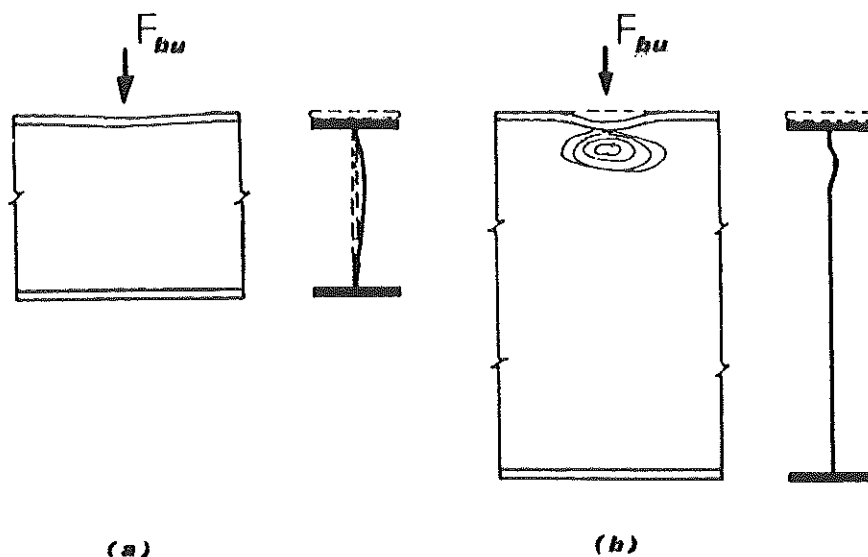


Figure 31 - Instability modes of column web: buckling (a) and crippling (b)

It is important to mention that the buckling strength M_{bb} , contrary to the pseudo-plastic moment $M_{b ppl}$, is strongly dependent on the initial out-of-flatness of the web (see for instance figure 11.a). The amplitude of this imperfection is generally unknown by the designers; their values have consequently been chosen on base of rolling tolerances [13] and those of the k coefficient which will be defined in the next sub-sections have been calibrated accordingly.

The initial out-of-flatnesses measured in laboratory seem however to be generally lower than those proposed in [13], what results in a too safe theoretical approximation of the actual buckling load. Numerical simulations have shown that the variation of the buckling load may reach 25 - 30 % according to the value of the out-of-flatness.

This has not to be forgotten when comparisons between theory and experiments are performed.

6.3.1. Interior HE columns.

For what concerns the interior columns (figure 3.b) with HE sections, it has been shown [3] that the pseudo-plastic moment of the column web, $M_{b_{pp1}}$, defined in section 4.2. (formula 6), constitutes a lower bound value for the web buckling load.

This may be easily explained by referring to figure 32.

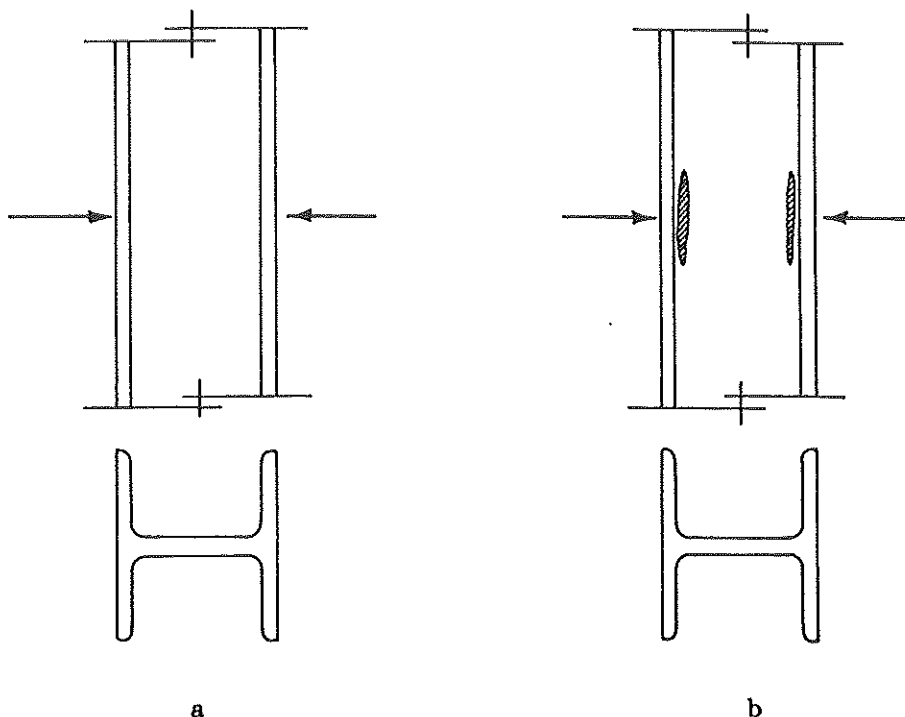


Figure 32 - Support conditions of the column web according to the load level

In the elastic range of the web behaviour (figure 32.a), the column web may be considered as rigidly connected to the column flanges: its instability load is consequently high. The increase of the loading and the resultant yielding of the web just under the column flanges (figure 32.b) lead to a modification of the support conditions for the web and consequently to a considerable decrease of the buckling load.

A collapse by instability in the elastic range behaviour has never been encountered, even for relatively slender column webs (HEA) and the numerical simulations have shown that the actual buckling load is always greater or equal to the pseudo-plastic moment $M_{b_{pp1}}$ which then constitutes a lower bound value for the instability load.

The buckling strength M_{b_b} given by formula (19.b) is consequently based on the assumption that the web is pinned on the column flanges ; it has

to be compared to $M_{b\text{pp1}}$ in order to determine the actual buckling load of the web, M_{bub} :

$$M_{\text{bub}} = M_{b\text{pp1}} \quad \text{if } M_{b\text{pp1}} > M_{\text{bb}} \quad (21.a)$$

$$M_{\text{bb}} \quad \text{if } M_{b\text{pp1}} < M_{\text{bb}} \quad (21.b)$$

The coefficient k which accounts for the type of loading - cross nodes symmetrically loaded - and for the web support conditions - hinges - may be taken equal to 1.0.

6.3.2. Exterior HE columns.

The fact that transverse loads are only applied to one side of the column web increases significantly the buckling strength M_{bb} of the web, whereas the pseudo-plastic moment $M_{b\text{pp1}}$ is independent of the node arrangement (cross or "T"). The k coefficient in formula (20) will consequently be chosen equal to 2.0 for "T" nodes.

The resulting formula (19) for the assessment of the web instability load, which has been discussed in the previous sub-section, may be applied in the case of exterior columns with HE sections.

6.3.3. Extension to IPE columns.

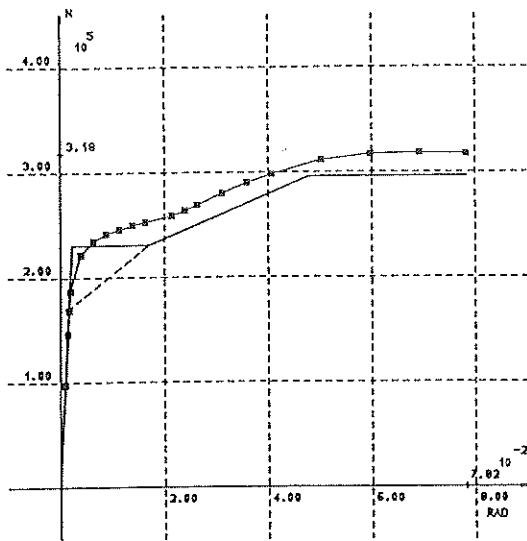
Profiles with IPE sections being usually used as beams and not as columns, specific numerical simulations of joints with IPE columns have not been performed. Some test results (joints with end plate connections) are however available and the application of formula (19) has allowed to demonstrate its validity (see sub-section 9.2.1.).

It must however be noted that the collapse by attainment of the pseudo-plastic moment $M_{b\text{pp1}}$ corresponds rather to a web crippling than to a web buckling.

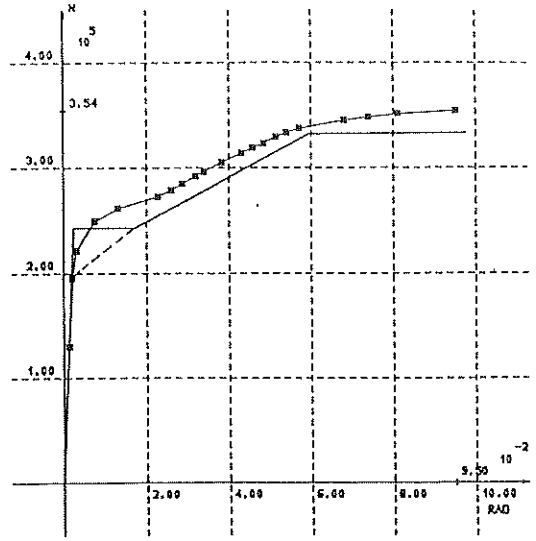
7. COMPARISON OF THE MODELS AND FORMULAE WITH THE RESULTS OF NUMERICAL SIMULATIONS

7.1. $V_n - \gamma$ curves.

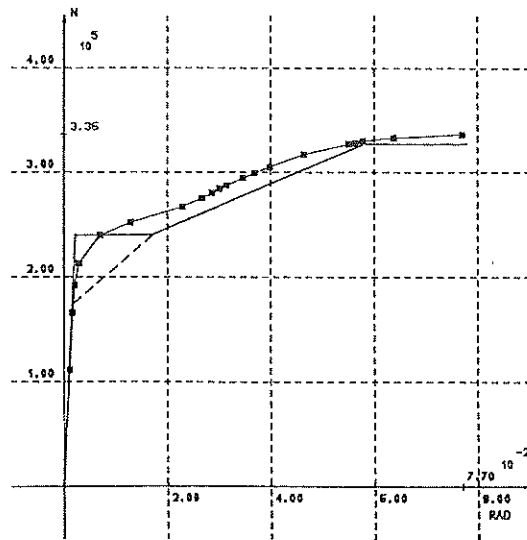
The model which has been applied to the studied nodes A and B (figures 5 and 6) in figures 33 and 34 (without stiffeners) and 35 (with stiffeners) allows to predict in a quite satisfactory way the main characteristics of the non-linear shear curves.



a-FS

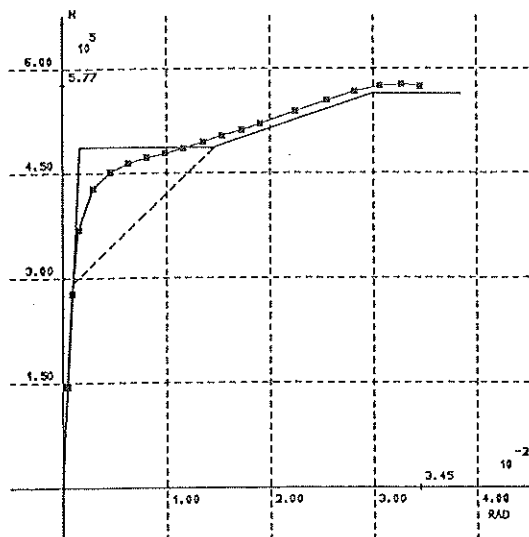


b-FP

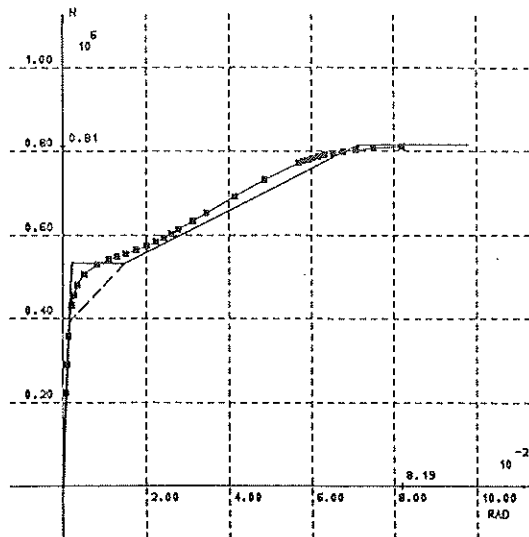


c-MP

Figure 33 - $V_n - \gamma$ curves : comparison between numerical simulations and model (unstiffened "T" joint A).

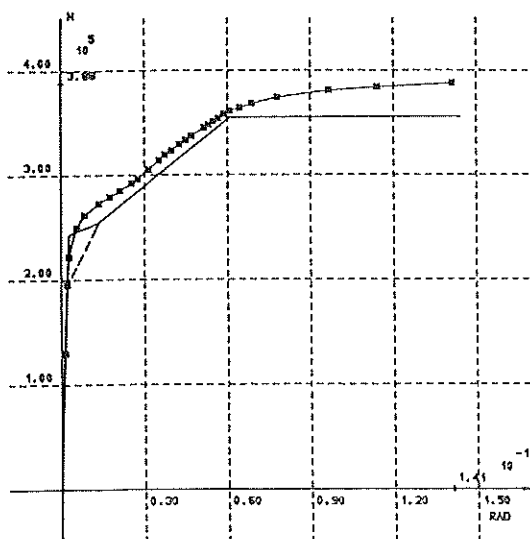


a-FS

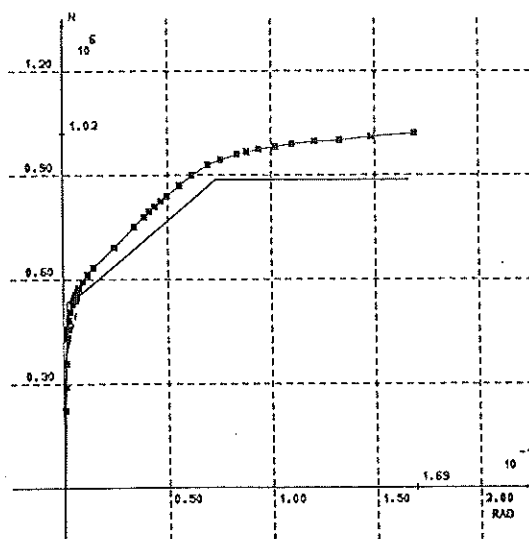


b-FP

Figure 34 - $V_n - \gamma$ curves : comparison between numerical simulations and model (unstiffened "T" joint B).



a-Joint A



b-Joint B

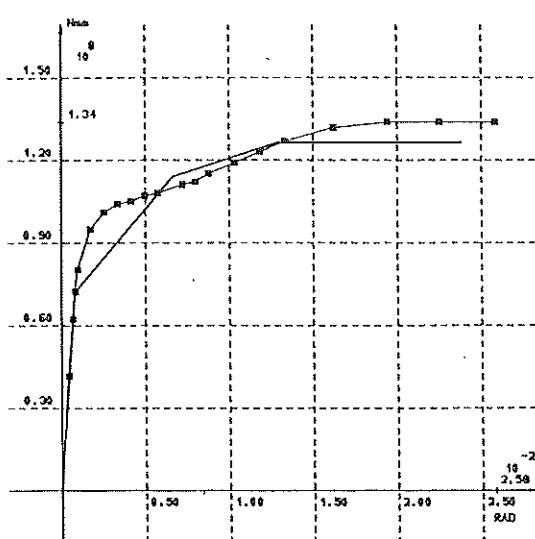
Figure 35 - $V_n - \gamma$ curves : comparison between numerical simulations and model (stiffened "T" joints - FP)

7.2. Load-introduction curves.

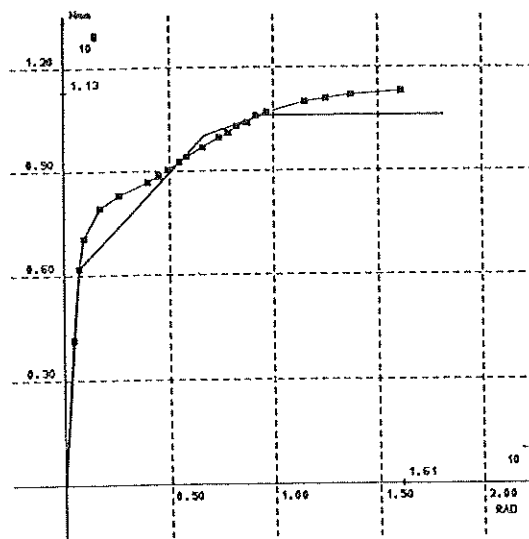
Figures 36 and 37 present the comparison of the proposed model with the $M_b - \phi$ curves recorded during the numerical simulation of the behaviour of the studied nodes A and B (figures 5 and 6).

The numerical simulation of the same joints A and B has also been carried out in a cruciform configuration (figure 3.b) for the load case reported on figure 38. The comparison of the related $M_b - \phi$ curves and the model appears on figure 39.

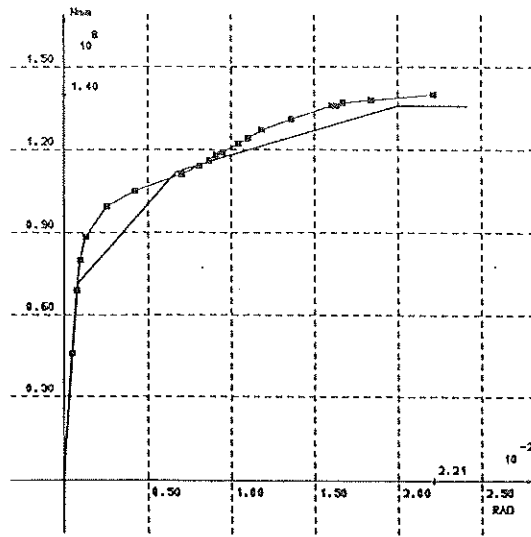
The prediction of the main characteristics of the curves is seen to be in a close agreement with the numerical results in each case.



a-FS

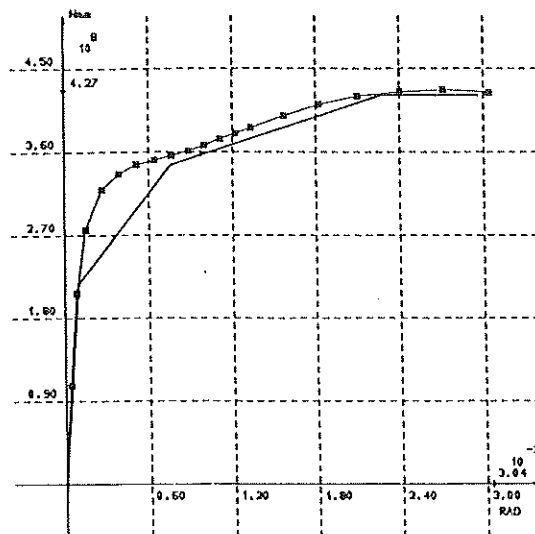


b-FP

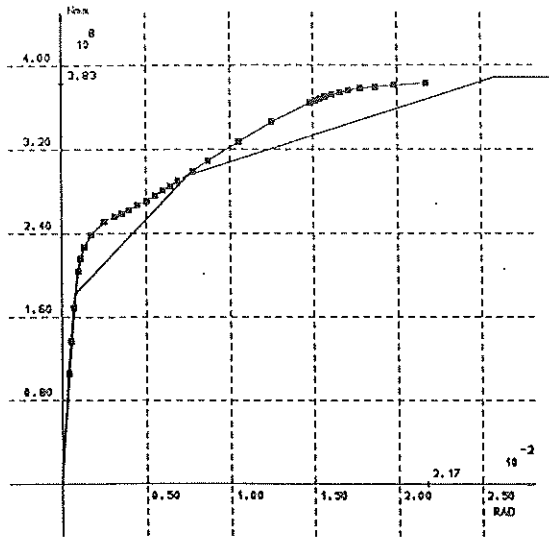


c-MP

Figure 36 - $M_b - \phi$ curves : comparison between numerical simulations and model ("T" joint A)

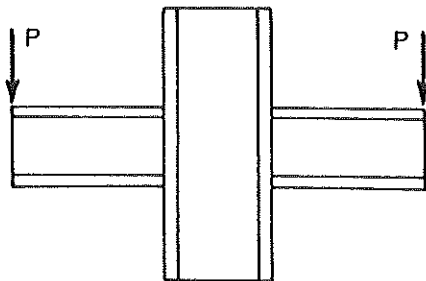


a-FS



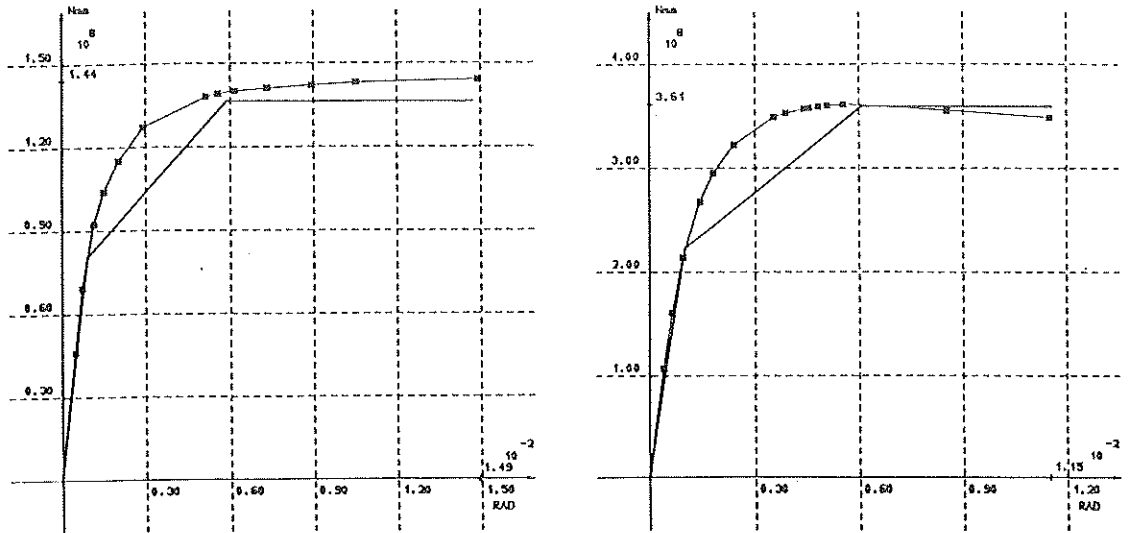
b-FP

Figure 37 - $M_b - \phi$ curves : comparison between numerical simulations and model ("T" joint B)



FS = simple bending in the beams

Figure 38 - Load case for the cruciform arrangement



a - "cross" joint A

b - "cross" joint B

Figure 39 - $M_b - \phi$ curves : comparison between numerical results and model
(cruciform arrangement - FS)

7.3. Ultimate loads

The good agreement between the predicted and the actual ultimate loads may be seen on figures 33 to 37 and on figure 39.

Table 1 summarizes the results of these comparisons. A similarity between the predicted and the actual modes of collapse has been registered for each joint.

Joints				Ultimate moments M_{bu} (kNm)					
				Collapse by shear (form.17)	Collapse by web excessive yielding (form.18)	Collapse by web instability (form.19)	Theoretical value	Numerical value	
"T"	A	Unstif.	FS	136.3	127.2	182.3	127.2	134.5	
			MP	136.9	136.1	181.1	136.1	140.6	
			FP	106.0	118.7	169.2	106.0	113.0	
	B	Stif.	FP	113.0	-	-	113.0	123.0	
			Unstif.	FS	565.2	474.4	421.4	421.4	427.4
				FP	393.6	440.3	386.7	386.7	383.3
cross	A	Unstif.	FS	-	181.7	136.0	136.0	144.0	
			FS	-	556.5	302.7	359.2	361.0	

Table 1 - Comparison of actual and predicted ultimate loads M_{bu} for welded joints

8. PASSAGE FROM MULTI-LINEAR MODELS TO MORE CONTINUOUS DEFORMABILITY CURVES

The reproach which may be addressed to the multi-linear model is the sudden and unrealistic modification of the stiffness at the intersection of two zones characterized respectively by a constant stiffness, as well as the gap, sometimes significative between the actual curve and the model in the range of moderate rotations. These flaws are inherent in the multi-linear model. The introduction of some defined characteristics of the deformability curves in an adequate mathematical expression allows to obtain full non-linear curves with a more continuous shape.

The generic mathematical function $pM = pM(\theta)$ that is likely to represent the shear and the load-introduction behaviour of a column web panel must (figure 40) :

- i) be such that $(pM) = 0$ when $\theta = 0$;
- ii) be asymptotic to $(pM) = (pM)_u$ when θ is increasing infinitely ;
- iii) comply with the coordinates $((pM)_y, \theta_y)$;
- iv) comply with the coordinates $((pM)_{st}, \theta_{st})$.

From the several mathematical expressions which were investigated and compared with tests results, the following one is suggested :

$$(pM) = (pM)_u (1 - \exp [-f(\theta)]) \quad (22)$$

with :

$$f(\theta) = a\theta^b + c\theta \geq 0 \quad (23)$$

Parameters a and b can be determined by above conditions (iii) and (iv), wherefrom :

$$a = -(\beta + c\theta_y)/\theta_y^b = -(\alpha + c\theta_{st})/\theta_{st}^b \quad (24.a)$$

$$b = \ln [(\alpha + c\theta_{st})/(\beta + c\theta_y)] / \ln (\theta_{st}/\theta_y) \quad (24.b)$$

with :

$$\alpha = \ln [1 - (pM)_{st}/(pM)_u] \quad (25.a)$$

$$\beta = \ln [1 - (pM)_y/(pM)_u] \quad (25.b)$$

According to above requirement (i), parameter b must be strictly positive ; therefore parameter c cannot exceed a limiting value c_{max} :

$$c \leq c_{max} \quad (26)$$

with :

$$c_{max} = (\beta - \alpha) / (\theta_{st} - \theta_y) \quad (27)$$

At last it is easily demonstrated that only positive (or zero) values of c can warrant the existence of an horizontal asymptot.

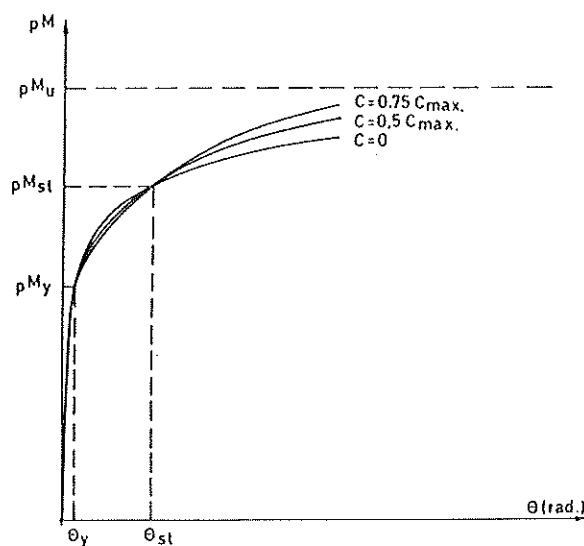
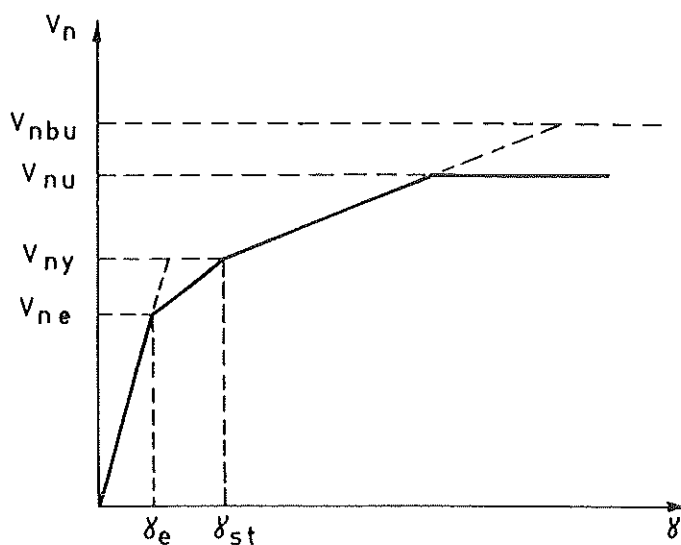


Figure 40 - Conditions to be fulfilled by the mathematical formulation and influence of the c value on the shape of a pM- θ curve

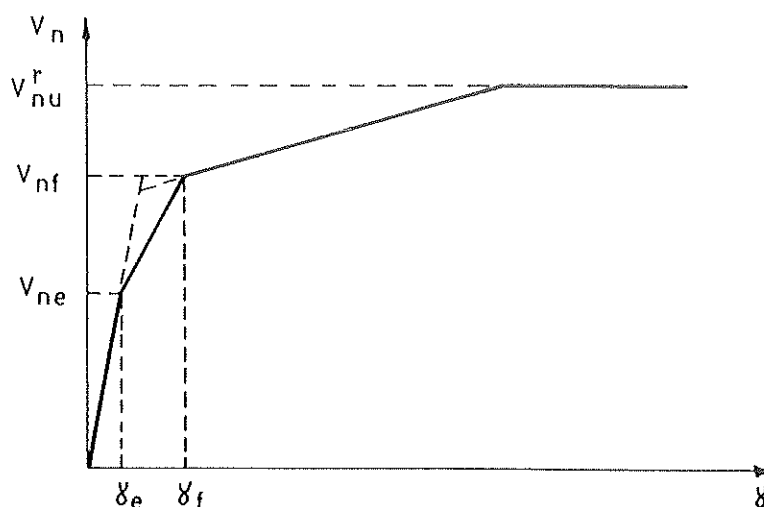
The definition of the characteristic values pM_y , pM_{st} , pM_u , θ_y and θ_{st} are given in table 2 as well as in figure 41 for each component of the column web panel deformability.

	Shear curve for an unstiffened joint	Shear curve for a stiffened joint	Load-introduction curve for an unstiffened joint
θ pM	γ V_n	γ V_n	ϕ M_b
θ_y θ_{st} pM_y pM_{st} pM_u	$\left. \begin{matrix} \gamma^e \\ \gamma^{st} \\ V_{ne} \\ V_{ny} \\ V_{nbu} \end{matrix} \right\} \begin{matrix} \\ \\ \text{(sect.5.2)} \\ \\ \text{(sect.6.1)} \end{matrix}$	$\left. \begin{matrix} \gamma^e \\ \gamma^f \\ V_{ne} \\ V_{nf} \\ V_{nbu} \end{matrix} \right\} \begin{matrix} \\ \\ \text{(sect.5.2 and 5.3)} \\ \\ \text{(sect.5.3 nbu and 6.1)} \end{matrix}$	$\left. \begin{matrix} \phi_y \\ \phi_{st} \\ M_{by} \\ M_{bst} \\ M_{buy} \end{matrix} \right\} \begin{matrix} \\ \\ \text{(sect. 4.2)} \\ \\ \text{(sect. 6.2)} \end{matrix}$

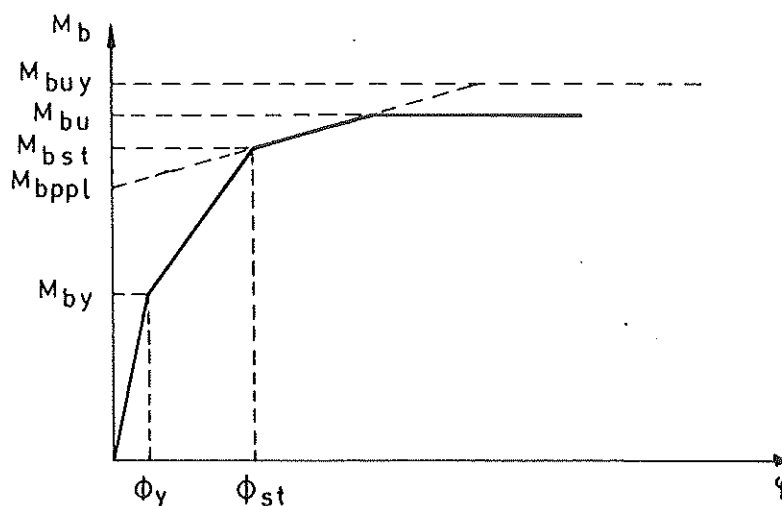
Table 2 - Significance of the characteristic values in the mathematical expression according to the deformability component of the column web panel



(a) $V_n - \gamma$ curve for an unstiffened joint - see figure 27



(b) $V_n - \gamma$ curve for a transversally stiffened joint - see figure 30



(c) $M_b - \phi$ curve for an unstiffened joint - see figure 13

Figure 41. - Characteristic values of the deformability components for a column web panel

The curves resulting from the proposed mathematical expression are asymptotic to $(pM) = (pM)_u$ when θ is increasing infinitely; it may be noted that $(pM)_u$ represents, for a specified deformability component of the panel, the ultimate strength - the loss of stability being not accounted for - relative to this particular component (as clearly mentioned in table 2); this ultimate load is not necessarily that of the whole panel which has been evaluated in chapter 6. The deformability curves for a given column web panel resulting from the use of formula (22) will consequently have to be truncated by means of a horizontal line corresponding to the actual collapse load of the panel.

The shape of the $pM-\theta$ curves is largely dependent on the value of the parameter c , as it is clearly shown in figure 40.

By comparing the results of the mathematical model suggested here with those got from the numerical simulations and from experiments (see following chapter), a very simple value $c = 0.75 c_{\max}$ may be recommended whatever be the deformability component.

The use of this non-linear formulation is illustrated in figure 42 for the deformability components of the "T" joint A subject to simple bending (figures 5 and 6).

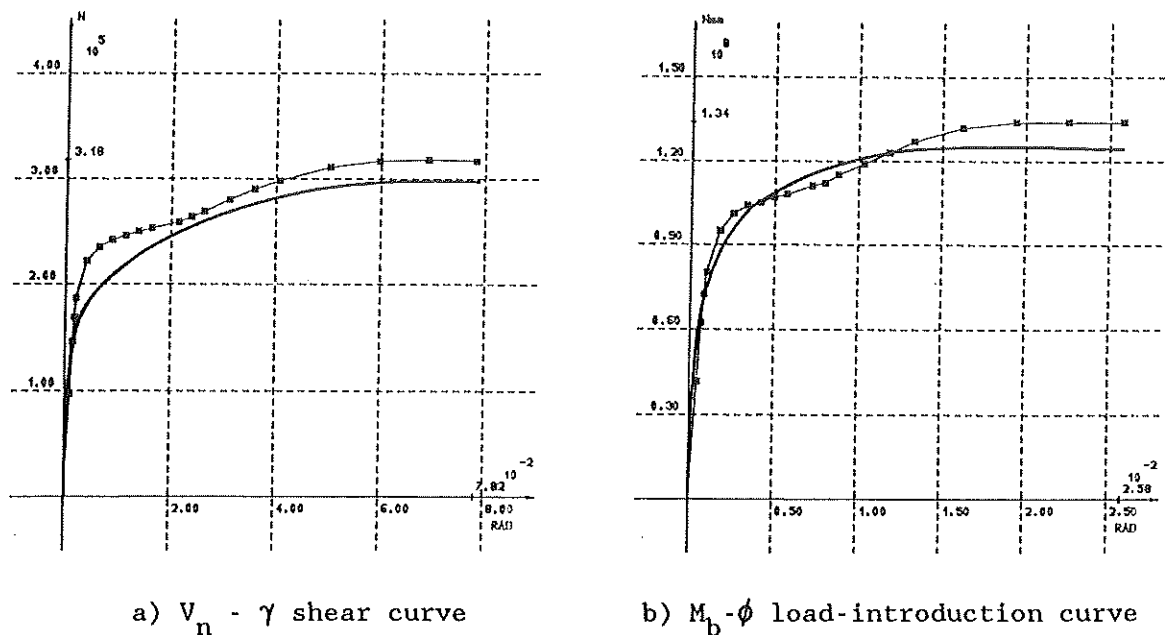


Figure 42 - Non-linear modelling of unstiffened "T" joint A

It complies with the coordinates (pM_y, θ_y) and does not develop, as it should be, a linear elastic behaviour in the region of small bending moments. The reason of doing so is the desire of simplicity when expressing mathematically the $pM-\theta$ curve. As demonstrated in figure 42, this simplification is quite justified; indeed the difference between the theoretical approach and the actual behaviour is not significant at all.

9. VALIDATION OF THE MODELS FOR JOINTS WITH STEEL BOLTED CONNECTIONS.

9.1. Shear curves.

The validity of the proposed model for steel bolted joints has been also checked by means of comparisons with shear moment-rotation curves resulting from the experimental tests on unstiffened joints with extended end plate

connections which have been performed in Liège four years ago - in the frame of a CRIF-IRSIA research - and which have been presented and discussed in [9].

The close agreement between the theoretical model and the experimental results has been demonstrated. Two examples are shown on figure 43.

The bending resistance of the column flanges in unstiffened joints has been neglected, as above-explained, because of its small importance. It is however increased, for joints with end-plate connections, by the bending resistance of the end-plate; this explains the actual, though not significant, difference between the model and the experimental result for the test 010, the end-plate thickness of which is relatively important (20 mm) in comparison with that of the column flange (12,5 mm).

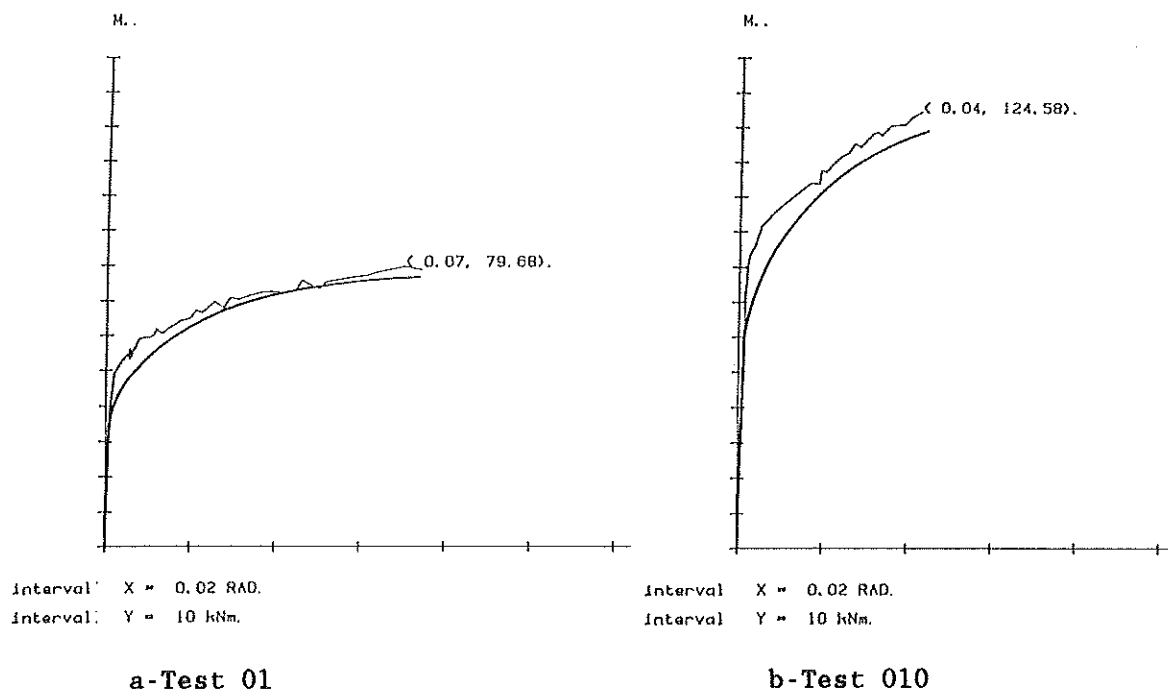


Figure 43 - $V_n - \gamma$ curves : comparison between experimental results and model (joints with end-plate connections).

Experimental shear deformability curves have also been registered for joints with cleated connections in the frame of the above-mentioned CRIF-IRSIA research [9] as well as in that of an other research [11] launched in the Department M.S.M. of the University of Liège with the financial help of ARBED Recherches (ECSC Research - agreement N° 7210-SA/507). The shear deformability for such joints is however limited and does not permit a significant comparison with the theoretical model.

At our knowledge, no other shear deformability curves are available in

spite of the numerous experimental tests which have been performed for many years in different countries.

It has to be noted that, because of the different points of application of the tensile and compressive forces carried over from the beam(s) to the column, according to the type of connection(s), the vertical dimension of the column web panel is not necessarily equal to the distance d_b between the gravity centers of the beam flanges, as for welded joints. It shall be consequently referred to figure 49 where the vertical dimensions of the web panel is defined for joints with extended end plate connections (d_b as for welded joints) and for joints with flange cleated connections (d_r).

9.2. Load-introduction curves.

To our knowledge, load introduction $M_b-\phi$ curves have never till now been registered during experimental tests in laboratory.

They have however been reported recently in Liège for the steel joint with flange cleated connections which have been tested in the frame of the ECSC Research [11], but the "trapezoidal" deformability of the column webs has been shown to be quite negligible for each test. On account of the lack of experimental load-introduction curves, the accuracy of the formula for the assessment of the collapse load of webs submitted to transverse loads in bolted joints will consequently be checked (in 9.2.1.) by comparison with the results of experimental tests, the collapse of which is due to the failure of the web, whereas the validity of the model for the prediction of the whole load-introduction curves (presented in section 4.2) will be discussed in 9.2.2.

The approach described in the previous chapters for the modelling of the load-introduction effect and the prediction of the related ultimate load may be applied to bolted joints, as this will be demonstrated in 9.2.1. and 9.2.2., on condition of very limited modifications linked up to the length of diffusion of the forces in the tension and compression zones, through the cleats or the end-plate, the column flange and the radii of fillet; all the details, which may be found in [10], are summarized in sub-section 9.2.3.

9.2.1. Check of the ultimate load.

The validity of the extending to the calculation of bolted joints of the formulae presented in chapter 6 for the assessment of the collapse loads of column web subject to transverse forces is illustrated by means of the comparison with the results of five tests on joints with extended end-plate

connections. Tests 9, 20 and M3A have been performed by ZOETEMEIJER [12] in the Netherlands whereas tests 013 and 014 originate from Liège [9]. Table 3 summarizes the main characteristics of the joints as well as the comparison between the actual and predicted collapse loads.

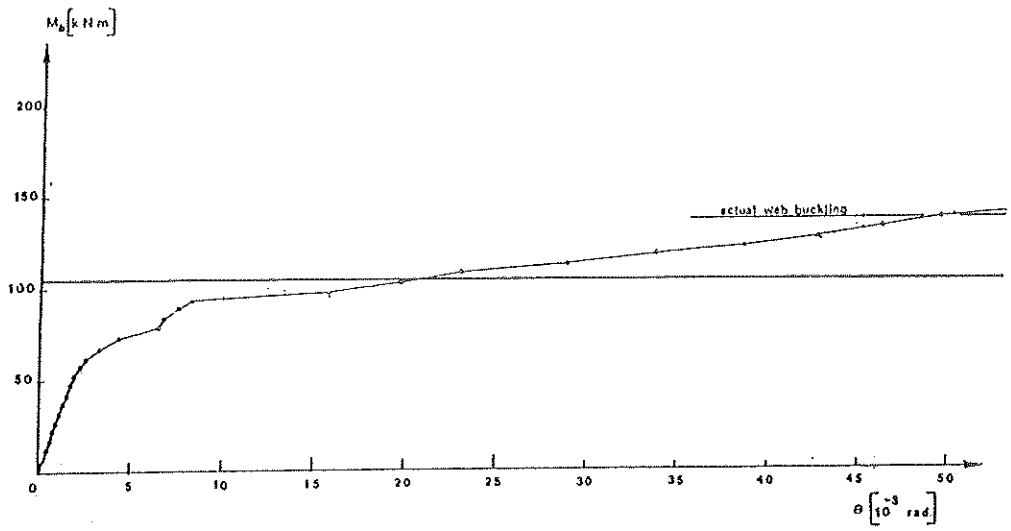
Joints					Ultimate moments M_{bu} (kNm)		
Test number	Testing arrangement	Column type	Beam type	Reference	Collapse mode (see chap.6)	Theoretical ultimate value	Experimental ultimate value
9	"T"	HE200A	IPE300	[12]	web buckling $M_{bub} = M_{bppl}$	104.5	143.0
20	"T"	HE300A	IPE400	[12]	web buckling $M_{bub} = M_{bppl}$	248.8	246.0
M3A	cruciform	HE240A	IPE300	[12]	web buckling $M_{bub} = M_{bppl}$	135.3	145.0
013	"T"	IPE240	IPE200	[9]	web crippling $M_{bub} = M_{bppl}$	61.0	62.7
014	"T"	IPE300	IPE200	[9]	web crippling $M_{bub} = M_{bppl}$	72.3	83.6

Table 3 - Comparison of actual and predicted ultimate loads M_{bu} for joints with end plate connections.

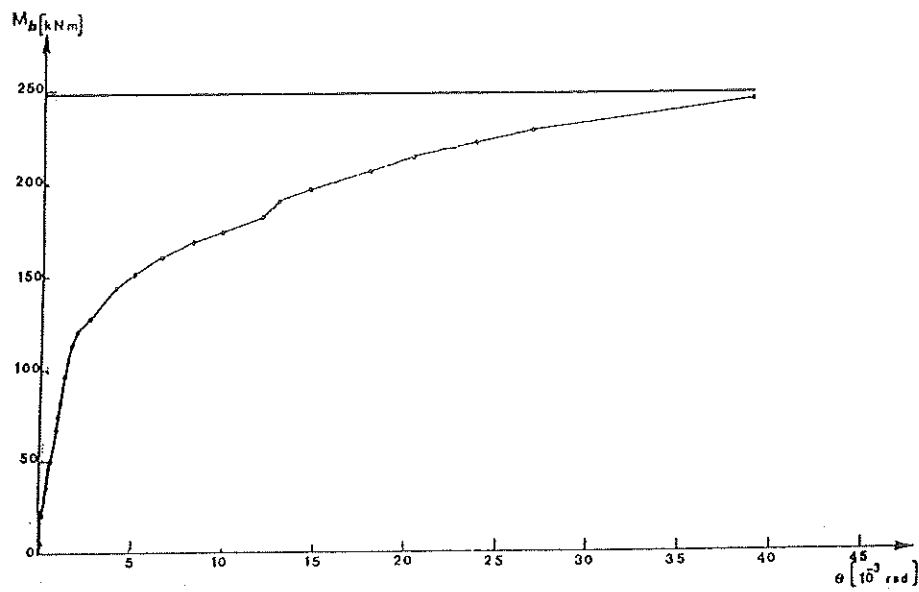
The collapse of the CRIF-IRSIA test 013 and 014 (figures 44.d and 44.e) is associated to the crippling of the column web, whereas the "T" test 20 (figure 44.b) and the cruciform test M3A (figure 44.c) fail rather by web buckling when the value of the pseudo-plastic moment is reached.

The predicted ultimate strengths constitute a good approximation of the actual ones.

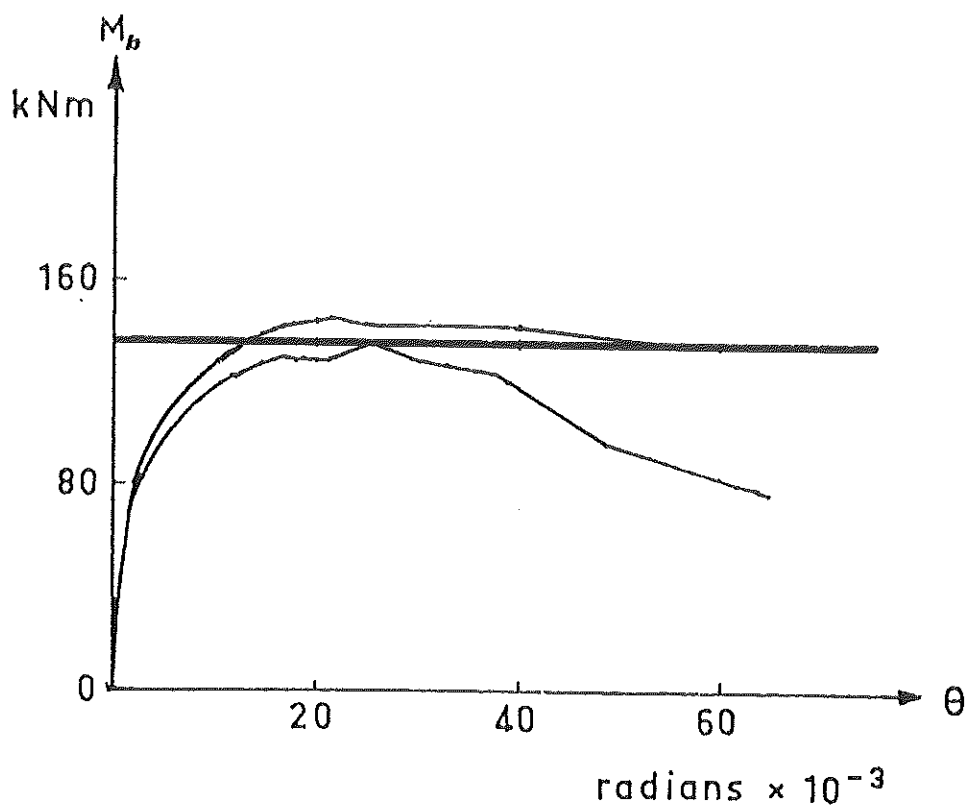
The safe but significant divergence between the theoretical and the experimental ultimate loads for the test 09 (figure 44.a) may be explained without any doubt, as explained in 6.3, by the low initial out-of-flatness of the actual column webs in comparison with those, chosen on base of rolling tolerances, which has been considered for the assessment of the theoretical buckling load M_{bb} .



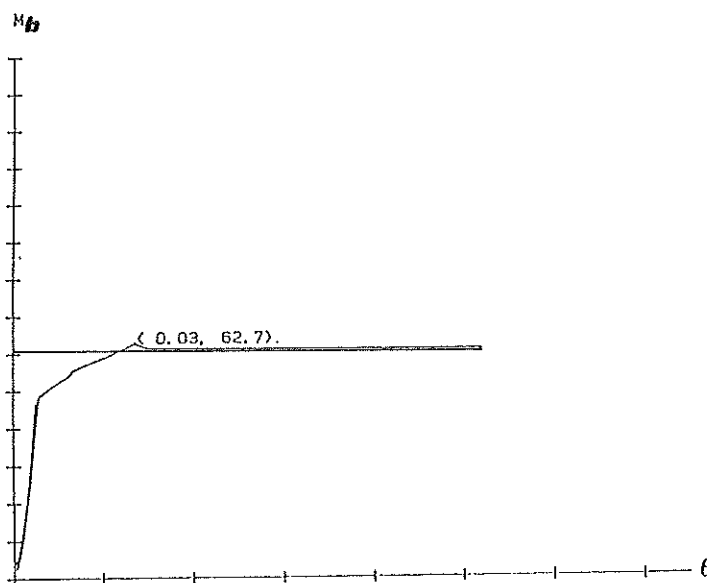
a-Test 09



b-Test 20

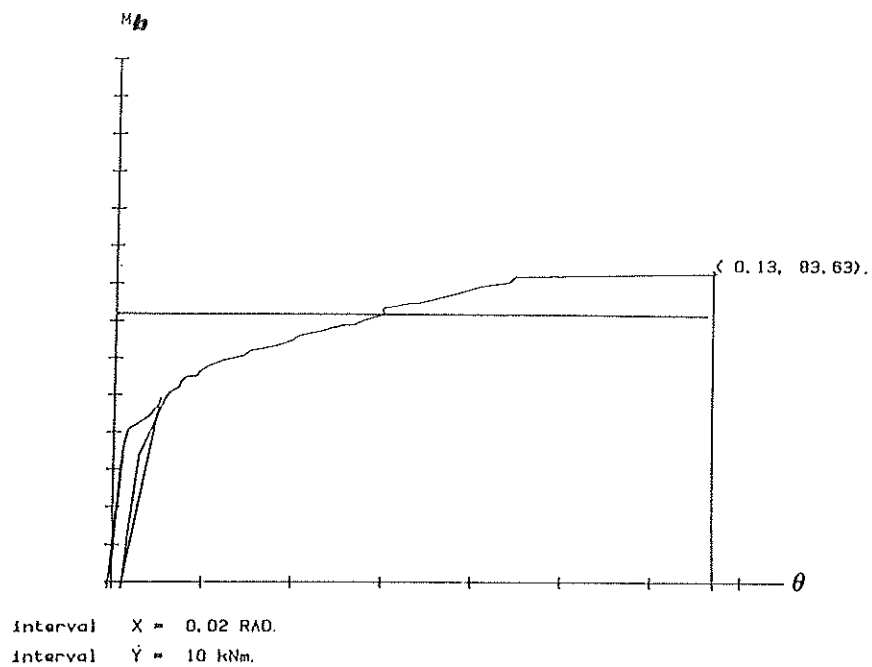


c-Test M3A



interval X = 0.02 RAD.
 interval: Y = 10 kNm.

d-Test 013



e-Test 014

Figure 44 - Comparison of theoretical ultimate loads with experimental ones (joints with bolted connections).

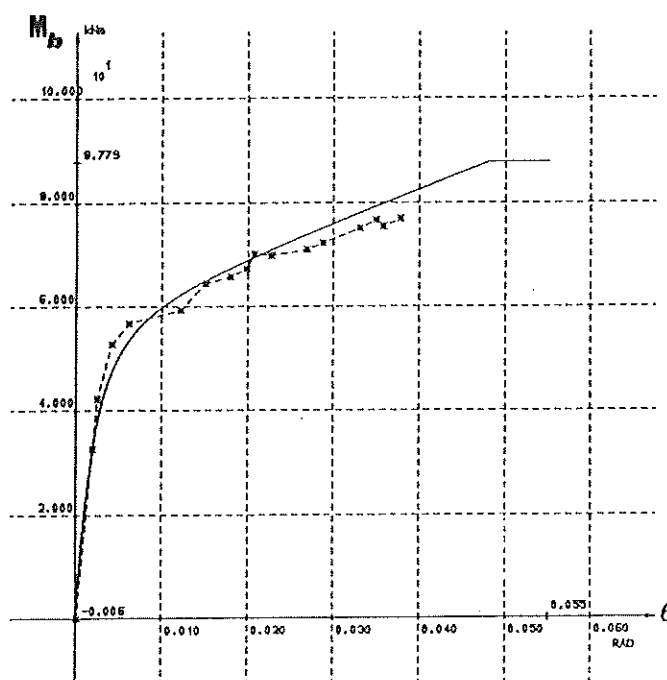
9.2.2. Check of the deformability model.

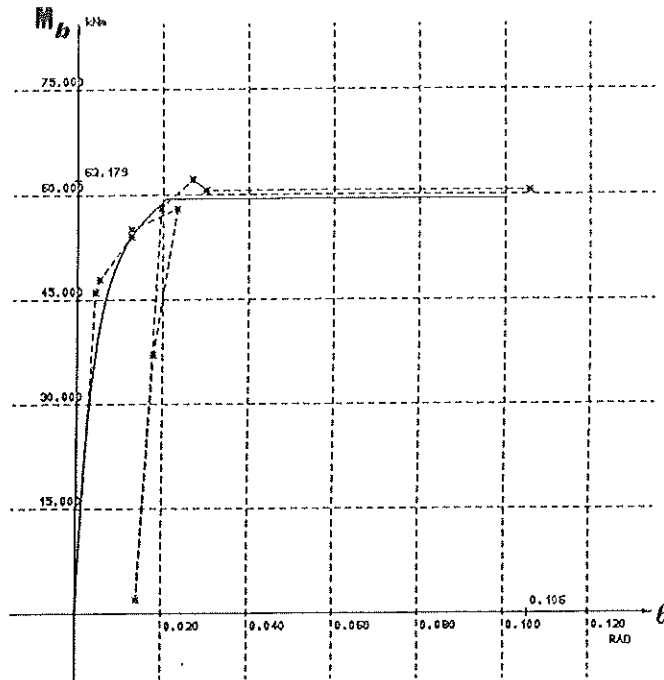
As explained in chapter 2, the deformability of a beam-to-column joint has to be divided into the shear deformability of the column web panel and the deformability of the connection(s). This report is devoted to the study of the shear and of the load-introduction; the latter constitutes only one of the components of the connection deformability. The study of the other components of the connection deformability has also been performed in Liège and has recently led to the proposal of mathematical models, similar to those described in this report, for the prediction of the non-linear deformability $M_b-\phi$ curves of :

- extended end plate connections [10] ;
- flange cleated connections [10] ;
- composite connections (web cleat and lower and/or upper flange cleats) [11].

The comparison between experimental connection deformability curves and the theoretical modelling allows to validate the mathematical approach for the prediction of the load-introduction behaviour, particularly in the case of the composite joints, the deformability of which is mainly, and sometimes almost exclusively (for high percentages of slab reinforcement) associated to the load-introduction deformability of the column web subject to transverse compressive forces.

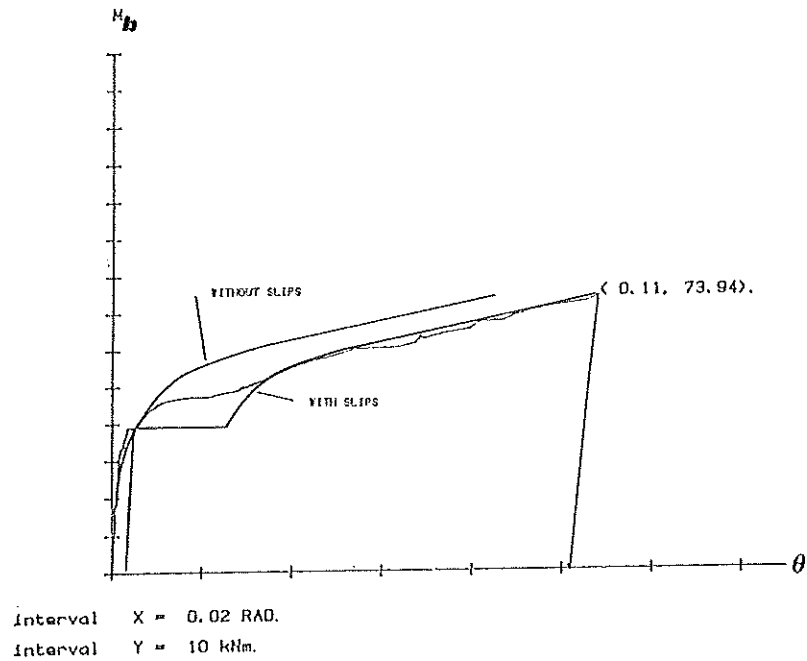
Two examples are reported on figures 45 to 47 for each type of studied connection.



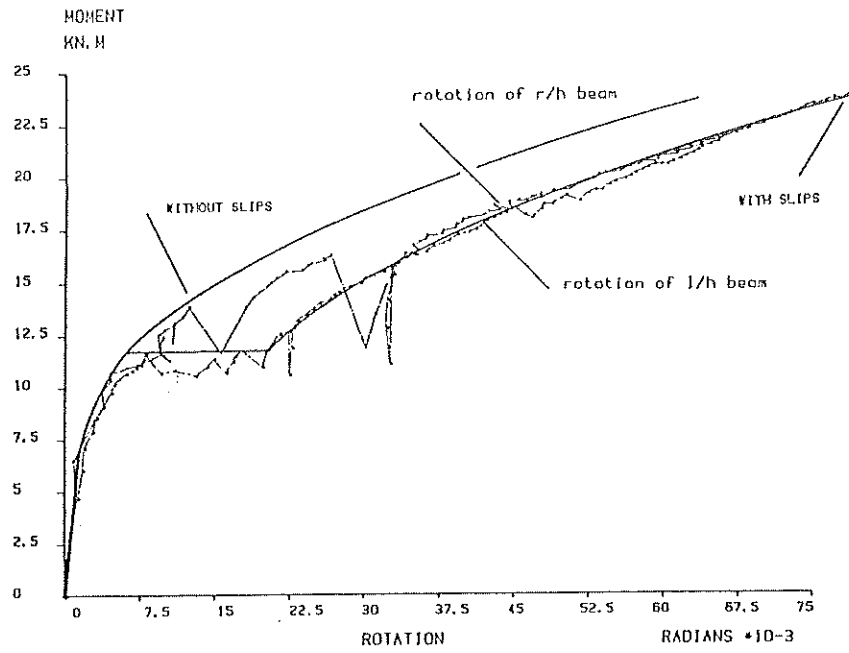


b-Test 013

Figure 45 - Comparison between experimental results and the response of the theoretical model for the prediction of the connection behaviour (tests on joints with extended end plate connections [9]).



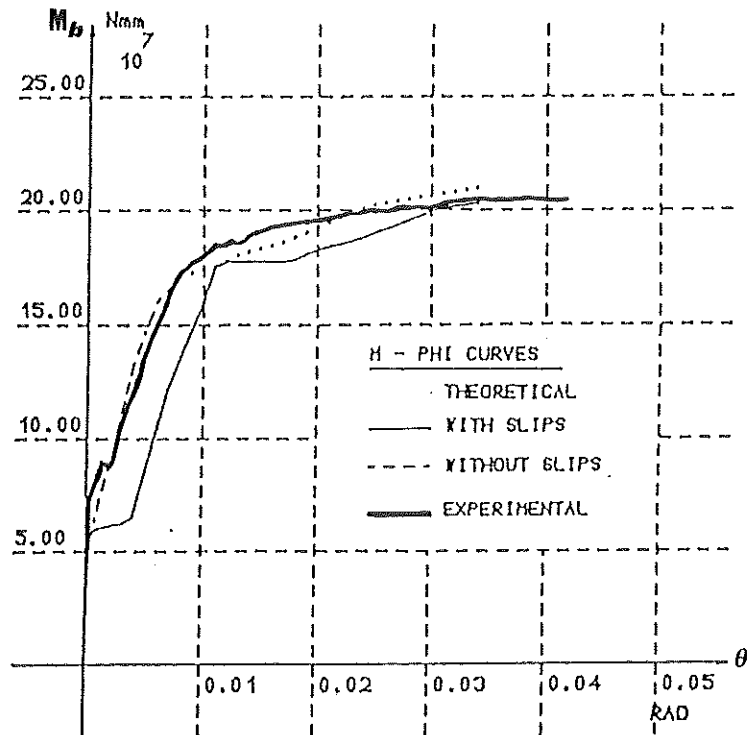
a-Test 03 [9]



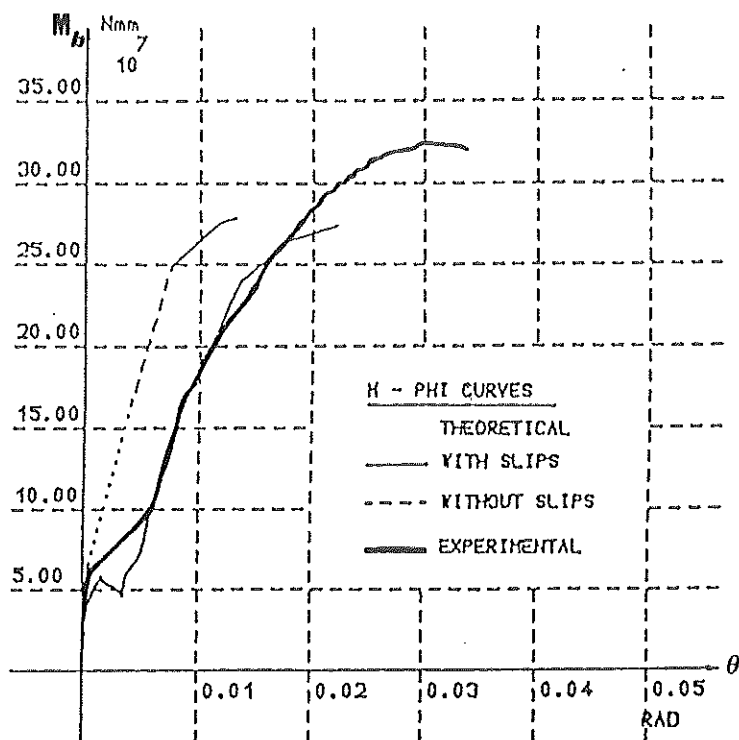
b-Test JT08 [14]

Figure 46 - Ibidem

(tests on joints with flange cleated connections).



a-Test 30 x 2c.5 (rebars of 10 mm)



b-Test 30 x 2c.7 (rebars of 18 mm)

Figure 47 - Ibidem

(tests on composite joints - connections with a web cleat and a lower flange cleat [11]).

According to the initial position of the bolts in their holes, the slip between the cleats and the beam may or not occur during the loading of the flange cleated connections and also of the composite connections; this justifies the necessity to report two different theoretical curves corresponding respectively to the development of the maximum permissible slip (which depends on the hole clearances) and to the absence of slip. The influence of this parameter on the connection deformability can be observed on figures 46 and 47 and is found relatively significant.

The collapse of the composite joint 30 x 2c.7 is associated to the buckling of the column web. As explained in 6.3., the safe but important divergence between the actual and the predicted ultimate loads may be explained by the very low initial out-of-flatness of the column web actually measured in laboratory in comparison with that, chosen on base of rolling tolerances, which has been considered for the assessment of the theoretical buckling load of the web.

9.2.3. Amendments of the formulae for bolted joints.

As illustrated in figure 49.a, the deformability of the column web in a welded joint is similar in the compression and tension zones of the joint. The numerical simulations presented in chapter 3 have clearly shown that the initial out-of-flatness of the column web, which affects the value of the buckling load M_{bb} (formula 19.b) in a significant way, modifies very slightly the deformability of the compression zone of the web before buckling with respect to that of the tension zone. The equality of Δ_c and Δ_t allows to refer directly to the moment M_b carried over by the joint and to the rotation ϕ , as described in figure 49.a.

The length of application of the compressive and tensile forces F_b to the column is limited to the thickness of the beam flanges. The influence of this parameter on the load-introduction deformability curves is quite negligible (except for M_{bpl} - formula (6) - and for M_{buy} - formula (18)) so that concentrated forces have been considered in the model proposed in 4.2. as well as in the formulae for the assessment of the ultimate strength of the web (sections 6.2. and 6.3.).

The different modes of application of the beam loads to the column web in the compressive and tensile zones of joints with bolted connections requires to refer separately to the corresponding $F_b - \Delta$ curves (figure 49) The general shape of these $F_b - \Delta$ curves is given in figure 48.

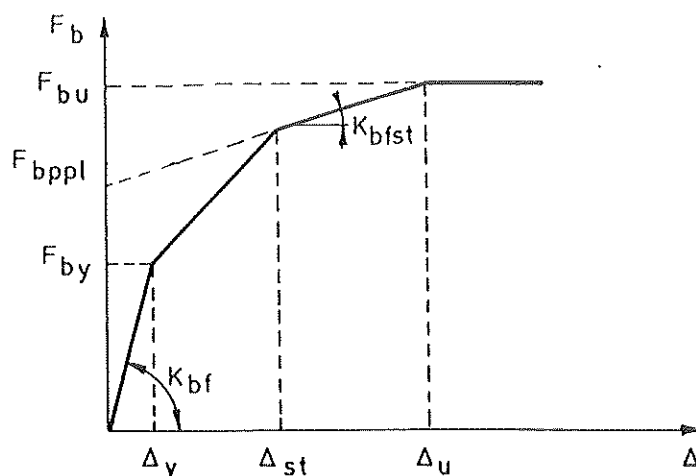


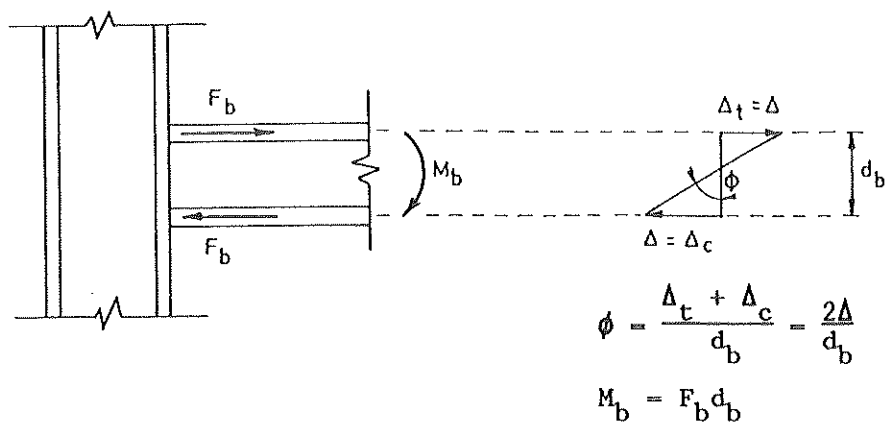
Figure 48 - Characteristics of the multi-linear model for prediction of $F_b - \Delta$ curves

The definitions of the main characteristics are equivalent to those provided in section 4.2. and in chapter 6 except that it is here referred to the forces F_b and to the displacements Δ (Δ_c or Δ_t) and not to M_b and ϕ as in figure 13.

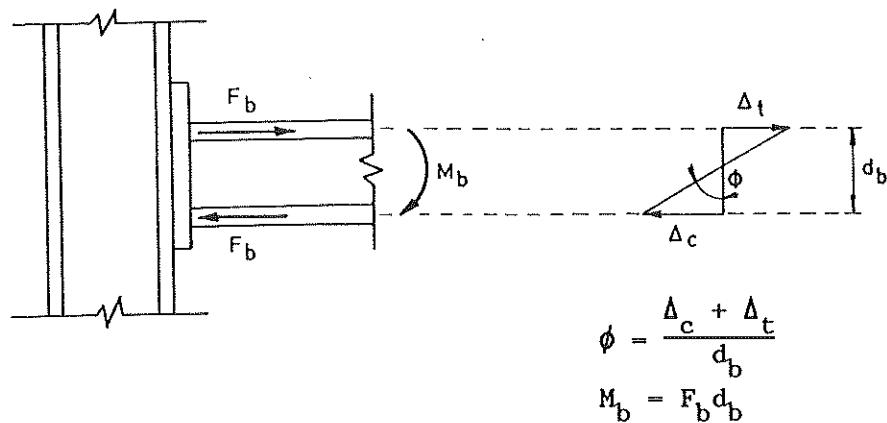
The relations between M_b and F_b , as well as between ϕ and Δ , are given in figure 49.b and 49.c respectively for joints with extended end plate and flange cleated connections. The large diffusion of the forces F_b into the cleats or the end plate, in the compression zone, and into the column flange in the tension zone requires to account, in the case of bolted connections, for the length of application of the forces F_b to the column web.

The slightly amended values [10] of K_{bf} , F_{by} , F_{bppl} as well as the ultimate load F_{buy} (associated to the web resistance) and the buckling strength F_{bb} of the web (only in compression), which allows, as explained in chapter 6, to assess the actual ultimate strength F_{bu} of the web, are presented in tables 4 and 5 respectively for joints with extended end plate and flange cleated connections.

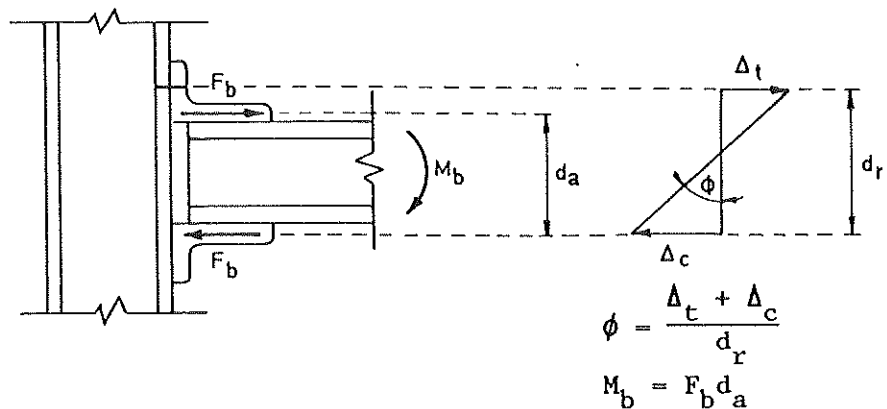
As for the welded joints, Δ_{st} and K_{bfst} are given by :



a) Welded joints



b) Joints with end plate connections



c) Joints with flange cleated connections

Figure 49 - Definition of M_b and ϕ according to the connection type.

$$\Delta_{st} = \epsilon_{st} h_w/2 \quad (27.a)$$

$$K_{bfst} = K_{bf}/50 \quad (27.b)$$

Because of the stiffening of the column flange by the beam web for joints with welded connections, the column flange has been considered in section 4.2. (see figure 15) as infinitely stiff in the zone located between the beam flanges. The assumption is no more valid for joints with bolted connections so that formula (3) has to be replaced by the following one :

$$\sigma_i = \frac{F_b \lambda}{2\mu s_c} \quad (28)$$

μ is defined in table 5.

All the other parameters appearing in formulae (27) and (28) as well as in tables 4 and 5 have been defined in section 4.2. and in chapter 6.

Formulae	Web under compression	Web under traction
$K_b = \frac{2k}{\lambda} \mu$ $F_{by} = \frac{2 s_c}{\lambda} \mu \sigma_{iy}^c$ with $\mu = \frac{\xi}{1 - e^{-\xi \cos \xi}}$ $\xi = \frac{b}{2L}$ $L = 1/\lambda$	$b = t_b + 2a \sqrt{2} + 2 t_e$ with : t_b = beam flange thickness ; a = weld throat thickness t_e = end plate thickness	$b = t_b + 2 w_e$ with t_b = beam flange thickness ; w_e = length of the extended part of the end plate in the tensile zone
$F_{b\text{pppl}} = s_c l_p \sigma_{iy}^c$	$l_p = t_b + 2a\sqrt{2} + 2t_e + 5(t_c + r_c)$ with: t_b =beam flange thickness a =weld throat thickness t_e =end plate thickness t_c^e =column flange thickness r_c =radius of fillet of the column	$l_p = b_m$ where: b_m is taken as equal to the total effective length of the bolt pattern in the tensile zone of the connection, obtained from J.3.3.1. in the appendix J of the chapter 6 of EC3
$F_{b\text{uy}} = s_c l_p \sigma_{iu}^c$		
$F_{bb} = \mu \sqrt{F_{by} F_{bcr}}$ where: F_{by} and μ are given here above; F_{bcr} is given by formula (20)	$b = t_b + 2a \sqrt{2} + 2 t_e$ with: t_b =beam flange thickness a =weld throat thickness t_e =end plate thickness	-

Table 4 - Modified values of the load-introduction curves for joints with extended end plate connections.

Formulae	Web under compression	Web under traction
$K_b = \frac{2k}{\lambda} \mu$ $F_{by} = \frac{2 s_c}{\lambda} \mu \sigma_{iy}^c$ <p>with $\mu = \frac{\xi}{1 - e^{-\xi \cos \xi}}$</p> $\xi = \frac{b}{2L}$ $L = 1/\lambda$	$b = 2t_a + (2 - \sqrt{2}) r_a$ <p>with: t_a = lower cleat thickness r_a = radius of fillet of the lower flange cleat</p>	$b = 2 n_a$ <p>with n_a = distance between the bolt centre and the edge of the vertical leg of the upper flange cleat connecting the beam upper flange to the column</p>
$F_{bpyl} = s_c l_p \sigma_{iy}^c$	$l_p = 2t_a + (2 - \sqrt{2}) r_a + 5(t_c + r_c)$ <p>where : t_a = lower cleat thickness r_a = radius of fillet of the lower flange cleat t_c = column flange thickness r_c = radius of fillet of the column</p>	$l_p = b_m$ <p>where b_m is taken as equal to the total effective length of the bolt pattern in the tension zone of the connection, obtained from J.3.3.1. in the appendix J of chapter 6 of EC3 (for one bolt row only)</p>
$F_{buy} = s_c l_p \sigma_{iu}^c$		
$F_{bb} = \mu \sqrt{F_{by} F_{bcr}}$ <p>where : F_{by} and μ are given here above ; F_{bcr} is given by formula (20).</p>	$b = 2t_a + (2 - \sqrt{2}) r_a$ <p>with: t_a = lower cleat thickness r_a = radius of fillet of the lower flange cleat</p>	

Table 5 - Modified values of the load-introduction curves for joints with flange cleated connections.

10. IMPROVEMENT OF THE EC3 FORMULAE FOR THE ASSESSMENT OF THE DESIGN RESISTANCE OF COLUMN WEB PANELS.

The analysis and the design of building frames by means of sophisticated non-linear programs requires an accurate prediction, similar to that described here above for the shear and the load-introduction effects in column web panels, of all the deformability components of the beam-to-column joints, whereas only some simplified characteristics of the actual joint behaviour such as the secant or the initial stiffness and the plastic moment capacity are needed in the daily design practice.

Formulae for the assessment of the design resistance of a sheared column web panel ($V_{n,Rd}$) and of an unstiffened column web subject to a transverse compressive ($F_{c,Rd}$) or tensile ($F_{t,Rd}$) force are proposed in this respect in the annex J of Eurocode 3 for joints with end plate or welded connections [15].

Their validity will be discussed in this chapter, but it first appears necessary to clearly define the design resistance of a column web panel subject to shear and to transverse loads.

At each step of loading, the web panel is subject to a shear force V_n (figure 2.c) and to transverse forces F_b (figure 2.b).

The design resistance of the column web panel will be defined as the minimum load level leading to the attainment of the design resistance of the panel under shear ($V_n = V_{n,Rd}$) or under transverse loads ($F_b = F_{c,Rd}$ or $F_b = F_{t,Rd}$).

Two remarks are to be made before discussing the EC3 formulae :

- present report is dealing with joints, the members of which are constituted of hot-rolled H and I sections; that explains why the specific formulae related to the joints with welded sections are not reported in the following of the chapter (even if the proposals for improvement which will be proposed may be also applied to them),
- all the formulae listed here below should be divided by a safety factor γ_{MO} associated to the resistance of members and cross-sections ; this safety factor shall be taken as equal to 1.0 for class 1,2 or 3 cross-sections, what explains why it has been omitted in this chapter.

10.1. Resistance of the shear panel.

The following formula for the assessment of the design resistance of a sheared column web panel is proposed in the annex J of Eurocode 3 chapter 6 :

$$V_{n.Rd} = A_{sh} \cdot f_y / \sqrt{3} \quad (29)$$

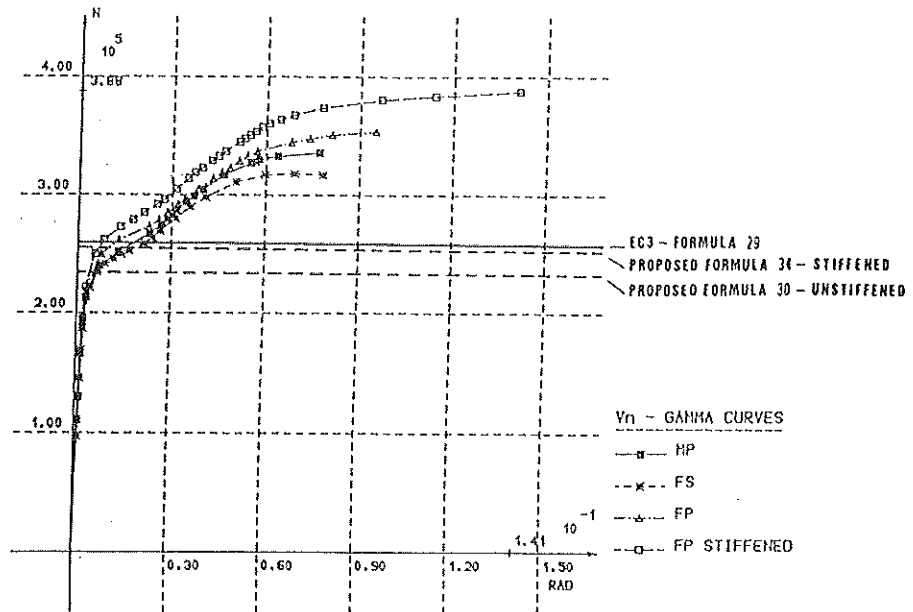
where : - f_y is the yield stress of the column web ;
 - A_{sh} is the sheared column web area defined in figures 28 and 53.a.

This formula is recommended in EC3 independently of the presence or not of transverse stiffeners (figure 29.a) welded on the column web.

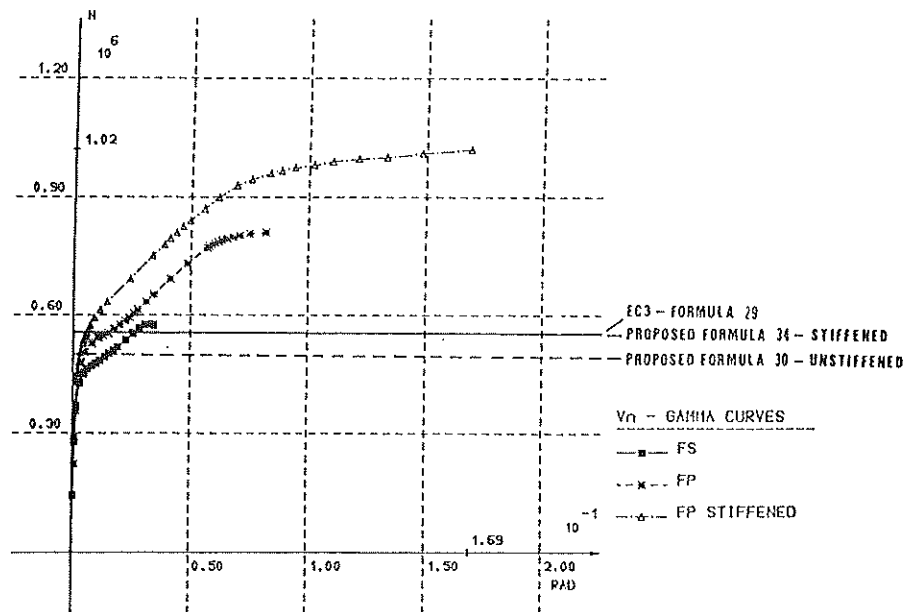
This formulation differs from that proposed in section 5.2. for unstiffened web panels - formula (10) - by an unsafer definition of the maximum shear stress (the actual stress interaction in the web is not accounted for).

The application of formula (29) to the fully welded joints studied numerically and to the joints with end plate connections tested in laboratory has led to the following main conclusions :

- for most of the unstiffened joints (see examples on figures 50 and 51), the stress interaction results in a moderate reduction of the design resistance of the shear web panel assessed by formula (29); the frame effect which has been shown to be negligible for unstiffened joints (section 5.2.) and which has not been accounted for in the computation of the design resistance of the sheared panel compensates partly this reduction so that the design resistance assessed by formula (29) constitutes generally a slightly unsafe approximation of the actual one.
- the stress interaction in the web may however lead sometimes to more pronounced decrease of the design resistance of web panels evaluated by means of formula (29), as seen in figures 50.b (FS) and 51.a, and consequently to the development of large shear rotations incompatible with the definition of the associated secant rigidity given in annex J of EC3 chapter 6 [3].
- formula (29) leads to safe assessments of the actual design resistance of stiffened web panels (the frame effect which is not negligible in these cases is indeed not accounted for in this formula).

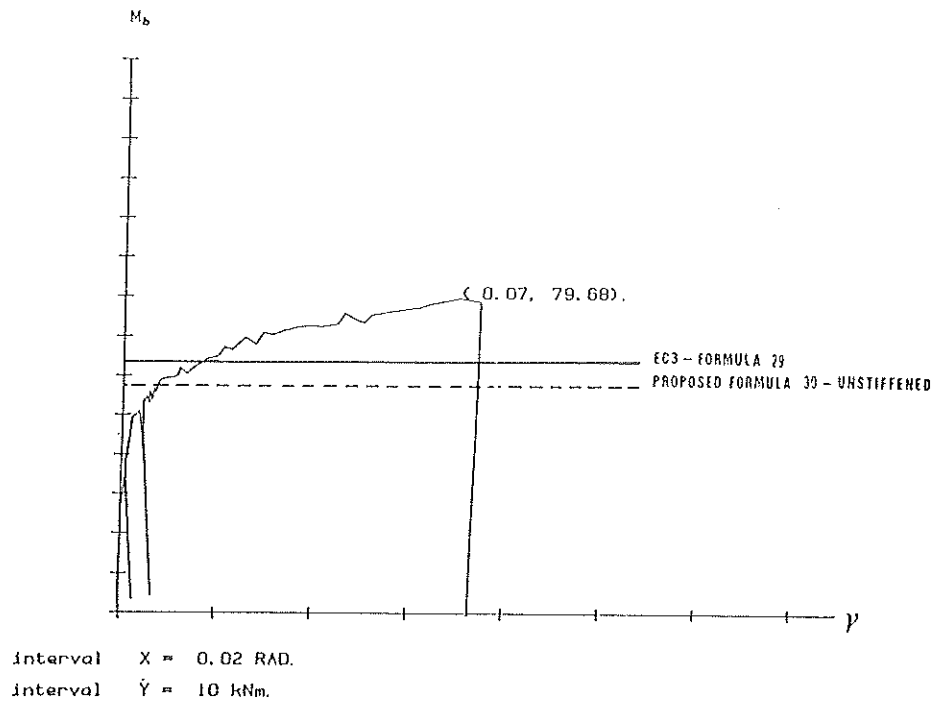


a-"T" joint A

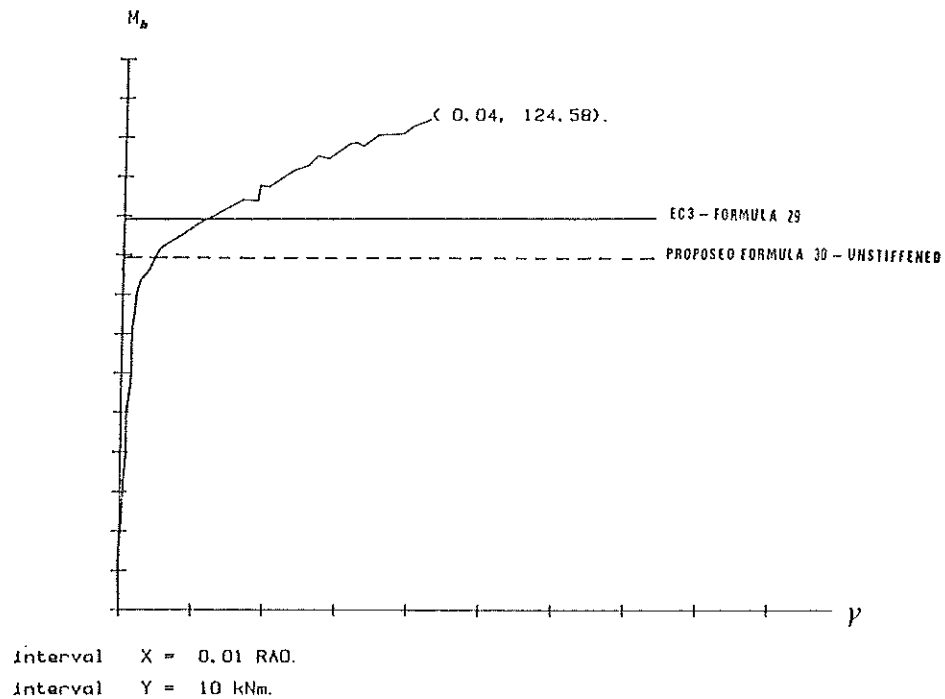


b-"T" joint B

Figure 50 - Characteristic $V_n - \gamma$ curves. Assessment of the design resistance according to the EC3 and new proposed formulae. Fully welded joints studied numerically.



a-Test 01



b-Test 010

Figure 51 - Characteristics shear curves.

Assessment of the design resistance according to the EC3 and new proposed formulae. Joints with extended end plate connections [9].

For sake of simplicity, it is suggested not to account for the stress interaction - what would complicate the use of the formula and is not really necessary because of the relatively limited influence of this factor - but to compensate it by a fictitious reduction of the shear web area of the column.

The proposed improved formula for unstiffened web panels writes :

$$V_{nr.Rd} = A_{r.sh} \cdot f_y / \sqrt{3} \quad (30)$$

where : f_y is the yield stress of the column web ;

$A_{r.sh}$ is the reduced area of the sheared column web given by :

$$A_{r.sh} = \chi_s A_{sh} \quad (31)$$

where χ_s is the reduction factor.

The web panel shear capacity of the joints, the characteristic $V_n - \gamma$ curves of which were available, has been evaluated by means of :

- formula (10) which accounts for the stress interaction (V_{ny}) ;
- formula (29) which does not account for it ($V_{n.Rd}$).

The values are reported in table 6. The ratio between $V_{n.Rd}$ and V_{ny} which represents the influence of the stress interaction on the shear capacity is nothing else than the reduction factor χ_s . Its values are also listed in table 6, that covers :

- the usual types of sections : HE and IPE ;
- various loading patterns ;
- values of σ_n/f_y ratios up to 50 % (range of practical interest according to KATO [8] - see section 4.1.).

The limited influence of the stress interaction on the plastic capacity of the sheared web panels appears clearly in table 6. A single but nevertheless safe (the frame effect, which has been neglected, increases always slightly the actual shear capacity) and accurate value is chosen for the reduction factor :

$$\chi_s = 0.9 \quad (32)$$

Unstiffened tee joints		Type of loading (Fig. 6)	V_{ny} (kN)	$V_{n,Rd}$ (kN)	Ratio χ_s
welded connec- tions (Fig. 5)	A	FS	232,39	259,73	0,89
	A	FP	244,18	259,73	0,94
	A	MP	241,18	259,73	0,93
	B	FS	488,30	557,49	0,88
	B	FP	537,82	557,49	0,96
end plate connec- tions [9]	01	FS	276,49	317,97	0,87
	07	FS	299,6	317,97	0,94
	010	FS	278,68	317,97	0,88
	013	FS	316,09	340,70	0,93
	014	FS	448,92	474,09	0,95

Table 6 - Values of the reduction factor χ_s

The design resistances resulting from the use of formulae (30) to (32) constitute satisfactory assessments of the actual ones (see figures 50 and 51) as far as the shear force V_n acting on the panels is evaluated by means of the formula (7). The use of formula (8), which is recommended by many authors, may lead (it depends on the joint loading) to too safe evaluations of the shear plastic capacity of the web (see figure 52 for instance for joint A).

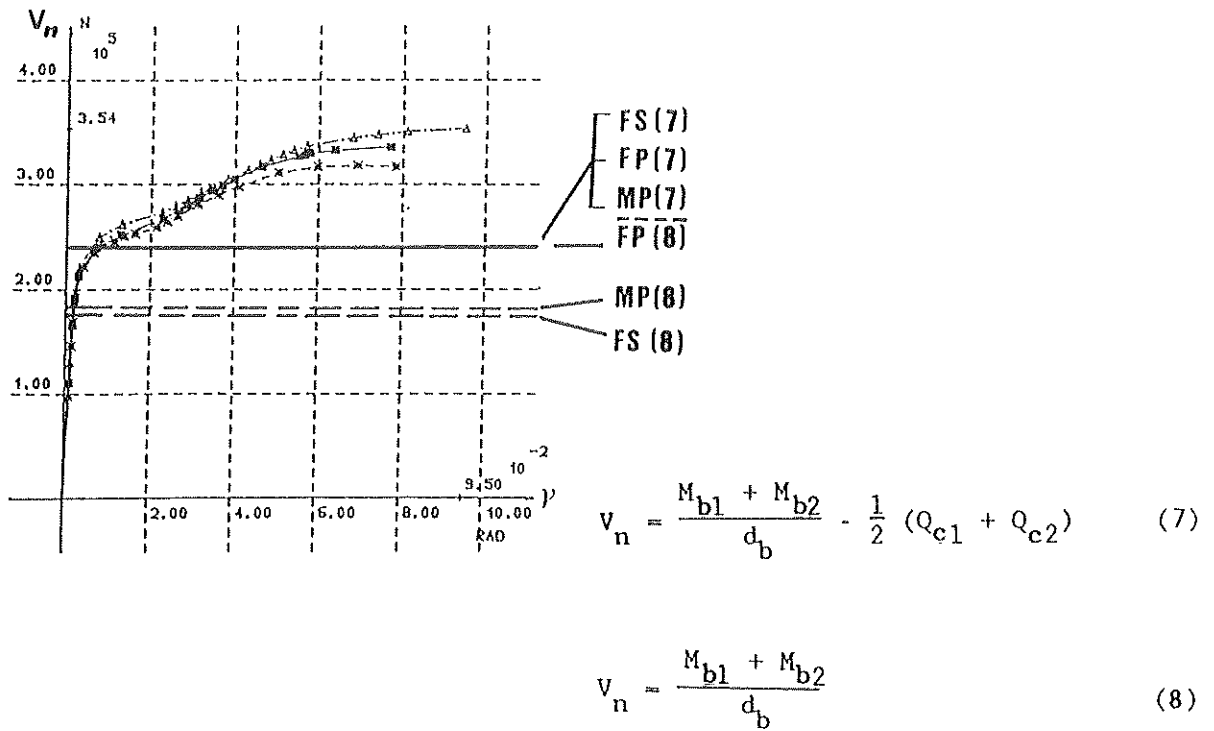


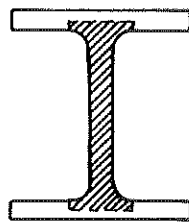
Figure 52 - Proposed rule for the assessment of the shear plastic capacity. Influence of the mode of evaluation for V_n ("T" joint A).

For simplicity, it is allowed, in section 5.4.6. of EC3 chapter 5, to replace the determination of the actual web shear area A_{sh} (fig. 53.a) for H and I sections (load parallel to web) by that of the following expression:

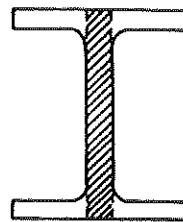
$$A_{sh} = 1.04 A_w \quad (33.a)$$

with $A_w = h_c \cdot s_c \quad (33.b)$

where : A_w is the column web area defined in figure 53.b ;
 h_c is the overall column depth ;
 s_c is the column web thickness.



a - A_{sh}



b - A_w

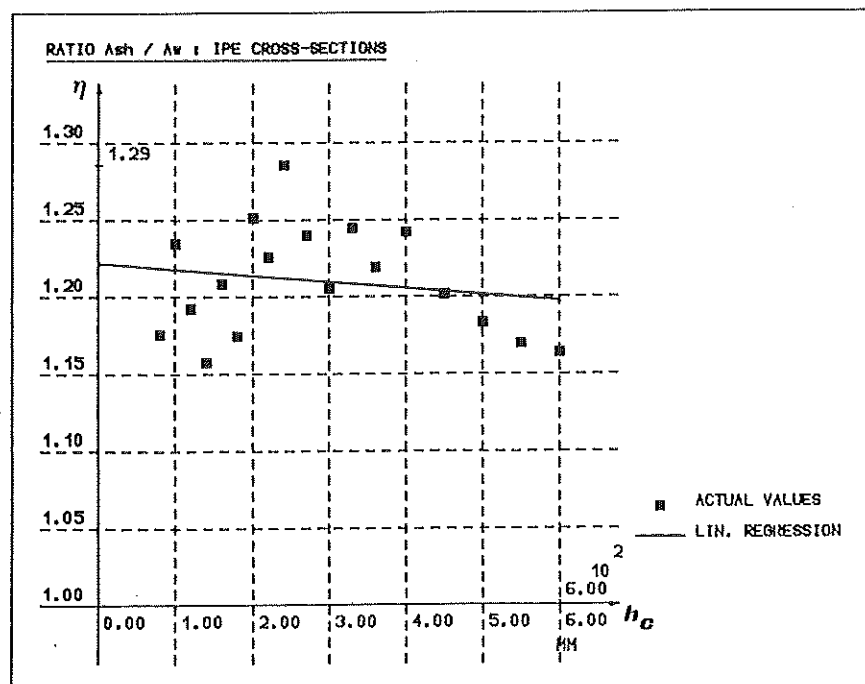
Figure 53 - Column web sheared areas

The values of the ratio η between A_{sh} and A_w versus the column depth h_c have been reported in figures 54.a to 54.c respectively for IPE, HEA and HEB cross-sections.

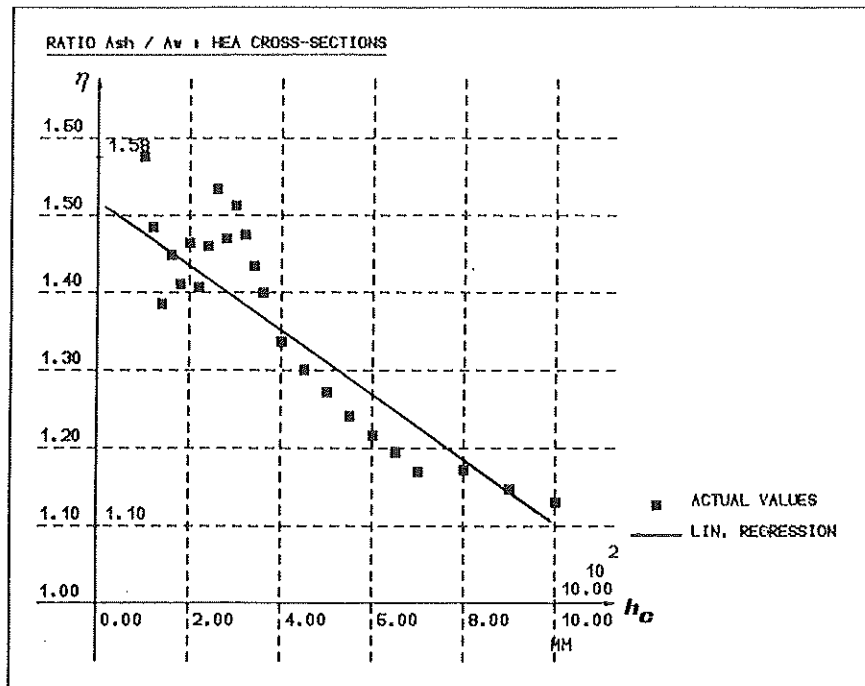
The constant value 1.4 of the coefficient η , suggested by EC3, is seen to be quite unrealistic.

Linear regressions have been used in order to obtain more realistic estimations of this coefficient. The exact results are reported in figure 54; they have been slightly modified in order to simplify their formulation:

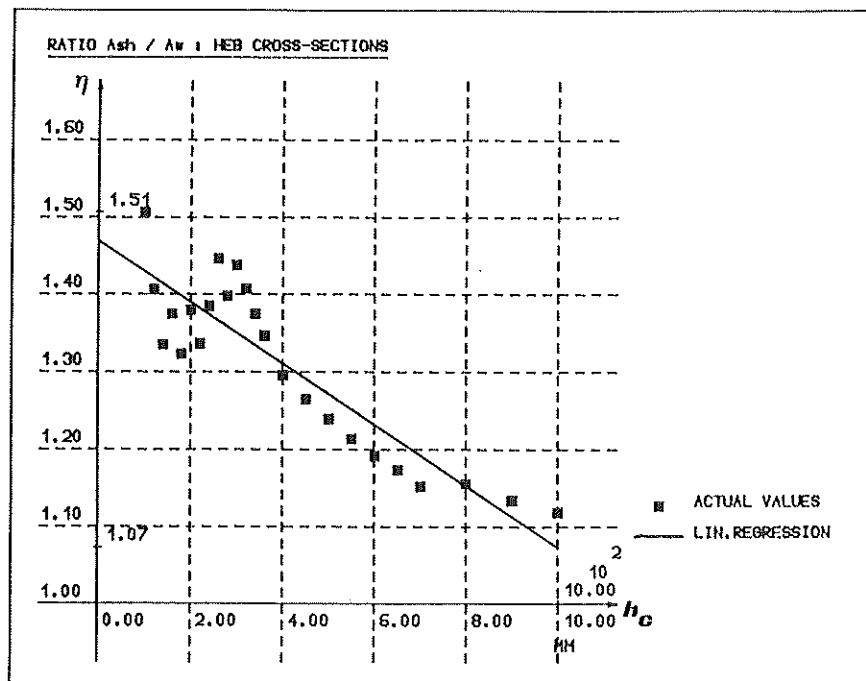
- IPE sections : $\eta = 1.2$
- HEA sections : $\eta = 1.5 - 0.4 \cdot 10^{-3} h_c$ (h_c in mm)
- HEB sections : $\eta = 1.45 - 0.4 \cdot 10^{-3} h_c$ (h_c in mm)



a - IPE cross-sections



b - HEA cross-sections



c - HEB cross-sections

Figure 54 - Values of the η coefficient

The design resistance for sheared web panels of transversally stiffened joints is easily evaluated by adding the additional contribution V_{cy} due to the frame effect (formula 15) to the shear capacity $V_{nr,Rd}$ defined here above.

$$V_{nr,Rd}^r = V_{nr,Rd} + V_{cy} \quad (34)$$

The cogency of this approach may also be seen in figure 50.

10.2. Resistance to the introduction of transverse loads.

The following formulae for the assessment of the design resistance of an unstiffened column web subject respectively to a transverse compression and tensile force are proposed in the annex J of EC3 chapter 6 :

compression zone

$$F_{c,Rd} = f_y \cdot s_c [1.25 - 0.5 \sigma_n / f_y] \cdot b_{c,eff} \leq f_y \cdot s_c \cdot b_{c,eff} \quad (35.a)$$

$$\text{with : } \cdot b_{c,eff} = t_b + 2 \sqrt{2} a + 5 (t_c + r_c) \quad (35.b)$$

for welded joints

$$\cdot b_{c,eff} = t_b + 2 \sqrt{2} a + 2t_e + 5 (t_c + r_c) \quad (35.c)$$

for joints with end plate connections.

tension zone

$$F_{t,Rd} = f_y \cdot s_c \cdot b_{t,eff} \quad (36)$$

with : $\cdot b_{t,eff} = b_{c,eff}$
for welded joints

$$\cdot b_{t,eff} = \text{total effective length of the bolt pattern in the tension zone of the connection, obtained from J.3.3.1. in the appendix J of EC3 chapter 6.}$$

In these expressions :

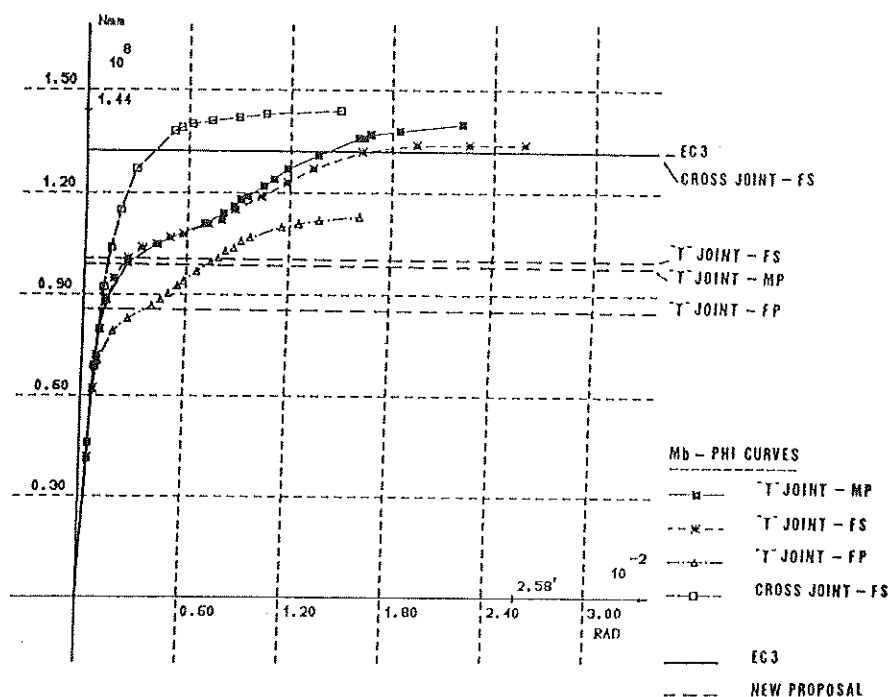
- f_y = column web yield stress ;
- s_c = column web thickness ;
- σ_n = the maximum compression normal stress in the web of the column due to axial force and bending moment ;
- t_b = beam flange thickness ;
- a = weld throat thickness ;

- t_c = column flange thickness ;
- r_c = radius of fillet of the column.

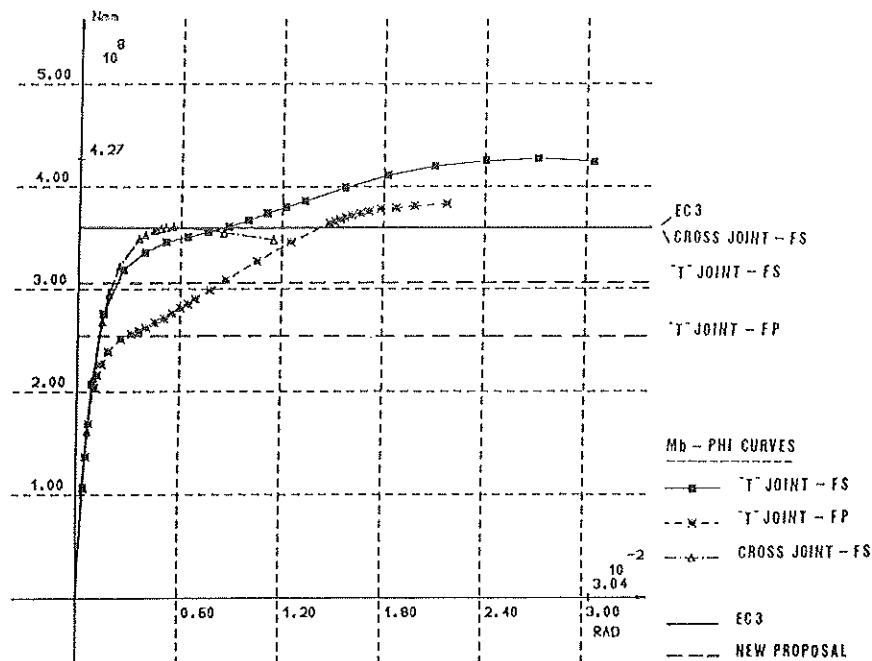
These formulae differ from those proposed in sections 4.2. and 9.2.3. - the design resistance corresponds to the pseudo-plastic force (or moment) presented in section 4.2. - by an unsafer definition of the maximum compressive or tensile stress in the web ; this is linked to the fact that the actual interaction between σ_1 and τ stresses (see figure 9) has not been accounted for in the EC3 rules.

The application of the EC3 and new proposed formulae to the fully welded joints studied numerically and to the joints with extended end plate connections tested in laboratory (see table 7) led to the conclusion that, contrarily to what has been shown in table 6 for the shear resistance, the design resistance of a web subject to transverse loads is highly dependent on the values of the shear stresses in the web panel, and consequently to the actual joint loading. This influence, which may lead to substantial decreases (see factor χ_{1i} in table 7), has to be accounted for, even in a simplified computation of the design resistance of the web transversally loaded.

Examples of application of the formulae are given in figure 55.



a - Joint A



b - Joint B

Figure 55 - Characteristic $M_b - \phi$ curves

Assessment of the design resistance by the EC3 and new proposed formulae.

Fully welded joints.

The approach presented in this report identifies itself obviously to the EC3 one for cruciform joints symmetrically loaded for which the web panel is not subject to shear stresses.

In conclusion the design resistance of a column web will be assessed by means of the following formula :

$$F_{b,Rd} = F_{b,ppl} = s_c l_p \sigma_{iy}^c \quad (37)$$

It will be referred to section 4.2. as well as to tables 4 and 5 in view to determine l_p and σ_{iy}^c in the compression and tension zones of joints with welded, extended end plate and flange cleated connections.

Unstiffened joints		Type of loading (fig.6 and 38)	Testing arrangement: tee(T) or cruciform(C)	$M_{b,ppl}$ (form. 6) kNm	$M_{b,Rd}$ (EC3) kNm	Ratio χ_{li}
welded connections (Fig. 5)	A	FS	T	101.0	133.0	0.76
	A	FP		86.9	133.0	0.65
	A	MP		99.6	133.0	0.75
	B	FS		306.2	359.2	0.85
	B	FP		257.8	359.2	0.72
	A	FP	C	133.0	133.0	1.0
	B	FP		359.2	359.2	1.0
end plate connections [9,12,14]	01	FS	T	78.0	89.7	0.87
	07	FS		77.8	91.8	0.85
	010	FS		127.6	143.7	0.89
	013	FS		61.0	67.2	0.91
	014	FS		72.4	79.0	0.92
	T9	FS		104.5	112.8	0.93
	T20	FS	248.8	263.7	0.94	
	JT3	FS	C	57.3	57.3	1.0

Table 7 - Influence of the stress interaction on the design resistance of web transversally loaded.

10.3. Resistance of the whole panel.

The validity of the EC3 formulae for the assessment of the design resistance of sheared column web panels and of webs subject to transverse loads has been discussed successively in both previous sections.

In reality the design resistance of the whole column web panel is defined as the minimum load level loading to the attainment of the design resistance of the panel under shear or under transverse loads.

The unsafe character of the EC3 rules has consequently to be quantified by considering simultaneously, and not successively, the shear and the load-introduction resistance of the web panel.

The complete study of two examples in this section will allow to demonstrate that the use of the EC3 formulae for the assessment of the design resistance of the whole panel may lead to unsafe and generally unacceptable results.

The geometrical configuration of the cruciform joints A (figure 5) and O1 [9], respectively with a welded and an extended end plate connection, is chosen. A second beam similar to the first one is connected to the other column flange in order to obtain a symmetrical cruciform joint (figure 56). The cantilever beams are respectively loaded by concentrated gravity forces P_1 and P_2 .

P_2 is assumed to be greater or equal to P_1 . The ratio between P_2 and P_1 , termed ρ , may vary then between 0.0 and 1.0 :

- $\rho = 1.0$ means that the joint is cruciform and symmetrically loaded (no shear in the web panel) ;
- $\rho = 0.0$ corresponds to a tee joint (maximum shear in the panel).

The length of the members results in bending-to-shear ratios in the column, in the beams and in the connections which are realistic and similar to those encountered in practice.

The design resistances of the web under shear and transverse loads have been calculated, for 11 different values of the ratio ρ varying between 0.0 and 1.0, by means, on the one hand, of the EC3 formulae and, on the other hand, of the corresponding theoretical expressions which have been presented in sections 4.2., 5.2. and 9.2.3. and which have been validated by comparison with results of experimental tests and numerical simulations in chapter 7.

These values are reported for joint A and O1 respectively, in figures 57.a and 57.b.

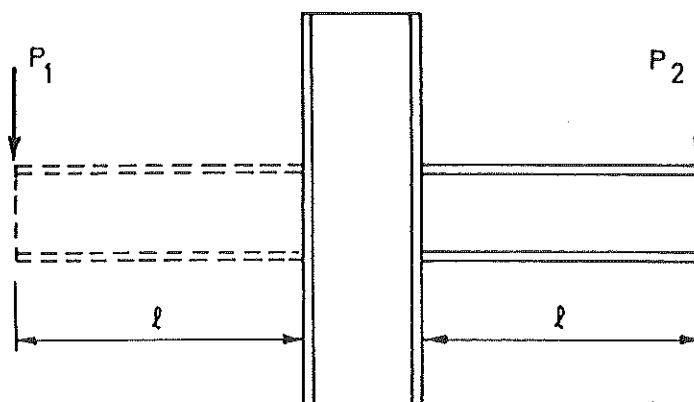
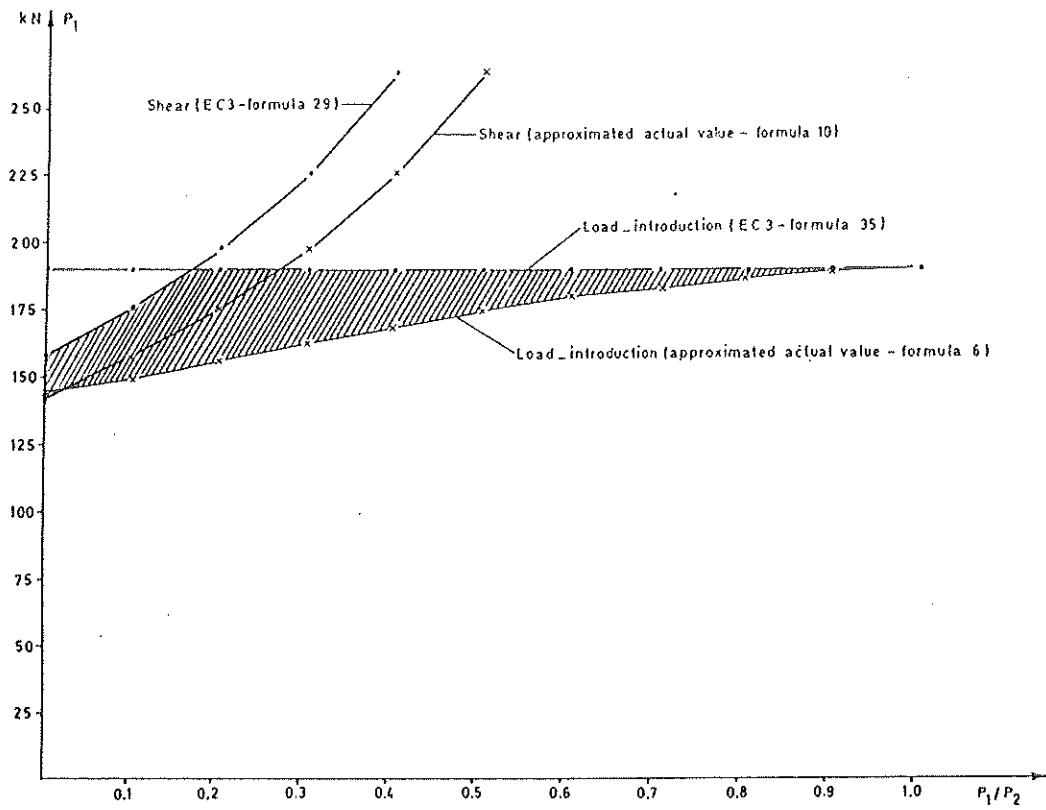
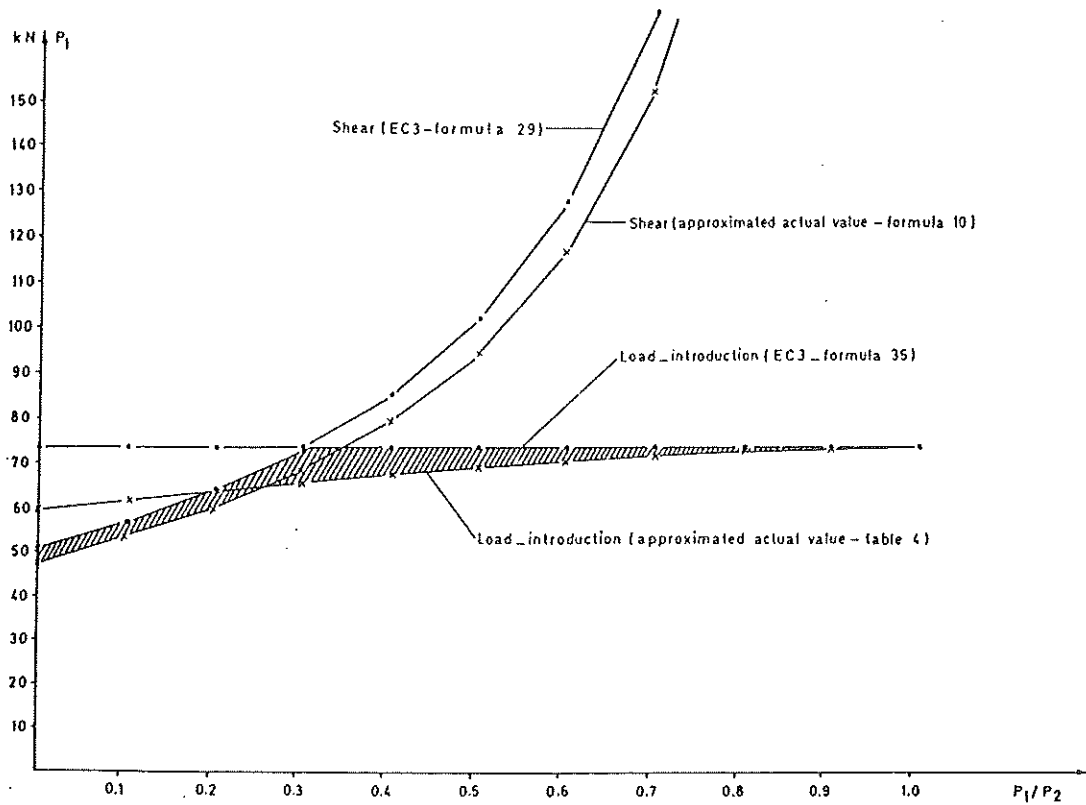


Figure 56 - Geometrical configuration and loading for the joints studied on next figure.



a - Joint A (welded connections)



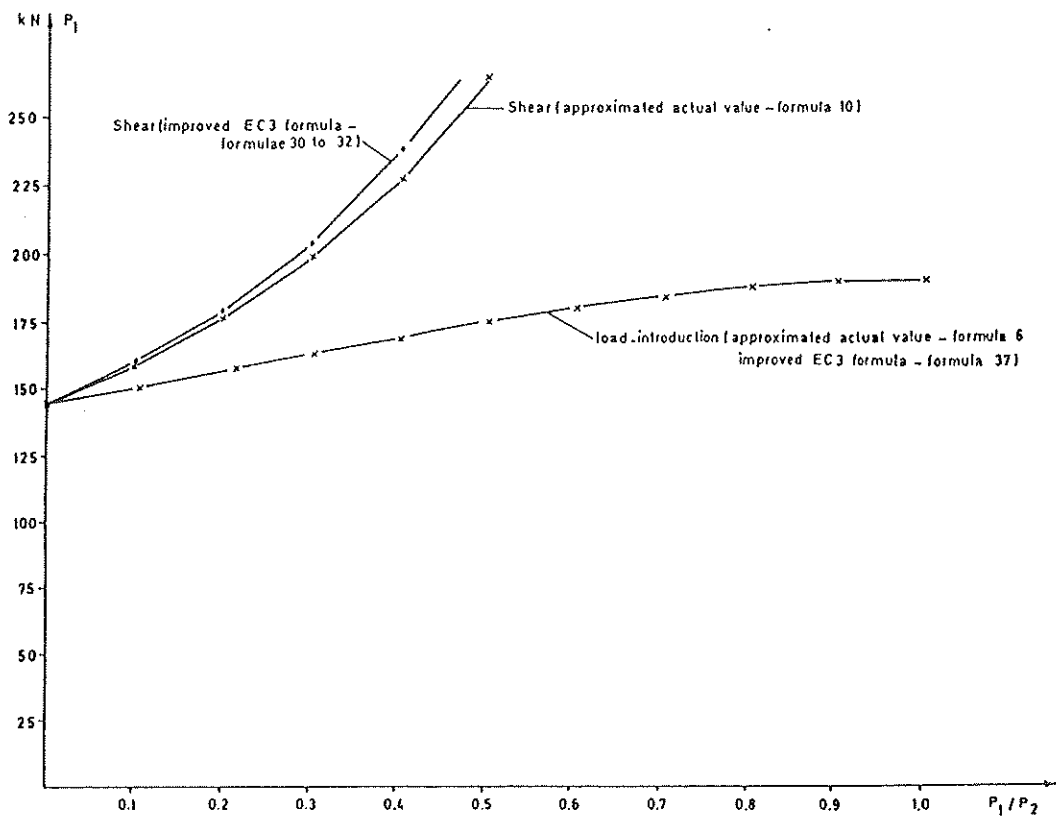
b - Joint 01 (extended end plate connections)

Figure 57 - Design resistance of a column web panel
Unsafe character of the EC3 formulae

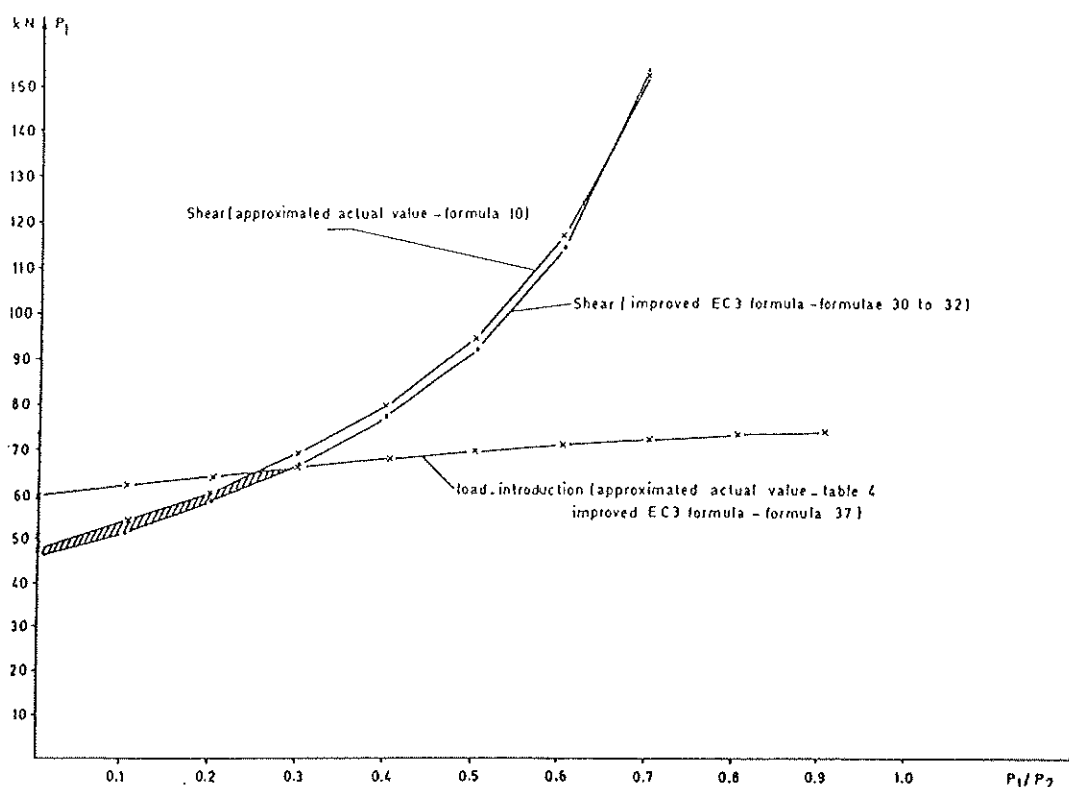
From these examples, as well as from several others which have been studied but are not reported here, it may be stated that :

- the attainment of the plastic capacity of the column web panel is generally associated to the shear resistance only for values of ρ close to 0.0 ;
- the unsafe character of the formula for the assessment of the resistance of a transversally loaded column web is not very significant for values of ρ close to 1.0...
- ... but much more pronounced for intermediate values of ρ (it reaches 24% for joint A and 11% for joint 01).

Figures 58.a and 58.b present the results of a similar comparison, on the same joints, based on modified formulae of EC3 as described in sections 10.1 and 10.2; the cogency of these amendments is well demonstrated.



a - Joint A (welded connections)



b - Joint 01 (extended end plate connections)

Figure 58 - Design resistance of a column web panel

Cogency of the modifications of the EC3 formulae

The unsafe character of the EC3 formulae has to be seriously accounted for, more especially as the design resistance of the web under transverse loads may, in some cases, correspond to the ultimate resistance of the web in the compression zone as explained in chapter 6 and as shown, for instance, in figure 55.b for the cruciform joint B.

This results then in a lack of strength reserve and of rotation capacity for the web subject to transverse compressive forces.

This situation has egged the authors of the annex J of EC3 chapter 6 to clearly specify the modes of collapse to which a substantial rotation capacity is associated : the yielding of the joint in the tension zone and of the web panel in shear.

This implies two possible uses of the EC3 formulae :

- a) if a rotation capacity of the joint is required (for a plastic frame design for instance), the joint design has to be performed in order to avoid a collapse by lack of strength in its compression zone ;
- b) if a rotation capacity of the joint is not required, no condition relative to the collapse mode has to be formulated.

It may be asked, besides, whether the rotation capacity is sufficient when the actual design resistance of the joint is only slightly lower than that of the compression zone of the column web.

A less restrictive attitude may however be recommended. It lies on the following thoughts:

- a) as shown in chapter 6, the instability load F_{bub} (see figure 59) of a web subject to (a) transverse compression force(s) may identify itself to the buckling strength F_{bb} of the web if $F_{bb} > F_{btpl}$ (figure 59.a) or to the pseudo-plastic resistance F_{btpl} of the web if $F_{bb} \leq F_{btpl}$ (figure 59.b) ;

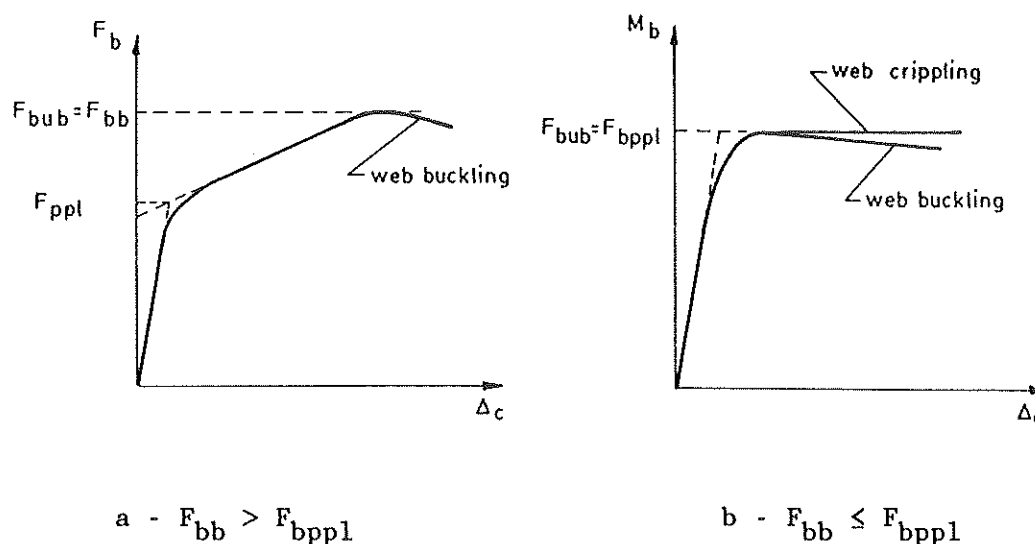


Figure 59 - Relative values of F_{btpl} and F_{bub}

- b) the results of the experimental tests on joints with extended end plate connections carried out in Liège [9] and in Delft [12] as well as the numerical simulations of welded joints presented in this report allow to characterize the post-critical behaviour of the web : the decrease of the compression force F_b versus the displacement Δ_c associated to a web buckling is seen to be not very important when $F_{bub} = F_{bb}$ (figure 59.a) and quite limited when $F_{bub} = F_{btpl}$ (figure 59.b); it is almost inexistant in figure 59.b for a web crippling.

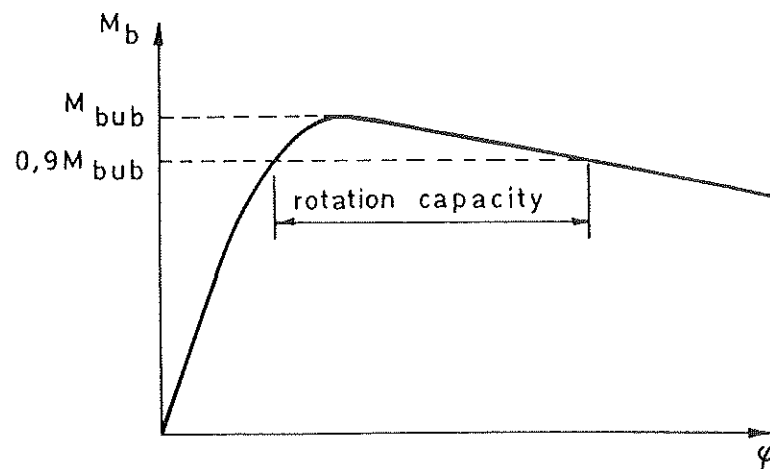
If it is assumed that the strength of the web in the compression zone is the determining factor for the joint resistance, the approach suggested consists :

- 1) in the determination of the pseudo-plastic resistance $F_{b,pp1}$ of the web, of its buckling strength F_{bb} and consequently of the ultimate strength F_{bub} ;
- 2) in the definition of the design resistance $F_{b,Rd}$ of the web subject to (a) transverse compression force(s) by the following formula :

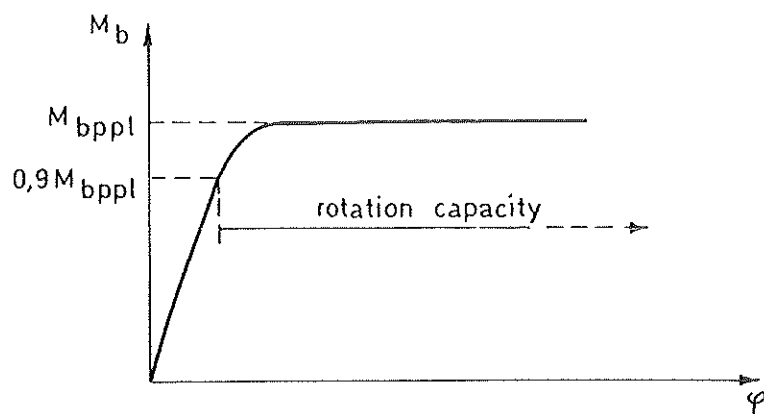
$$F_{b,Rd} = \min (F_{b,pp1} ; 0.9 F_{bub}) \quad (38)$$

This definition of the design resistance allows to dispose of a substantial rotation capacity, whatever the instability mode of the web may be, by slightly reducing the previously defined design resistance $F_{b,pp1}$ only for the webs characterizes by $F_{bub} \leq 1.1 F_{b,pp1}$ (see figure 60.a and 60.b), what is not necessary in the other cases, when $F_{bub} > 1.1 F_{b,pp1}$ (see figure 60.c).

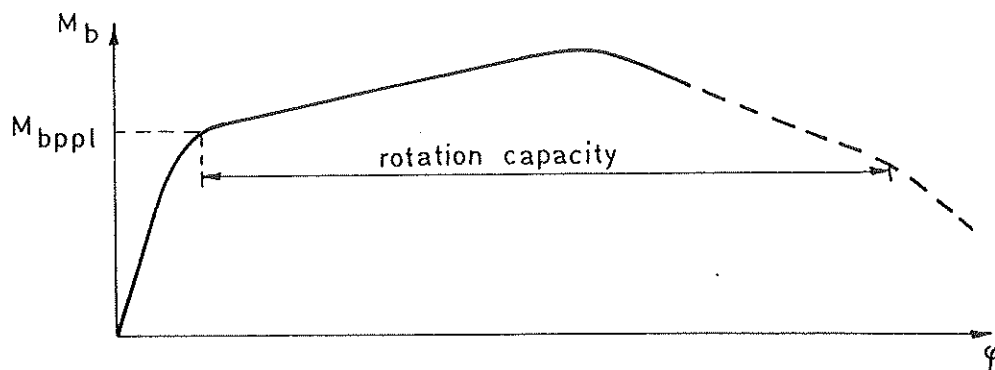
The value of the reduction factor 0.9 appearing in (38) has been determined on base of the study of the available numerical and experimental results.



a - Web buckling ($M_{b,pp1} \leq M_{bub} \leq 1.1 M_{b,pp1}$)



b - Web crippling ($M_{bub} = M_{bppl}$)



c - Web buckling ($M_{bub} > 1.1 M_{bppl}$)

Figure 60 - Rotation capacity associated to the use of formulae (38).

This approach requires obviously the computation of two characteristics, $F_{b\text{pp1}}$ and $F_{b\text{b}}$, instead of a single one in Eurocode 3; this could be avoided by defining the design resistance of the compression zone of the column web as equal to $0.9 F_{b\text{pp1}}$ whatever the mode of instability may be. This simplified formulation corresponds to the approach described here above when the instability of the web is associated to a crippling (figure 60.b) or to a buckling with $F_{b\text{ub}} = F_{b\text{pp1}}$; it is however too safe in the other cases, and in particular in that of a buckling with $F_{b\text{ub}} > 1.1 F_{b\text{pp1}}$ (figure 60.c).

10.4. Summary of the proposals.

This last section presents a summary of the proposals for the improvement of the EC3 formulae for the assessment of the design resistance of a column web panel in a joint with welded or extended end plate connections.

The extending to the joints with flange cleated connections is also considered in this summary.

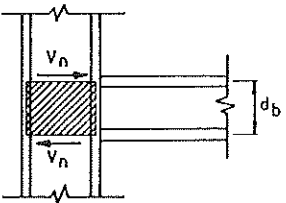
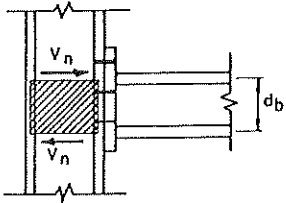
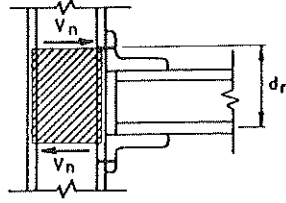
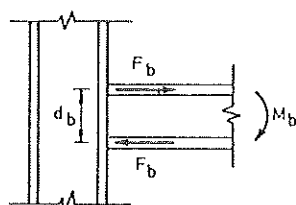
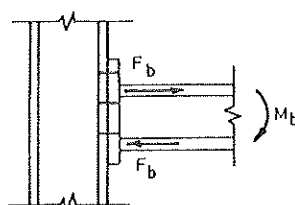
DESIGN RESISTANCE OF A SHEARED COLUMN WEB PANEL	
 <p>welded connection</p>	 <p>extended end plate connection</p>
 <p>flange cleat connection</p>	
<p><u>Unstiffened web panel</u></p> $V_{nr.Rd} = 0.9 A_{sh} f_y / \sqrt{3}$ <p>f_y = yield stress of column web ; A_{sh}^c = column web sheared area given in table 11 or approximated by $\eta \cdot h_c \cdot s_c^c$ with :</p> <ul style="list-style-type: none"> - h_c = overall column depth ; - s_c^c = column web thickness - $\eta^c = 1.2$ for IPE₃ sections $= 1.5 - 0.4 \cdot 10^{-3} h_c$ (h_c en mm) for HEA sections - $\eta^c = 1.45 - 0.4 \cdot 10^{-3} h_c$ (h_c en mm) for HEB sections 	
<p><u>Transversally stiffened web panel</u></p> $V_{nr.Rd}^r = V_{nr.Rd} + V_{cf}$ <p>with $V_{cf} = 4 M_{pf} / d$</p> <p>M_{pf} = plastic moment of the column flange given in table 11 ; $d = d_b$ for welded and extended end plate connections ; $= d_r$ for flange cleated connections.</p>	

Table 8

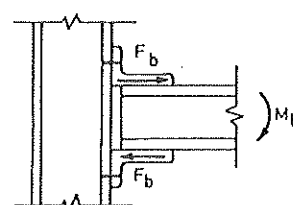
DESIGN RESISTANCE OF A COLUMN WEB SUBJECT TO TRANSVERSE TENSILE FORCES



welded connection



extended end plate connection



flange cleat connection

Unstiffened web panel

$$F_{bt.Rd} = s_c l_p \sigma_{iy}^c$$

σ_{iy}^c = maximum elastic tensile stress in the web which accounts for the stress interaction, in the tension zone of the web, between σ_i and shear τ stresses by means of :

$$\sqrt{\sigma_{iy}^c{}^2 + 3 \tau^c{}^2} = f_y$$

with:

$$\sigma_i = F_b [1/\lambda + 2(1 + 1/d_b \lambda)/(d_b \lambda^2) + d_b/6]^{-1} / s_c$$

for welded connections ;

$$= F_b \lambda / 2 \mu s_c$$

for bolted connections ;

$$\tau = V_n / A_{sh} \text{ (see table 8)}$$

In these expressions :

λ = geometrical characteristic of the column cross-section given in table 11 ;

s_c = column web thickness ;

$$\mu = \xi / (1 - e^{-\xi} \cos \xi)$$

with :

$$\xi = b \lambda / 2$$

$$b = t_b + 2w_e \text{ for extended end plate connections}$$

with : t_b = beam flange thickness ;

w_e = length of the extended part of the end plate in the tension zone

= $2n_a$ for flange cleated connections (see table 5)

$$l_p = t_b + 2\sqrt{2} a + 5(t_c + r_c) \text{ for welded connections}$$

with : a = welded throat thickness ;

t_c = column flange thickness ;

r_c = radius of fillet of the column

= b_m for bolted connections where b_m is taken equal to the effective length of the bolt pattern in the tension zone of the connection obtained from J.3.3.1. in the appendix J of EC3 chapter 6.

$F_{bt.Rd}$ may be reduced by a factor $(1.25 - 0.5 \sigma_n / f_y)$ when $\sigma_n > 0.5 f_y$; σ_n represents the normal stress acting in the column web, just under the applied force, and resulting from the normal load and the bending moment in the column.

Table 9

DESIGN RESISTANCE OF A COLUMN WEB SUBJECT TO TRANSVERSE COMPRESSION FORCES

Types of connections covered : see table 9

Unstiffened web panel

$$F_{bc.Rd} = \min(F_{b ppl}; 0.9 F_{bub})$$

$$F_{b ppl} = s_c l_p \sigma_{iy}^c$$

with:

σ_{iy}^c = maximum elastic compression stress in the web which accounts for the stress interaction, in the compression zone of the web, between σ_x and shear τ stresses; it is defined as in table 9, except that :

$b = t_b + 2a\sqrt{2} + 2t_e$ for extended end plate connections with:
 t_b = beam flange thickness;
 a = weld throat thickness;
 t_e = end plate thickness.

$b = 2t_a + (2-\sqrt{2})r_a$ for flange connections with :
 t_a = cleat thickness;
 r_a = radius of fillet of the lower flange cleat.

$l_p = t_b + 2a\sqrt{2} + 5(t_c + r_c)$ for welded connections with :
 t_c = column flange thickness ;
 r_c = radius of fillet of the column.
 $= t_b + 2a\sqrt{2} + 2t_e + 5(t_c + r_c)$ for extended end plate connections
 $= 2t_a + (2-\sqrt{2})r_a + 5(t_c + r_c)$ for flange cleated connections.

s_c = column web thickness.

$$F_{bub} = \max(F_{b ppl}; F_{bb})$$

with :

$$F_{bb} = \mu \sqrt{F_{by} F_{bcr}}$$

with:

$$F_{by} = s_c \left[\frac{1}{\lambda} + 2 \left(\frac{1 + 1/d_b \lambda}{d_b \lambda^2} + d_b/6 \right) \right] \sigma_{iy}^c$$

for welded connections ;
 $= 2s_c \mu \sigma_{iy}^c / \lambda$ for bolted connections.

$$F_{bcr} = (h_c - 2t_c) s_c k \frac{\pi^2 E}{12(1-\nu^2)} \left(\frac{s_c}{h_c - 2t_c} \right)^2$$

In these expressions :

λ = geometrical characteristic of the column cross-section given in table 11 ;

d_b is given in table 9 for end plate connections ;

μ is given in table 9 (but modified values of b for the compression zone are given in this table ;

$k = 1.0$ or 2.0 according as the joint is a cruciform or a tee one.

$F_{bc.Rd}$ may be reduced by a factor $(1.25 - 0.5 \sigma_n / f_y)$ when $\sigma_n > 0.5 f_y$; see table 9.

Table 10

SECTIONS	Ash (cm ²)	If (cm ⁴)	Zf=Mpf/fy (cm ³)	L=1/λ (mm)
IPE 80	3.58	0.12	0.44	16.43
IPE 100	5.08	0.24	0.71	20.36
IPE 120	6.31	0.31	0.93	22.69
IPE 140	7.64	0.41	1.19	24.99
IPE 160	9.66	0.69	1.67	28.91
IPE 180	11.25	0.85	2.05	31.15
IPE 200	14.00	1.50	2.88	36.12
IPE 220	15.88	1.83	3.49	38.51
IPE 240	19.14	3.00	4.76	43.82
IPE 270	22.14	3.45	5.50	46.28
IPE 300	25.68	4.03	6.43	48.73
IPE 330	30.81	6.28	8.52	54.90
IPE 360	35.14	7.79	10.39	58.40
IPE 400	42.69	11.50	13.29	64.87
IPE 450	50.85	13.86	15.71	68.76
IPE 500	59.87	17.16	18.96	73.17
IPE 550	72.34	24.87	24.16	80.46
IPE 600	83.78	31.17	29.40	85.48
IPE 750*137	92.90	18.40	23.75	81.37
IPE 750*147	105.41	19.29	24.37	79.55
IPE 750*161	110.98	25.96	30.58	84.74
IPE 750*173	116.44	34.20	37.55	89.81
IPE 750*185	121.12	42.69	44.12	94.12
IPE 750*196	127.27	51.84	50.75	97.69
IPE 750*210	131.52	66.63	60.71	103.35
IPE 750*222	139.76	77.29	67.39	105.65

SECTIONS	Ash (cm ²)	If (cm ⁴)	Zf=Mpf/fy (cm ³)	L=1/λ (mm)
HE 100 A	7.56	1.29	2.58	27.60
HE 120 A	8.46	1.40	2.90	30.15
HE 140 A	10.12	1.72	3.60	32.78
HE 160 A	13.21	2.90	5.02	37.66
HE 180 A	14.47	3.33	5.90	40.56
HE 200 A	18.08	5.19	7.81	45.49
HE 220 A	20.67	6.48	9.73	48.70
HE 240 A	25.18	10.12	13.14	54.54
HE 260 A	28.76	13.89	16.14	60.18
HE 280 A	31.74	15.57	18.14	62.50
HE 300 A	37.28	22.39	23.24	68.42
HE 320 A	41.13	26.78	27.24	71.94
HE 340 A	44.95	30.28	30.20	74.60
HE 360 A	48.96	34.11	33.32	77.25
HE 400 A	57.33	40.85	38.46	81.57
HE 450 A	65.78	49.97	45.38	87.94
HE 500 A	74.72	60.61	52.92	94.21
HE 550 A	83.72	66.94	57.10	98.42
HE 600 A	93.21	73.74	61.43	102.47
HE 650 A	103.19	81.01	65.93	106.40
HE 700 A	116.97	89.70	70.94	109.55
HE 800 A	138.83	109.08	79.26	118.33
HE 900 A	163.33	128.45	89.66	125.40
HE 1000 A	184.56	138.99	95.10	130.77

SECTIONS	Ash (cm ²)	If (cm ⁴)	Zf=Mpf/fy (cm ³)	L=1/λ (mm)
HE 100 B	9.04	2.05	3.72	29.56
HE 120 B	10.96	2.77	4.99	33.50
HE 140 B	13.08	3.69	6.55	37.33
HE 160 B	17.59	6.22	9.32	42.41
HE 180 B	20.24	7.85	11.60	46.08
HE 200 B	24.83	11.92	15.41	51.62
HE 220 B	27.92	14.53	18.55	55.23
HE 240 B	33.23	20.83	23.66	60.80
HE 260 B	37.59	27.10	28.15	66.18
HE 280 B	41.09	30.12	31.30	68.86
HE 300 B	47.43	40.85	38.46	74.55
HE 320 B	51.77	47.74	43.66	78.18
HE 340 B	56.09	53.06	47.44	80.97
HE 360 B	60.60	58.79	51.38	83.71
HE 400 B	69.98	68.62	57.75	88.23
HE 450 B	79.66	81.91	66.27	94.72
HE 500 B	89.82	97.03	75.42	101.08
HE 550 B	100.07	105.83	80.41	105.44
HE 600 B	110.81	115.16	85.56	109.63
HE 650 B	122.04	125.05	90.88	113.67
HE 700 B	137.10	136.62	96.74	116.95
HE 800 B	161.75	161.87	106.48	125.67
HE 900 B	188.75	187.26	118.52	132.88
HE 1000 B	212.49	200.94	124.79	138.43

SECTIONS	Ash (cm ²)	If (cm ⁴)	Zf=Mpf/fy (cm ³)	L=1/λ (mm)
HE 100 M	18.04	11.54	13.59	38.31
HE 120 M	21.15	14.71	17.09	43.20
HE 140 M	24.46	18.48	21.08	47.83
HE 160 M	30.81	26.30	27.24	52.87
HE 180 M	34.65	31.77	32.38	57.18
HE 200 M	41.03	42.81	40.09	62.54
HE 220 M	45.31	50.40	46.51	66.68
HE 240 M	60.07	101.77	77.10	78.04
HE 260 M	66.89	121.98	87.89	83.23
HE 280 M	72.03	133.56	96.05	86.74
HE 300 M	90.53	234.13	143.95	98.14
HE 320 M	94.85	248.32	150.11	101.57
HE 340 M	98.63	248.32	150.11	103.54
HE 360 M	102.41	247.77	149.71	105.35
HE 400 M	110.18	247.22	149.31	108.84
HE 450 M	119.84	247.22	149.31	112.82
HE 500 M	129.50	246.67	148.91	116.35
HE 550 M	139.58	246.67	148.91	119.77
HE 600 M	149.66	246.12	148.50	122.86
HE 650 M	159.74	246.12	148.50	125.79
HE 700 M	169.82	245.56	148.10	128.45
HE 800 M	194.27	264.29	152.71	135.72
HE 900 M	214.43	263.73	152.31	140.24
HE 1000 M	235.01	263.73	152.31	144.50

Table 11 - Geometrical characteristics of the H and I profiles

REFERENCES

1. ANDERSON, D., BIJLAARD, F.S.K., NETHERCOT, D.A. AND ZANDONINI, R., 'Analysis and Design of steel frames with semi-rigid connections'. IABSE Survey S-39/87, IABSE Periodica 4/87.
2. JASPART, J.P. and de VILLE de GOYET, V., 'Etude expérimentale et numérique du comportement des structures composées de barres à assemblages semi-rigides'. Construction Métallique, N° 2, juin 1988, pp. 31 - 49.
3. ATAMAZ SIBAI, W. and JASPART, J.P., 'Etude du comportement jusqu'à la ruine des noeuds complètement soudés'. Internal Report IREM, Polytechnic Federal School of Lausanne, N° 89/7, and MSM, University of Liège, N° 194, October 1989.
4. FREY, F., LEMAIRE, E., de VILLE de GOYET, V., JETTEUR, P., STUDER, M. and ATAMAZ, W., 'FINELG, non linear finite element analysis program', MSM, University of Liège, IREM, Polytechnic Federal School of Lausanne, July 1986.
5. Manual on Stability of Steel Structures, ECCS Publication, N° 22, Bruxelles, 1976.
6. ATAMAZ SIBAI, W., 'Simulation numérique du comportement de deux assemblages de rive soudés non raidis', Internal Report 87/5, IREM, Polytechnic Federal School of Lausanne, June 1987.
7. ZOETEMEIJER, P., Report 6-80-5, Stevin Laboratory, Delft, February 1980.
8. KATO, B., 'Beam-to-column connection research in Japan', Journal of Structural Division, ASCE, Vol. 108, N° ST2, February 1982, pp.343-360.
9. JANSSE, J., JASPART, J.P. and MAQUOI, R., 'Experimental study of the non-linear behaviour of beam-to-column joints', Proceedings of a State-of-the-Art Workshop on Connections, Behaviour, Strength and Design of Steel Structures, Cachan, France, 25-27 May, 1987. Elsevier Applied Science Publishers, February 1988, pp. 26 - 32.
10. ZERIOOH, S. and JASPART, J.P., 'Prediction of moment-rotation curves for bolted end plate and flange cleated connections', Internal Report, University of Liège, MSM, Department, to appear.

11. JASPART, J.P., MAQUOI, R., ALTMANN, R. and SCHLEICH, J.B., 'Experimental and theoretical study of composite connections', to appear in the Report of the IABSE Symposium on Mixed Structures, including New Materials, Brussels, Belgium, September 5-7, 1990.
12. ZOETEMEIJER, P., 'A design method for the tension side of statically loaded, bolted beam-to-column connections', Heron, Vol. 20, 1974, N°1.
13. ALPSTEN, G.A., 'Variations in mechanical and cross-sectional properties of steel', ASCE-IABSE Int. Conf. on Planning and Design of Tall Buildings, Vol. 1b9, 1972.
14. DAVISON, J.B., KIRBY, P.A. and NETHERCOT, D.A., 'Rotational stiffness characteristics of steel beam-to-column connections', Journal of Constructional Steel Research, Vol. 8, 1987, pp. 17-54.
15. EUROCODE 3 : Design of Steel Structures.
Commission of the European Communities, April 1990.

User-Agent: Microsoft-Outlook-Express-Macintosh-Edition/5.02.2022
Date: Mon, 05 Feb 2001 16:35:18 +0000
Subject: remerciement
X-PH: V4.4@aix17.segi.ulg.ac.be
From: Luis Costa Neves <luis@dec.uc.pt>
To: Jean-Pierre JASPART <jean-pierre.jaspart@ulg.ac.be>

Cher Jean-Pierre

J'espère que tu vas bien, et que ton travail marche comme tu le souhaites. Je t'écris pour te remercier d'avoir demandé à Frédéric Cerfontaine de nous envoyer les documents demandés. Aujourd'hui même je lui ai envoyé un premier document produit par Luciano Lima, notre collègue brésilien qui est venu chez nous faire ses essais. D'autres lui seront envoyés au fur et à mesure qu'ils auront été produits.

Avec mes meilleures salutations, et à bientôt,

Luis Neves

33 1 30852137

rapport

J.P.

3.6.3